

# Receiver Design of Uplink Control and Shared Channel in 4G-LTE

Prasanna Kumar Pulimela

Roll No: EE12M1026

A Thesis Submitted to  
Indian Institute of Technology Hyderabad  
In Partial Fulfillment of the Requirements for  
The Degree of Master of Technology  
in Electrical Department




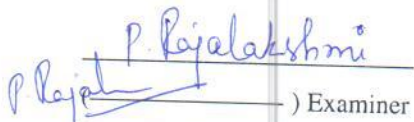
भारतीय प्रौद्योगिकी संस्थान हैदराबाद  
Indian Institute of Technology Hyderabad


Supervisor: Dr.Kiran Kuchi


# Approval Sheet


This Thesis entitled "Receiver Design of Uplink Control and Shared Channel in 4G-LTE" by Prasanna Kumar Pulimela is approved for the degree of Master of Technology from IIT Hyderabad.

  
\_\_\_\_\_ ) Examiner  
Dept. of Electrical Engineering  
IIT Hyderabad

  
\_\_\_\_\_ ) Examiner  
Dept. of Electrical Engineering  
IIT Hyderabad

  
\_\_\_\_\_ (Dr. Kiran Kuchi) Adviser  
Dept. of Electrical Engineering  
IIT Hyderabad

  
\_\_\_\_\_ (Sunitha) Chairman  
Dept. of Electrical Engineering  
IIT Hyderabad

  
\_\_\_\_\_ Chairman  
Dept of Electrical Engineering  
IIT Hyderabad.

# Declaration

I declare that this written submission represents my ideas in my own words, and where ideas or words of others have been included, I have adequately cited and referenced the original sources. I also declare that I have adhered to all principles of academic honesty and integrity and have not misrepresented or fabricated or falsified any idea/data/fact/source in my submission. I understand that any violation of the above will be a cause for disciplinary action by the Institute and can also evoke penal action from the sources that have thus not been properly cited, or from whom proper permission has not been taken when needed.

P. Prasanna Kumar  
(Signature)

P. Prasanna Kumar  
(P. Prasanna Kumar)

EE12M1026  
(Roll Number)

# Acknowledgments

Foremost, I would like to express my sincere gratitude to my adviser Prof. Kiran Kuchi for the continuous support of my Masters study and research. His guidance helped me in all the time of research and writing of this Masters thesis.

I would like to thank my lab mates Sibgath Alikhan, Sri Harsha and Srikanth Dama for all those valuable discussions in the lab.

Finally I would also like to thank my parents, sister, and younger brother. They were always supporting me and encouraging me with their best wishes.

# Abstract

This Work focuses on the Receiver Design of Physical Uplink Control Channel (PUCCH) and Physical Uplink Shared Channel (PUSCH) which includes different channel estimation techniques and different equalization techniques. Simulations are done in Matlab to verify algorithms. In addition to estimation and equalization algorithms, here i presented Channel Quality Indicator (CQI) decoding algorithm for PUSCH and PUCCH .

# Contents

<b>1</b>	<b>Introduction</b>	<b>9</b>
<b>2</b>	<b>Radio Channel Propagation</b>	<b>13</b>
2.1	Radio Channel Propagation . . . . .	13
2.1.1	Large-Scale Fading . . . . .	13
2.1.2	Small-Scale Fading . . . . .	15
<b>3</b>	<b>3GPP Specifications</b>	<b>21</b>
3.1	Definitions and Symbols . . . . .	21
3.2	Abbreviations . . . . .	22
3.3	Frame Structure . . . . .	22
3.3.1	Frame Structure Type 1 . . . . .	23
3.3.2	Frame Structure Type 2 . . . . .	24
3.4	Slot Structure and Physical Resources for Uplink . . . . .	24
3.4.1	Resource Grid . . . . .	24
3.4.2	Resource Elements . . . . .	25
3.4.3	Resource Blocks . . . . .	26
3.5	Simulation Parameters . . . . .	27
<b>4</b>	<b>Transmitter Structure of PUSCH</b>	<b>29</b>
4.1	Bit level Scrambling . . . . .	30
4.2	Modulation Mapper . . . . .	32
4.2.1	QPSK . . . . .	32
4.2.2	16QAM . . . . .	32
4.3	Transform Precoder . . . . .	33
4.4	Uplink Reference Signals . . . . .	34
4.4.1	Uplink Reference Signal Sequences . . . . .	35
4.4.2	Demodulation Reference signals . . . . .	38
4.5	Resource Element Mapping . . . . .	39
4.6	SC-FDMA Signal Generation . . . . .	40
<b>5</b>	<b>Transmitter Structure of PUCCH Formats 2,2a and 2b</b>	<b>41</b>
5.1	PUCCH Formats 2,2a and 2b . . . . .	42
5.2	PUCCH Mapping . . . . .	42

5.3	Demodulation Reference Signal . . . . .	44
<b>6</b>	<b>Receiver Design for PUSCH</b>	<b>47</b>
6.1	Channel Estimation . . . . .	47
6.1.1	Least Square Estimation . . . . .	49
6.1.2	LMMSE Channel Estimator . . . . .	50
6.1.3	DFT Based Channel Estimation with transform domain cutoff filter . . . . .	50
6.1.4	Linear Averaging Method . . . . .	52
6.2	Equalization . . . . .	52
6.2.1	ZF Equalization . . . . .	54
6.2.2	MMSE-LE Without Co-variance Estimation . . . . .	54
6.2.3	MMSE-LE With Co-variance Estimation . . . . .	55
6.3	Inverse Precoding . . . . .	56
6.4	Demodulation Section . . . . .	56
6.4.1	Soft Demodulation of Binary Modulation in an AWGN Environment . . . . .	56
6.4.2	Soft Demodulation in Rayleigh Fading Environment . . . . .	57
6.4.3	BER vs SNR Plots for MMSE-LE with and without Co-variance Estimation . . . . .	59
<b>7</b>	<b>Receiver design for PUCCH-Formats 2,2a and 2b</b>	<b>63</b>
7.1	Channel Estimation . . . . .	65
7.1.1	LS Estimation . . . . .	65
7.1.2	LMMSE Estimation . . . . .	66
7.1.3	DFT Based Channel Estimation . . . . .	67
7.1.4	2D-MMSE . . . . .	68
7.2	Interpolation . . . . .	69
7.3	Equalization . . . . .	70
7.3.1	ZF Equalization . . . . .	70
7.3.2	MMSE Equalization . . . . .	70
7.4	Demodulation . . . . .	70
7.4.1	Soft Demodulation of Binary Modulation in an AWGN Environment . . . . .	70
7.4.2	Soft Demodulation in Rayleigh Fading Environment . . . . .	71
7.4.3	Block Error Plots for PUCCH . . . . .	74
<b>8</b>	<b>CQI Decoding algorithm for PUSCH and PUCCH</b>	<b>77</b>
8.1	Channel Coding for Periodic Reporting . . . . .	77
8.2	Channel Coding for Aperiodic Reporting . . . . .	78
8.3	Decoding algorithm for APeriodic report-Long CQI . . . . .	79
8.3.1	Decoding algorithm for Aperiodic report -Short CQI . . . . .	81
8.4	Decoding algorithm for Periodic report-CQI . . . . .	81
<b>9</b>	<b>Miscellaneous-Concepts</b>	<b>85</b>
9.1	Orthogonal Frequency Division Multiplexing (OFDM) . . . . .	85





# 1 | Introduction

Evolved Universal Mobile Telecommunications Systems (UMTS) Terrestrial Radio Access (E-UTRA) is aimed at commercial deployment around 2010 timeframe. Long term goals for the system include support for high peak data rates (>100 Mbps downlink and >50 Mbps uplink), low latency (10ms round-trip delay), improved system capacity and coverage, reduced operating costs, multi-antenna support, efficient support for packet data transmission, flexible bandwidth operations (up to 20 MHz) and seamless integration with existing systems.

To reach these goals, a new design for the air interface is envisioned. Single-Carrier Frequency Division Multiple Access (SC-FDMA) is selected to efficiently meet E-UTRA performance requirements for Uplink (UL) and Orthogonal Frequency Division Multiple Access (OFDMA) is selected for Downlink(DL). An overview on the physical shared and control channels of the UMTS long term evolution (LTE) system can be found in [1,2].

The performance of the physical uplink shared channel (PUSCH) depends heavily on the channel state information (CSI) available at the receiver. The CSI is generally used for demodulation and equalization that is especially needed when SC-FDMA transmission scheme is employed. Different channel estimation methods such as the maximum-likelihood (ML) and the inverse fast Fourier transform (IFFT) can be found in the literature [6,7,8]. However, the performance of these channel estimation methods depends heavily on the signal-to noise ratio (SNR) and the number of allocated sub-carriers or equivalently resource blocks (RB) in the uplink.

The key aspects of the requirements are as follows [2,3,4,5]:

- Up to 100 Mbps with in a 20 MHz downlink spectrum allocation(5 b/s/Hz) and 50 Mb/s (2.5 b/s/Hz) with in a 20 MHz uplink spectrum allocation.
- Control-plane capacity: at least 200 users per cell should be supported in the active state for spectrum allocations up to 5 MHz.
- User-plane latency : less than 5 msec in an unloaded condition (i.e.,single user with single data stream) for small IP packet.
- Mobility: E-UTRAN should be optimized for low mobile speeds 0–15 km/h. Higher mobile speeds between 15 and 120 km/h should be supported with high performance. Connections shall be maintained at speeds 120–350 km/h (or even up to 500 km/h depending on the frequency band).
- Coverage: Throughput, Spectrum efficiency, and Mobility targets should be met for 5 km cells and with a slight degradation for 30 km cells.

- Enhanced multimedia broadcast multicast service (E-MBMS).
- Spectrum flexibility: shall operate in spectrum allocations of different sizes including 1.4MHz, 3 MHz, 5 MHz, 10 MHz, 15 MHz, and 20 MHz in both UL and DL.
- Radio Resource Management: enhanced support for end-to-end Quality of Service (QoS), efficient support for transmission of higher layers, and support of load sharing and policy management across different radio access technologies.

There are major differences between DL and UL in LTE, including different transmissions and multiple access schemes, and different types of channel and control information, which result, in different physical layer processing. Low complexity and high power efficiency are among major factors for the transmitter design in the UL. As a result, the multiple access in the UL is based on SC-FDMA due to its low peak-to-average power ratio (PAPR) compared to OFDMA which is used in the DL, subsequently has an impact on the resource allocation and base-band signal generation. Due to the SC-FDMA nature of the UL, each UE can be allocated contiguous resource blocks, unlike DL where each UE can be allocated non contiguous resource blocks in order to extract frequency diversity gain.

The user data in the UL direction is carried on the PUSCH, which has a 10 ms frame structure and is based on the allocation of time and frequency domain resources with 1 ms and Thus there are no fixed resources for the devices, and without prior signaling from the eNodeB (Base Station) only random access resources may be used. For this purpose the device needs to provide information for the UL scheduler of the transmission requirements (buffer status) it has as well as on the available transmission power resources.

## References

- [1].3GPP TR 21.905: "Vocabulary for 3GPP Specifications".
- [2].3GPP TS 36.201: "Evolved Universal Terrestrial Radio Access (E-UTRA): Physical Layer – General Description".
- [3]. B. Classon, K. Baum V. Nangia, R. Love, Y. Sun, R. Nory, K. Stewart, A. Ghosh, R. Ratasuk, X. Weimin, and J. Tan, "Overview of UMTS Air-Interface Evolution," 64th IEEE Vehicular Technology Conference, Montréal, Sept. 2006.
- [4].3GPP TS 36.213: "Evolved Universal Terrestrial Radio Access (E-UTRA): Physical layer procedures".
- [5].3GPP TS 36.214: "Evolved Universal Terrestrial Radio Access (E-UTRA): Physical layer – Measurements".
- [6]. T. Fukuhara, Y. Hao, Y. Takeuchi, and H. Kobayashi, "A novel channel estimation method for OFDM transmission technique under fast time-variant fading channel," 57th IEEE Vehicular Technology Conference, Jeju, Apr. 2003.
- [7]. Y. Kang, K. Kim and H. Park, "Efficient DFT-based channel estimation for OFDM systems on multipath channels," IEEE ITE Commun, vol. 1, Issue 2, pp. 197-202, April 2007.

[8] J.-J. van de Beek, O. Edfors, M. Sandell, S. K. Wilson, and P.O. Börjesson, "On channel estimation in OFDM systems," in Proc. 45th IEEE Vehicular Technology Conf., Chicago, pp. 815-819, July 1995.



## 2 | Radio Channel Propagation

This chapter focuses on the characteristics of the mobile radio channel, in the application of wireless communications, the signal propagates over a hostile radio channel, which leads to signal fading and distortion. Moreover, the received signal is corrupted by thermal noise generated at the receiver, which is usually modeled as additive white Gaussian noise (AWGN). Hence, when simulating the physical layer performance of a wireless communication system, channel distortion and thermal noise are often used as the primary sources of performance degradation.

### 2.1 Radio Channel Propagation

There are two types of mobile channel fading effects: large-scale and small-scale fading. Large-scale fading represents the average signal power attenuation due to motion over a large geographical area. Small-scale fading refers to the dynamic changes of signal amplitude and phase due to a small change of the antenna displacement and orientation, which is as small as a half-wavelength [1]. In a mobile radio channel, the received signal experiences both large-scale fading and small scale fading.

#### 2.1.1 Large-Scale Fading

The simplest model for large-scale fading is to assume the radio channel propagation takes place over an ideal free space (i.e., no objects that might absorb or reflect the radio frequency (RF) energy in the region between the transmit and receive antennas). In the idealized free space model the signal attenuation as a function of the distance between the transmit and receive antennas follows an inverse-square law. Let  $P_T$  and  $P_R(d)$  denote the transmit and received signal power respectively, where  $d$  denotes the distance between the transmit and receive antennas in meters. When the antennas are isotropic, the signal attenuation (or free space path loss) is given by [1]

$$L_o(d) = \frac{P_T}{P_R(d)} = \left(\frac{4\pi d}{\lambda}\right)^2 = \left(\frac{4\pi d f_c}{c}\right)^2 \quad (2.1)$$

where  $\lambda = \frac{c}{f_c}$  is the wavelength of the propagating signal,  $f_c$  is the carrier frequency in Hz and  $c = 3 * 10^8 \frac{m}{s}$  is the speed of light.

Suppose the transmit power is  $P_T = 1mW$  (i.e., 0dBm). Based on the free space path loss model in Equation (2.1), the received signal power as a function of distance and carrier frequency is shown in Figure 2.1. It is shown that the received signal power decreases as the distance between the transmit and receive antennas increases. Moreover, the use of a higher carrier frequency gives a larger signal attenuation. Given the received signal power threshold of  $-90dBm$ , a carrier frequency of 800MHz allows the spatial separation of the transmit and receive antennas up to 1km, while a carrier frequency of

5GHz can only support the spatial separation of 150m. Hence, a low carrier frequency is desirable for long-range wireless communication systems. For short-range wireless communication systems, a high carrier frequency can be used. Since the wireless channel does not behave as a perfect medium and there

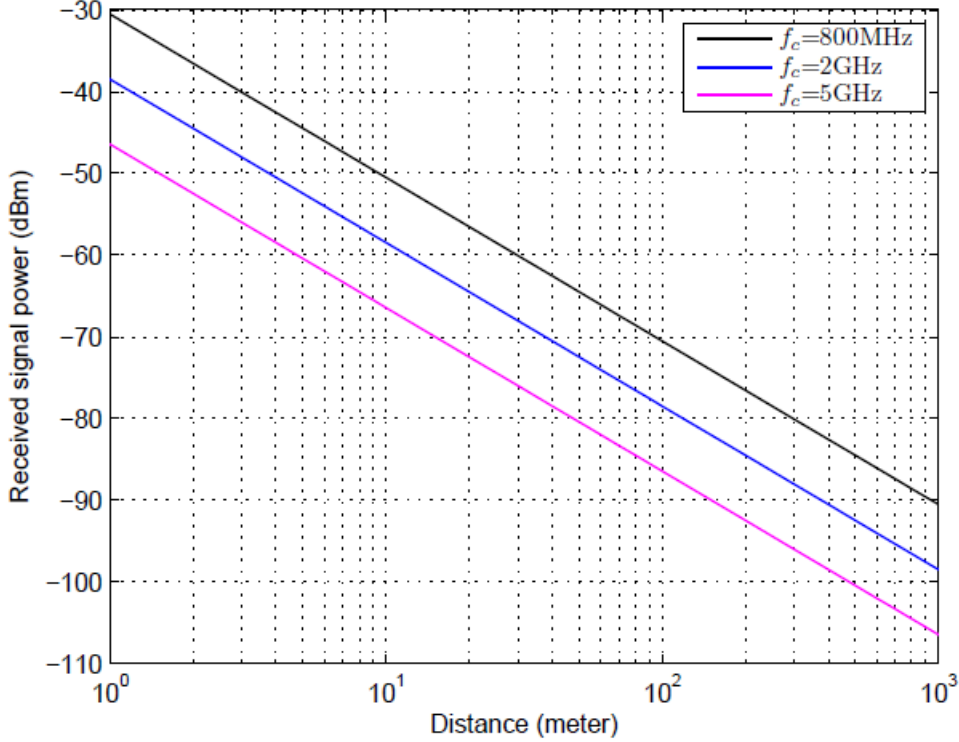


Figure 2.1: Received signal power as a function of antenna displacement based on a free space path loss model. The transmit signal power is 1mW (i.e. 0dBm)

are normally obstacles (e.g. hills, buildings, tree, etc.) in the region of signal propagation, the free space path loss model does not reflect the practical large-scale fading scenario. For mobile radio applications, the mean path loss as a function of distance between the transmitter and the receiver can be modeled as [2]

$$\bar{L}_s \propto \left(\frac{d}{d_o}\right)^n \quad (2.2)$$

where  $n$  denotes the path loss exponent and  $d_o$  denotes a reference distance. The above mean path loss model is often expressed in terms of dB, i.e.,

$$\bar{L}_s(dB) = L_o(d_o)(dB) + 10 * n * \log_{10}\left(\frac{d}{d_o}\right) \quad (2.3)$$

In the above mean path loss model, the reference distance  $d_o$  corresponds to a point located in the far field of the transmit antenna. The typical values of  $d_o$  are 1km for large cells, 100m for microcells and 1m for picocells [1]. The path loss  $L_o(d_o)$  at the reference distance  $d_o$  can be found using measured results [1]. The value of the path loss exponent depends on the carrier frequency, antenna height and propagation environment. In ideal free space,  $n = 2$  since the signal attenuation as a function of distance follows the inverse-square law. In the urban microcell,  $n > 2$  due to the presence of dense obstructions such as buildings [3].

The mean path loss model in Equations(2.3) is an average of the path loss at different sites for a given

distance between the transmitter and the receiver. For different sites, there is a variation about the mean path loss. When there are less obstacles between the transmitter and receiver, the path loss at this site is smaller than the mean path loss. However, for the same distance with the receiver located at a different site, the propagation paths may be blocked by tall buildings and the path loss at this site is higher than the mean. The measurement results in [4] show that the path loss  $L_S(d)$  can be modeled as a log-normal distributed random variable with a mean of  $\bar{L}_S$  in Equation(2.3). Therefore, the path loss model for large-scale fading can be described as [2]

$$\begin{aligned}\bar{L}_s(d)(dB) &= \bar{L}_s + X_v(dB) \\ &= L_o(d_o)(dB) + 10 * n * \log_{10}\left(\frac{d}{d_o}\right) + X_v(dB)\end{aligned}\quad (2.4)$$

where  $X_v$  denotes a zero-mean Gaussian random variable with a standard deviation of  $v$  (the values of  $X_v$  and  $v$  are both in dB). Since  $X_v$  has a normal distribution in a log scale,  $X_v$  is often stated as log-normal fading [5]. The value of the standard deviation  $v$  can be found from measurement results. The value of the standard deviation  $v$  can be found from measurement results. The typical value of  $v$  is 6-10dB or greater [2, 3]. For the path loss model used in the 3GPP spatial channel model (SCM),  $v = 10$ dB in the urban micro scenario [6]. Note that the log-normal fading is part of large-scale fading since its variation occurs at different sites or the change over a large geographical area.

### 2.1.2 Small-Scale Fading

Small-scale fading leads to dynamic changes in signal amplitude and phase, which is caused by a small change of antenna displacement (as small as a half-wavelength). This section describes the statistics and two mechanisms of small-scale fading.

#### Rayleigh Fading and Rician Fading

In a wireless channel, a signal can travel from the transmitter to the receiver through multiple reflective rays [1]. When multiple reflective rays arrive at the receiver simultaneously, they become unresolvable and the receiver sees it as a single path. Each arrived ray experiences a different level of signal attenuation and phase shift due to the characteristics of the wireless channel. When the arrived rays combine constructively, the received signal envelope (or amplitude) is high. When the arrived rays combine destructively, the received signal envelope is low. Hence, multiple simultaneous arrived rays cause a variation in the received signal envelope, which is referred to as multipath fading [1].

#### Rayleigh Fading

Suppose there is no dominant arriving ray, e.g. a non light-of-sight (NLoS) scenario. Assuming the arriving rays are large in number and statistically independently and identically distributed (i.i.d.). According to the central-limit theorem, the path (i.e. the sum of the arrived rays) seen by the receiver can be modeled as a Gaussian distributed random variable [7]. Hence, the received signal envelope (denoted as  $r$ ) has a Rayleigh probability density function (PDF) [7], i.e.

$$\begin{aligned}p(r) &= \frac{r}{\sigma^2} e^{-\frac{r^2}{2\sigma^2}}, & r \geq 0 \\ &= 0, & r < 0\end{aligned}\quad (2.5)$$

where  $2\sigma^2$  is the pre-detection mean power of the NLoS multipath signal. In the NLoS Rayleigh fading case,  $2\sigma^2 = E[r^2]$ . When the received signal envelope due to small-scale fading follows a Rayleigh distribution, such a wireless channel is referred to as a Rayleigh fading channel.

It is useful to derive the cumulative distribution function (CDF) of the received signal power in a Rayleigh fading channel, since it can provide information on the dynamic range of the received signal power variation. The CDF of the received signal power can be defined as the probability of the received signal power (denoted as  $r^2$ ) being smaller than a reference received signal power (denoted as  $r_o^2$ ). In a Rayleigh fading channel, the CDF of the received signal power is described by the CDF of a central chi-square distribution [7], i.e.

$$F(r_o^2) = \text{pr}(r^2 > r_o^2) = 1 - e^{-\frac{r_o^2}{2\sigma^2}}, \quad r, r_o \geq 0 \quad (2.6)$$

### Rician Fading

In a Rayleigh fading channel, there is no dominant arrived ray. However, when there is a dominant ray (e.g. a light-of-sight (LoS) scenario), the received signal envelope has a Rician PDF [5], i.e.

$$\begin{aligned} p(r) &= \frac{r}{\sigma^2} e^{-\frac{r^2+A^2}{2\sigma^2}} I_0\left(\frac{rA}{\sigma^2}\right), & r \geq 0 \\ &= 0, & r < 0 \end{aligned} \quad (2.7)$$

where  $A^2$  is the pre-detection received signal power from the dominant ray,  $2\sigma^2$  is the pre-detection mean power of the NLoS multipath signal, and  $I_0(\cdot)$  is the zero-th order modified Bessel function of the first kind. When a dominant ray exists, the received signal envelope follows a Rician PDF and such a wireless channel is referred to as a Rician fading channel. Note that when the dominant ray disappears (i.e.  $A = 0$ ), Equation(2.7) reduces to a Rayleigh PDF as shown in Equation (2.5).

In the literature, a Rician fading channel is often described in terms of its K-factor. The K-factor is defined as the ratio of the power of the dominant component to the power of the remaining random components (often expressed in dB) [5], i.e.

$$K = 10 * \log_{10}\left(\frac{A^2}{2\sigma^2}\right) \quad (2.8)$$

In the above equation, when  $A = 0$ ,  $K = -\infty$  dB corresponds to a Rayleigh fading channel. Due to the existence of the dominant component, the CDF of the received signal power in a Rician fading channel is described by the CDF of a non-central chi-square distribution [7], i.e.

$$F(r_o^2) = \text{pr}(r^2 > r_o^2) = 1 - Q_1\left(\frac{A}{\sigma}, \frac{r_o}{\sigma}\right), \quad r, r_o \geq 0 \quad (2.9)$$

Where  $Q_1(a, b)$  denotes the Marcum Q-function.

### Delay-Dispersive Channel

There are two mechanisms for small-scale fading. One of these is signal dispersion in the time-delay domain, which results in a frequency-selective channel. The other one is the time variation of a mobile channel, which results in a time-selective channel. In this section, the signal dispersion mechanism is



described. In the previous section, a single multipath signal was used to describe Rayleigh fading and Rician fading. However, there may be clusters of rays that arrive at the receiver with different time delays due to different propagation distances. When the relative time delay between the arrived clusters exceeds a symbol period, there is more than one resolvable path seen by the receiver. In other words, the received signal becomes dispersive in the time-delay domain.

Fig. 2.2(a) shows the impulse response for a delay-dispersive channel, where the symbol period is  $0.2\mu s$  and an 8-tap i.i.d. complex Gaussian channel is assumed. For an 8-tap i.i.d. complex Gaussian channel, there are 8 resolvable paths seen by the receiver. Each path is modeled as an i.i.d. complex Gaussian random variable and thus experiences Rayleigh fading individually. Since a wireless channel can be viewed as a linear filter to the transmit signal, the received signal is the convolution of the transmit signal and channel impulse response. Hence, a delay-dispersive channel introduces ISI into the received signal. Note that the ISI can lead to an irreducible error floor in the system performance, unless equalization is employed at the receiver to mitigate the ISI.

When converting a one-tap channel into the frequency domain, its frequency domain channel response is flat. Such a channel is called a flat fading channel. However, for a delay-dispersive channel, as shown in Fig. 2.2(a), its frequency domain channel response becomes selective as shown in Fig. 2.2(b) (where the carrier frequency is 2GHz and the signal bandwidth is 5MHz). Such a channel is called a frequency-selective fading channel. Note that a frequency-selective fading channel is a dual to a delay-dispersive channel [1] when viewing the signal distortion in the frequency domain.

The frequency selectivity of a wireless channel can be characterized by its coherence bandwidth. The

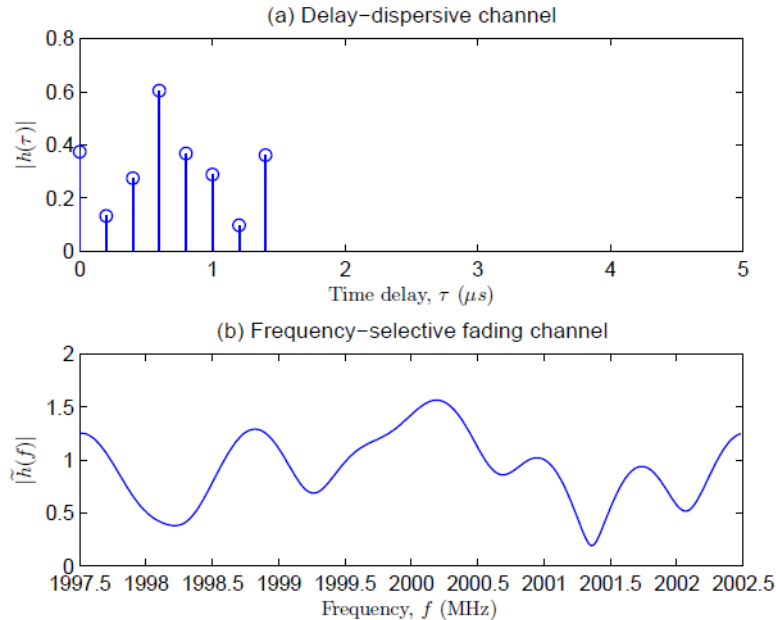


Figure 2.2:(a) Delay-dispersive channel (an 8-tap i.i.d. complex Gaussian channel). (b) Corresponding frequency-selective fading channel.

coherence bandwidth (denoted as  $f_o$ ) is a statistical measure of the range of frequencies over which the channel has approximately equal gain and linear phase [1]. Let  $r_l^2$  denote the average power of the  $l$  –  $th$  channel tap at a time delay of  $\tau_l$ . The mean excess delay (which represents the time for half the channel

power to arrive) is defined as [2]

$$\bar{\tau} = \frac{\sum_l r_l^2 \tau_l}{\sum_l r_l^2} \quad (2.10)$$

and the root mean square (RMS) delay spread is defined as [2]

$$\bar{\tau}_{RMS} = \frac{\sum_l r_l^2 (\tau_l - \bar{\tau})^2}{\sum_l r_l^2} \quad (2.11)$$

As a rule of thumb, a popular approximation of the coherence bandwidth with a correlation of at least 0.5 is given by [2]

$$f_o \approx \frac{1}{5\bar{\tau}_{RMS}} \quad (2.12)$$

When the transmit signal bandwidth is small compared to the coherence bandwidth (i.e. the symbol period is long compared to the channel delay spread), the received signal experiences a flat fading channel (i.e. an one-tap channel). In this case, channel- induced ISI does not occur. However, when this channel tap is faded, the system suffers from performance degradation due to low received signal-to-noise ratio (SNR). When the transmit signal bandwidth is larger than the coherence bandwidth (i.e. the symbol period is shorter than the channel delay spread), the received signal experiences a frequency-selective fading channel (i.e. a delay-dispersive channel). In this case, equalization is required at the receiver to mitigate the ISI. Since the probability of all the channel taps being in fades at the same time is very low, there is less fluctuation in the received SNR compared to a flat fading channel.

### Time-Varying Channel

A relative motion (as small as a half-wavelength) between the transmitter and the receiver can cause a significant fluctuation in the received signal power. In this section, the popular Jakes model [8] is used to describe the time variation mechanism of a mobile channel due to small-scale fading. In the Jakes model, it is assumed that the receiver is traveling at a constant velocity of  $vm/s$ , and  $N$  equal-strength rays arrive at the receiver simultaneously (that constitutes a single resolvable fading path). Jakes further assumes that the azimuth arrival angles of the rays (denoted as  $\alpha_n$ ) at the receiver are uniformly distributed from 0 to  $2\pi$  i.e.,

$$\alpha_n = \frac{2\pi n}{N}, \quad n = 0, 1, \dots, N-1 \quad (2.13)$$

Let  $\phi_n$  denote a random initial phase of the  $n$ -th ray. Assuming the mean channel power is normalized to 1 i.e.,  $E[|h(t)|^2] = 1$  the channel response at a time instant  $t$  is given by [8]

$$h(t) = \frac{1}{\sqrt{2N}} \sum_{n=0}^{N-1} \cos(2\pi f_d(\cos\alpha_n)t + \phi_n) + j \frac{1}{\sqrt{2N}} \sum_{n=0}^{N-1} \sin(2\pi f_d(\cos\alpha_n)t + \phi_n) \quad (2.14)$$

where  $f_d = \frac{v}{\lambda}$  is the maximum Doppler frequency and  $\lambda$  is the propagation wavelength in meters. Note that when  $N$  is large, according to the central-limit theorem,  $h(t)$  is well-approximated as a Gaussian random variable and thus leads to a flat Rayleigh fading channel.

Since the relative motion between the transmitter and the receiver (i.e., the distance traveled by the

receiver) is given by  $\Delta d = vt$ , the channel response  $h(t)$  in Equation (2.14) can be written as a function of  $\Delta d$ , i.e.

$$h(\Delta d) = \frac{1}{\sqrt{2N}} \sum_{n=0}^{N-1} \cos\left(\frac{2\pi\Delta d}{\lambda}(\cos\alpha_n) + \phi_n\right) + j \frac{1}{\sqrt{2N}} \sum_{n=0}^{N-1} \sin\left(\frac{2\pi\Delta d}{\lambda}(\cos\alpha_n) + \phi_n\right) \quad (2.15)$$

When the carrier frequency is  $f_c = 2\text{GHz}$  and  $\lambda = \frac{c}{f_c} = 0.15\text{m}$ , the coherence distance of the channel is small and the channel response can change dramatically with antenna displacements of just a few centimeters. This coherence distance can be translated to the coherence time via the traveling speed of the receiver. When the receiver is traveling at a high speed, the coherence time of the channel becomes shorter, which leads to a fast time-varying channel (or time-selective fading channel).

Let  $\Delta t$  a time difference the space-time correlation function of the Jakes model in Equation (2.14) is given by [9]

$$R(\Delta t) = E\left[h^*(t)h(t + \Delta t)\right] = J_0(2\pi f_d \Delta t) \quad (2.16)$$

where  $J_0(\cdot)$  denotes the zeroth order Bessel function of the first kind. It is shown in [10] that the coherence time of a mobile channel over which the channel response to a sinusoid has a correlation greater than 0.5 is approximately

$$T_o \approx \frac{9}{16\pi f_d} \quad (2.17)$$

For a FDE system, such as orthogonal frequency division multiplexing (OFDM) and single-carrier frequency domain equalization (SC-FDE), it is assumed that the channel response remains highly correlated during a symbol period (or a transmission block period). Otherwise, inter-carrier interference (ICI) occurs due to Doppler spectral broadening [2]. In the LTE standard, the symbol period is  $T_s = 66.67\mu s$ . In a high-speed train scenario with  $v = 350\text{km/hr}$ , the Doppler frequency is  $f_d = \frac{vf_c}{c} = 648\text{Hz}$  when the carrier frequency is  $f_c = 2\text{GHz}$ . Based on Equation(2.17), the channel coherence time  $T_o \approx 276\mu s$  is still long compared to the symbol period i.e.  $T_s = 66.67\mu s$ . Hence, the Doppler spectral broadening effect may not cause severe performance degradation in this high-mobility scenario.

## References

- [1] B. Sklar, "Rayleigh fading channels in mobile communication systems part I: characterization," IEEE Wireless Commun. Mag., vol. 35, no. 7, pp. 90–100, Jul.1997.
- [2] T. Rappaport, Wireless Communications. Upper Saddle River, New Jersey: Prentice Hall, 1996.
- [3] S. Seidel, T. Rappaport, S. Jain, M. Lord, and R. Singh, "Path loss, scatter- ing and multipath delay statistics in four european cities for digital cellular and microcellular radiotelephone," IEEE Trans. Veh. Technol., vol. 40, no. 4, pp. 721–730, Nov. 1991.
- [4] D. Cox, R. Murray, and A. Norris, "800-MHz attenuation measured in and around suburban houses," Bell Lab. Tech. J., vol. 63, no. 6, pp. 921–954, Jul.-Aug. 1984.
- [5] J. Parsons, The Mobile Radio Propagation Channel, 2nd ed. England: John Wiley and Sons, 2000.

- [6] D. Baum, J. Hansen, J. Salo, G. Galdo, M. Milojevic, and P. Kyosti, "An interim channel model for beyond-3G systems: extending the 3GPP spatial channel model (SCM)," in Proc. IEEE Vehicular Technology Conference (VTC'05- Spring), vol. 5, May 2005, pp. 3132–3136.
- [7] J. Proakis, Digital Communications, 4th ed. New York: McGraw-Hill, 2001.
- [8] W. Jakes, Microwave Mobile Communications. New York: John Wiley and Sons, 1974.
- [10] R. Steele and L. Hanzo, Mobile Radio Communications, 2nd ed. England: John Wiley and Sons, 1999.

## 3 | 3GPP Specifications

This chapter focuses on the Long Term Evolution(LTE) parameters for transmitter section which includes definitions and symbols, different form of Frame Structures, Slot Structures and Physical Resources for the UL.

### 3.1 Definitions and Symbols

Definitions and Symbols	
$(k, l)$	Resource element with frequency-domain index $k$ and time-domain index $l$ .
$f_o$	Carrier frequency.
$M_{SC}^{PUSCH}$	Scheduled bandwidth for uplink transmission, expressed as a number of subcarriers
$M_{RB}^{PUSCH}$	Scheduled bandwidth for uplink transmission, expressed as a number of Resource Blocks
$N$	A constant equal to 2048 for $\Delta f = 15\text{kHz}$ and 4096 for $\Delta f = 7.5\text{kHz}$ .
$N_{CS}$	Cyclic Shift value used for random access preamble generation.
$N_{CS}^{(1)}$	Number of cyclic shifts used for PUCCH formats 1/1a/1b in a resource block with a mix of formats 1/1a/1b and 2/2a/2b.
$N_{ID}^{cell}$	Physical layer cell identity.
$N_{RB}^{UL}$	Uplink bandwidth configuration, expressed in multiples of $N_{SC}^{RB}$ .
$N_{RB}^{min,UL}$	Smallest uplink bandwidth configuration, expressed in multiples of $N_{SC}^{RB}$ .
$N_{RB}^{max,UL}$	Maximum uplink bandwidth configuration, expressed in multiples of $N_{SC}^{RB}$ .
$N_{SC}^{RB}$	Resource block size in the frequency domain, expressed as a number of subcarriers.
$N_{PUCCH}^{RS}$	Number of reference symbols per slot for PUCCH.
$N_{symb}^{UL}$	Number of SC-FDMA symbols in an uplink slot.
$n_{PUCCH}^{(1)}$	Resource index for PUCCH formats 1/1a/1b.
$n_{PUCCH}^{(2)}$	Resource index for PUCCH formats 2/2a/2b.
$\eta_{PRB}$	Physical resource block number.
$\eta_{VRB}$	Virtual resource block number.
$n_{RNTI}$	Radio network temporary identifier.
$n_f$	System frame number.
$n_s$	Slot number within a radio frame.
$\Delta f$	Subcarrier spacing.
$T_f$	Radio frame duration.
$T_s$	Basic time unit.
$T_{slot}$	Slot duration.

Definitions and Symbols	
$Q_m$	Modulation order: 2 for QPSK, 4 for 16QAM and 6 for 64QAM transmissions.
$N_{RB}^{(2)}$	Bandwidth available for use by PUCCH formats 2/2a/2b, expressed in multiples of $N_{SC}^{RB}$ .
$N_{RB}^{HO}$	The offset used for PUSCH frequency hopping, expressed in number of resource blocks (set by higher layers).
$\beta_{PUSCH}$	Amplitude scaling for PUSCH.
$\beta_{PUSCH}$	Amplitude scaling for PUSCH.
$\beta_{PUCCH}$	Amplitude scaling for PUCCH.

### 3.2 Abbreviations

Abbreviations	
<b>3GPP</b>	Third Generation Partnership Project.
<b>4G</b>	Fourth Generation.
<b>CCE</b>	Control Channel Element.
<b>CDD</b>	Cyclic Delay Diversity.
<b>PBCH</b>	Physical Broadcast Channel.
<b>PCFICH</b>	Physical Control Format Indicator Channel.
<b>PDCCH</b>	Physical Downlink Control Channel.
<b>PDSCH</b>	Physical Downlink Shared Channel.
<b>PHICH</b>	Physical Hybrid-ARQ Indicator Channel.
<b>PMCH</b>	Physical Multicast Channel.
<b>PRACH</b>	Physical Random Access Channel.
<b>PUCCH</b>	Physical Uplink Control Channel.
<b>PUSCH</b>	Physical Uplink Shared Channel.
<b>eNodeB or BS</b>	Base Station.
<b>UE</b>	User Equipment or Mobile terminal.

### 3.3 Frame Structure

In LTE specifications, the size of elements in the time domain is expressed as a number of time units  $T_s = \frac{1}{15000 \cdot 2048}$  seconds. As the normal subcarrier spacing is defined to be  $\Delta f = 15kHz$ ,  $T_s$  can be regarded as the sampling time of an FFT-based OFDM transmitter/receiver implementation with FFT size  $N_{FFT} = 2048$ . Different FFT sizes are supported depending on the transmissions bandwidths. The set of parameters shown in the Table 3.1. In the time domain, the downlink and uplink multiple **Transmission Time Interval (TTI)**s are organized into radio frames with duration  $T_f = 307200 \cdot T_s = 10ms$ . For flexibility, LTE supports both Frequency Division Duplexing(FDD) and Time Division Duplexing (TDD) modes. Most of the design parameters are common to FDD and TDD in order to reduce the terminal complexity and maximize reuse between the designs of FDD and TDD systems. Accordingly, LTE supports two kinds of frame structures:

- Frame Structure Type 1: Used for the **LTE FDD** mode systems
- Frame Structure Type 2: Used for the **LTE TDD** mode systems

Transmission bandwidth [MHz]	1.4	3	5	10	15	20
Occupied bandwidth [MHz]	1.08	2.7	4.5	9.0	13.5	18.0
Guardband [MHz]	0.32	0.3	0.5	1.0	1.5	2.0
Guardband, % of total	23	10	10	10	10	10
Sampling frequency [MHz]	1.92 $1/2 \times 3.84$	3.84	7.68 $2 \times 3.84$	15.36 $4 \times 3.84$	23.04 $6 \times 3.84$	30.72 $8 \times 3.84$
FFT size	128	256	512	1024	1536	2048
Number of occupied subcarriers	72	180	300	600	900	1200
Number of resource blocks	6	15	25	50	75	100
Number of CP samples (normal)	$9 \times 6$ $10 \times 1$	$18 \times 6$ $20 \times 1$	$36 \times 6$ $40 \times 1$	$72 \times 6$ $80 \times 1$	$108 \times 6$ $120 \times 1$	$144 \times 6$ $160 \times 1$
Number of CP samples (extended)	32	64	128	256	384	512

Table 3.1: Typical Parameters

### 3.3.1 Frame Structure Type 1

Frame structure type 1 is applicable to both full duplex and half duplex FDD. There are three different kinds of units specified for this frame structure, illustrated in Figure 3.1. The smallest one is called a **Slot**, which is of length  $T_{slot} = 15360.T_s = 0.5ms$ . Two consecutive slots are defined as a **Subframe** of length 1 ms, and 20 slots, numbered from 0 to 19, constitute a **Radio Frame** of 10 ms. Channel dependent scheduling and link adaptation operate on a subframe level. Therefore, the subframe duration corresponds to the minimum uplink/downlink TTI, which is 1ms duration. Each slot consists of a number

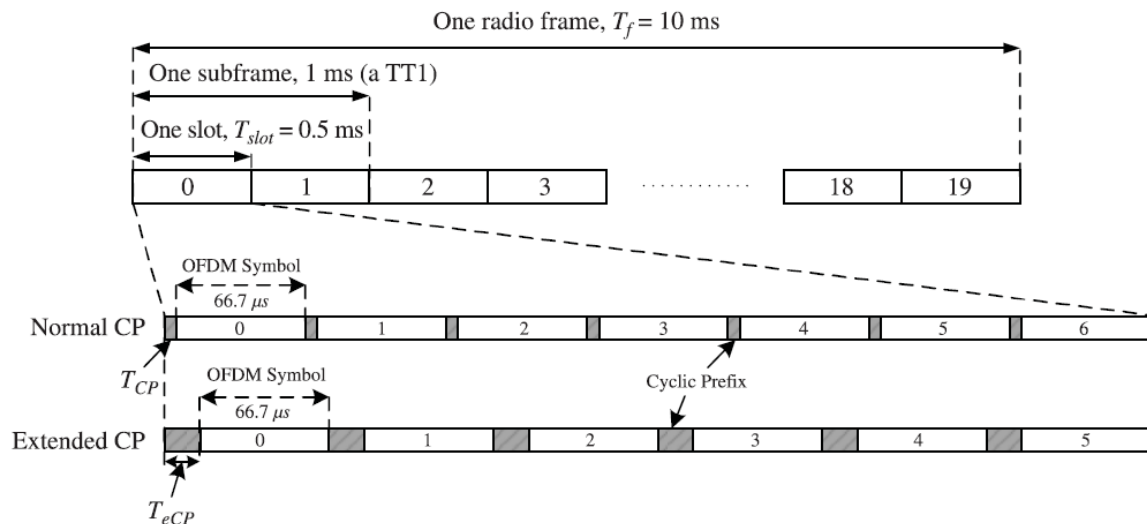


Figure 3.1: FDD Frame Structure

of OFDM/SCFDMA symbols including **Cyclic Prefix (CP)**. CP is a kind of guard interval to combat inter-OFDM-symbol interference, which should be larger than the channel delay spread. Therefore, the length of CP depends on the environment where the network operates, and it should not be too large as it

brings a bandwidth and power penalty. With a subcarrier spacing  $\Delta f = 15kHz$ , the OFDM/SCFDMA symbol time is approximately  $66.7\mu s$ . LTE defines two different CP lengths: a **Normal CP** and an **Extended CP**, corresponding to seven and six OFDM/SCFDMA symbols per slot, respectively.

For FDD, uplink and downlink transmissions are separated in the frequency domain, each with 10 subframes. In half-duplex FDD operation, the UE cannot transmit and receive at the same time while there are no such restrictions in full-duplex FDD.

### 3.3.2 Frame Structure Type 2

Frame structure Type 2 is applicable to TDD mode. Each radio frame of length  $T_f = 307200.T_s = 10ms$ , which consists of two half frames of length  $153600.T_s = 5ms$  each. Each half frame consists of five subframes of length  $1ms$ . There are special subframes, which consists of three fields: Downlink Pilot Time Slot (DwPTS), Guard Period (GP), and Uplink Pilot Time Slot (UpPTS). The TDD Frame structure is Shown in the Figure 2.2

- **The DwPTS field :** This is the downlink part of the special subframe, and can be regarded as ordinary but shorter downlink subframe for downlink data transmission. Its length can be varied from three up to twelve OFDM symbols.
- **The UpPTS field :** This is the uplink part of the special subframe, and has a short duration with one or two SCFDMA symbols. It can be used for transmission of uplink sounding reference signals and random access preambles.
- **The GP field :** The remaining symbols in the special subframe that have not been allocated to DwPTS or UpPTS are allocated to the GP field, which is used to provide the guard period for the DL to UL and UL to DL switch.

The total length of these three special fields has a constraint of  $1ms$ . With the DwPTS and UpPTS duration mentioned above, LTE supports a guard period ranging from two to ten OFDM symbols, sufficient for cell size up to and beyond 100 km. All other subframes are defined as two slots, each with length  $T_{slot} = 0.5ms$ . The Figure 3.2 shows the TDD Frame Structure.

This frame structure depends on the uplink-downlink configuration. Seven uplink-downlink configurations with either 5 ms or 10 ms DL to UL switch point periodicity are supported, as illustrated in Table 3.2. Where "D" and "U" denote subframe reserved for downlink and uplink, respectively, and "S" denote the special subframe. In case of 5 ms switch-point periodicity, the special subframe exists in both half-frames, in case of 10 ms switch-point periodicity, the special subframe exists in the first half-frame only. Subframes 0,5 and the field DwPTS are always reserved for downlink transmission, while UpPTS and the subframe immediately the special subframe are always reserved for uplink transmission.

## 3.4 Slot Structure and Physical Resources for Uplink

### 3.4.1 Resource Grid

The transmitted signal in each slot is described by a resource grid of  $N_{RB}^{UL} \cdot N_{SC}^{RB}$  sub carriers and  $N_{symb}^{UL}$  SC-FDMA symbols. The resource grid is illustrated in Figure 3.3

The quantity  $N_{RB}^{UL}$  depends on the uplink transmission bandwidth configured in the cell and shall fulfill



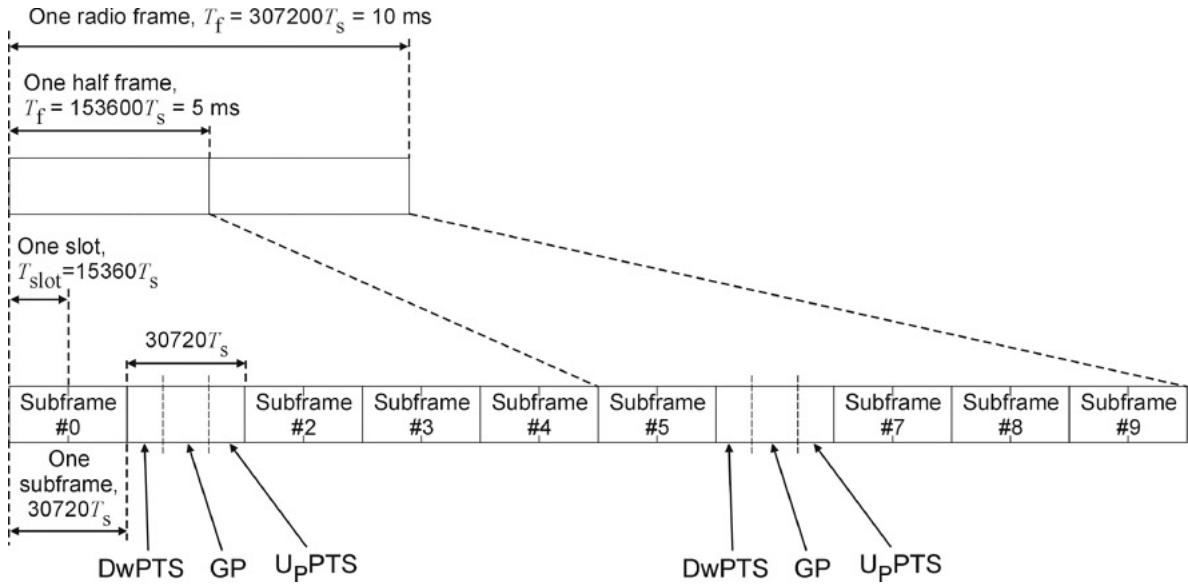


Figure 3.2: TDD Frame Structure

Uplink-Downlink Configuration	Downlink-to-Uplink Switch-Point Periodicity	Subframe Number									
		0	1	2	3	4	5	6	7	8	9
0	5 ms	D	S	U	U	U	D	S	U	U	U
1	5 ms	D	S	U	U	D	D	S	U	U	D
2	5 ms	D	S	U	D	D	D	S	U	D	D
3	10 ms	D	S	U	U	U	D	D	D	D	D
4	10 ms	D	S	U	U	D	D	D	D	D	D
5	10 ms	D	S	U	D	D	D	D	D	D	D
6	5 ms	D	S	U	U	U	D	S	U	U	D

Table 3.2:UL/DL Configuration.

$N_{RB}^{\min,UL} \leq N_{RB}^{UL} \leq N_{RB}^{\max,UL}$ . Where  $N_{RB}^{\min,UL} = 6$  and  $N_{RB}^{\max,UL} = 110$  are the smallest and largest uplink bandwidths respectively. The number of SC-FDMA symbols in a slot depends on the **CP** length configured by the higher layer parameter **UL-Cyclic Pre fix Length** and is given in the following Table .

Configuration	$N_{SC}^{RB}$	$N_{symp}^{UL}$
Normal Cyclic Prefix	12	7
Extended Cyclic Prefix	12	6

### 3.4.2 Resource Elements

Each element in the resource grid is called a resource element and is uniquely defined by the index pair  $(k, l)$  in a slot, where  $k = 0, \dots, N_{RB}^{UL} \cdot N_{SC}^{RB} - 1$  and  $l = 0, \dots, N_{symp}^{UL} - 1$  are the indices in the frequency and time domains, respectively. Resource element  $(k, l)$  corresponds to the complex value  $a_{k,l}$ . Quantities

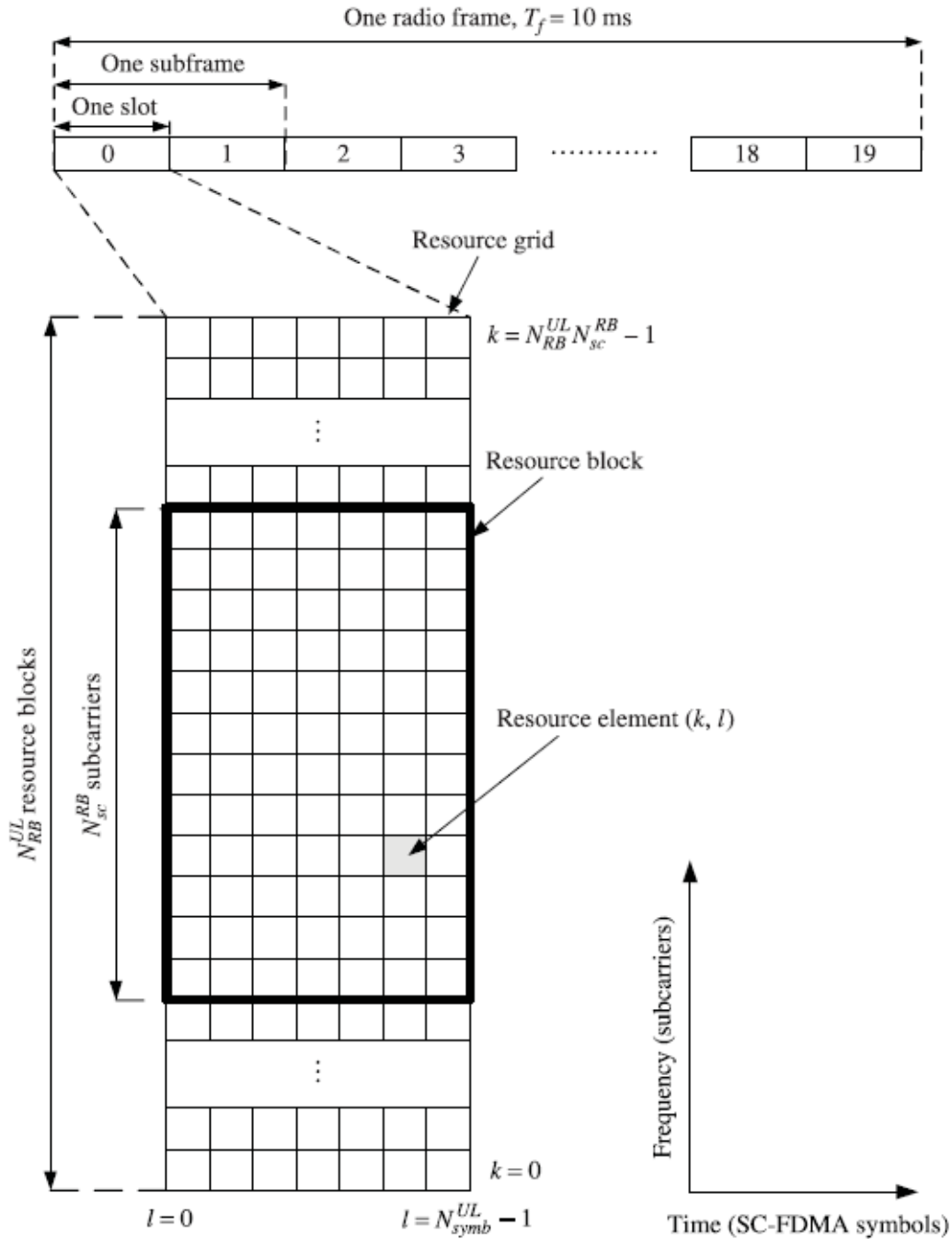


Figure 3.3:Uplink Resource grid

$a_{k,l}$  corresponding to resource elements not used for transmission of a physical channel or a physical signal in a slot shall be set to zero.

### 3.4.3 Resource Blocks

A physical resource block is defined as  $N_{\text{symb}}^{\text{UL}}$  consecutive SC-FDMA symbols in the time domain and  $N_{\text{SC}}^{\text{RB}}$  consecutive subcarriers in the frequency domain, where  $N_{\text{symb}}^{\text{UL}}$  and  $N_{\text{SC}}^{\text{RB}}$  given in the above table. A physical resource block in the uplink thus consists of  $N_{\text{symb}}^{\text{UL}} \cdot N_{\text{SC}}^{\text{RB}}$  elements, corresponding to one slot in the time domain and 180 kHz in the frequency domain.

The relation between the physical resource block number  $n_{PRB}$  in the frequency domain and resource elements  $(k, l)$  in a slot is given by

$$\eta_{PRB} = \left\lfloor \frac{k}{N_{SC}^{RB}} \right\rfloor \quad (3.1)$$

### 3.5 Simulation Parameters

For the baseband system simulation we assume that the some of the default parameters for the **PUSCH** as given below

Simulation Parameters	
Bandwidth of the System (BW)	20MHz,10MHz,5MHz
Size of the FFT and IFFT (N)	2048,1024,512
$n_{RNTI}$	8 , vary between 0 to 65535
CellID	79 , vary between 0 to 503.
$N_{SC}^{RB}$	12
$N_{symp}^{UL}$	7
Cyclic Prefix	Normal
$\Delta f$	15 KHz
$N_c$	1600, Used to generate the pseudo random sequence
Wide band Configuration	ON
Frame Structure Type	FDD
$RB_{START}$	0, Starting Resource block given by higher layers Range [0 to $N_{UL}^{RB} - 1$ ]
Group Hopping	Disable
Sequence Hopping	Disable
Frequency Hopping	Disable
$T_s$	$\frac{1}{N*\Delta f}$ , Sampling time
$T_{slot}$	15360 * $T_s$ , Slot duration
$T_f$	307200 * $T_s$ , Frame duration
$N_{subframe}$	0, For FDD and TDD vary depend on the UL-DL configuration
$\Delta_{ss}$	0, Configurable portion of the sequence-shift pattern for PUSCH (sib2 groupAssignmentPUSCH)



## 4 | Transmitter Structure of PUSCH

Uplink (UL) Physical Channel Processing involves the transmission of block of bits which are arrived from the channel coder or Rate Matching to the antenna ports. In this section mainly focusing on the transmission of user data bits ie transmitter structure of shared channel ie PUSCH. In addition to that in the receiver section different channel estimations are investigated.

The baseband signal representing the physical uplink shared channel is defined in terms of the operations shown in Figure 4.1a. For comparison, Figure 4.1b duplicates the transmitter portion of a generic SC-FDMA system. LTE specifies two rate 1/3 channel coding techniques: tail-biting convolution coding and

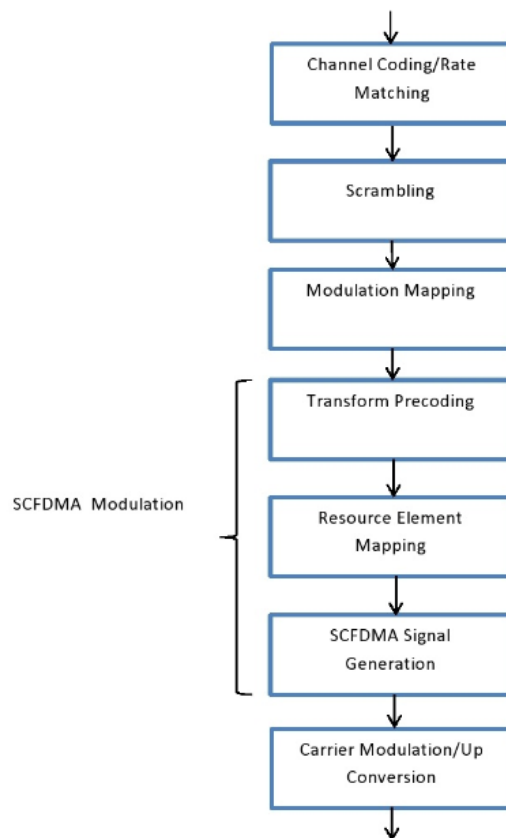


Figure 4.1a: Uplink Physical Channel Processing.

turbo coding [1]. Each coder produces three separate bit streams, corresponding to code rate 1/3. The bit streams are interleaved separately and the interleaved streams are fed to a circular rate matching buffer. The output bits of the circular buffer are scrambled with a length-31 Gold sequence [2]. Depending on channel quality, the PUSCH can use QPSK and 16-QAM modulations. The PUCCH can use BPSK and

QPSK modulations. The output symbols of the modulation mapping operation correspond to the input signal of Figure 4.1a.

Transform precoding corresponds to the DFT operation which is shown in Figure 4.1b. In PUSCH, the size of the DFT-precoding corresponds to the number of scheduled subcarriers used for PUSCH transmission in an SC-FDMA symbol,  $M_{sc}^{PUSCH}$ . The baseband signal representing the PUSCH is defined in terms of

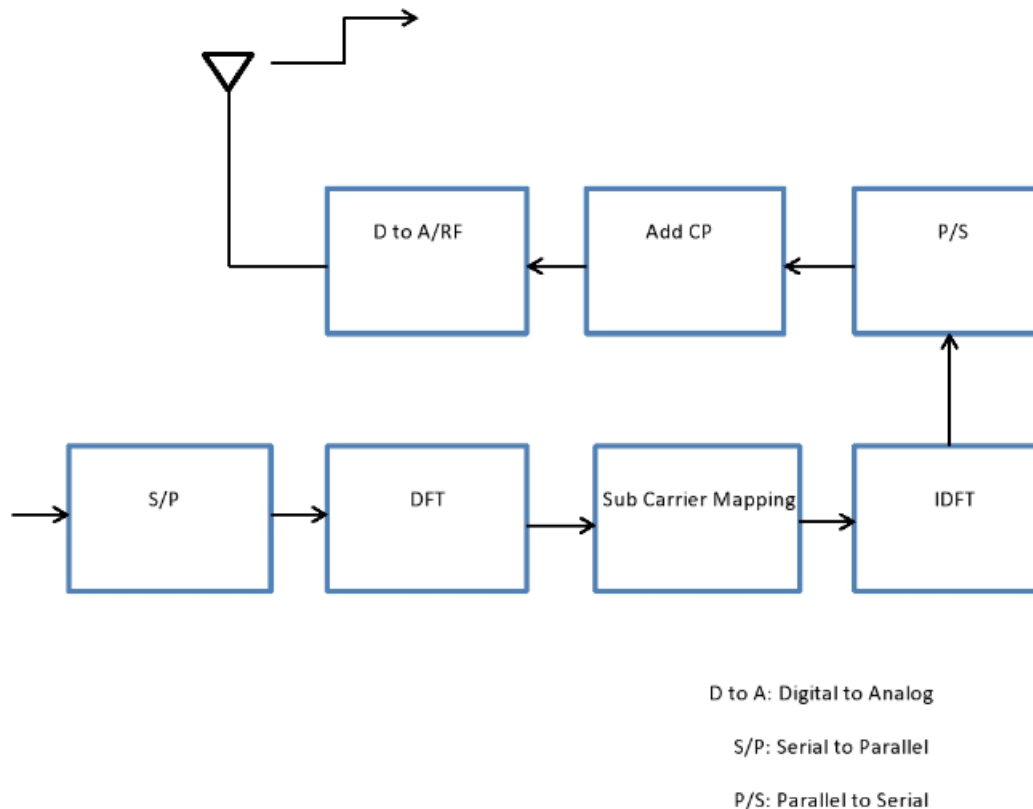


Figure 4.1b : SCFDMA Structure.

the following steps:

- Bit level Scrambling
- Modulation Mapper
- Transform Precoder
- Resource Element Mapping
- SC-FDMA Signal generation

#### 4.1 Bit level Scrambling

LTE UL scrambling implies that the block of bits delivered from channel coding/rate matching is multiplied (exclusive-or operation) by a bit-level scrambling sequence shown in the Figure 4.1c. In general, scrambling of the coded data helps to ensure that the receiver-side decoding can fully utilize the processing

gain provided by the channel code. Without scrambling, the channel decoder at BS could, at least in principle, be equally matched to an interfering signal as to the target signal, thus not being able to properly suppress the interference. By applying different scrambling sequences for different mobile terminals, the interfering signal(s) after de-scrambling are randomized, ensuring full utilization of the processing gain provided by the channel code. The uplink scrambling is mobile-terminal specific, i.e. different mobile terminals use different scrambling sequences. By using a scrambling code eNodeB can separate signals

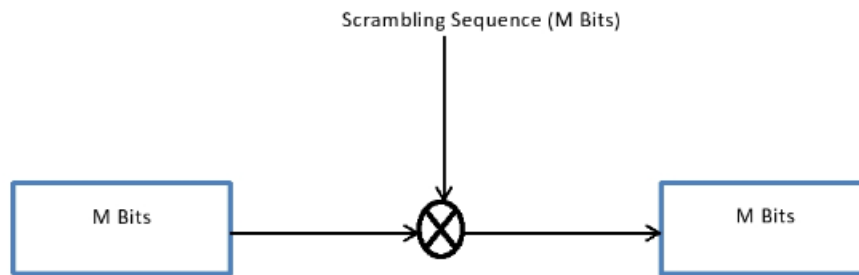


Figure 4.1c : Uplink Scrambling.

coming simultaneously from any different UE's and UE can separate signals coming simultaneously from many different eNodeB's.

The block of bits  $b(0), b(1), \dots, b(M_{bit} - 1)$ , where  $M_{bit}$  is the number of bits transmitted on the physical uplink shared channel in one subframe, shall be scrambled with a UE-specific scrambling sequence prior to modulation, resulting in a block of scrambled bits  $\tilde{b}(0), \tilde{b}(1), \dots, \tilde{b}(M_{bit} - 1)$ .

The Pseudo code is given as

```

Set i=0
while i < Mbit
if b(i) = x      //ACK/NACK or Rank Indication placeholder
 $\tilde{b}(i) = 1$ 
elseif b(i) = y  //ACK/NACK or Rank Indication repetition placeholder bits
 $\tilde{b}(i) = \tilde{b}(i - 1)$ 
else            // Data or channel quality coded bits, Rank Indication coded bits or ACK/NACK coded bits
 $\tilde{b}(i) = (b(i) + c(i)) \bmod 2$ 
endif
endif
i=i+1
endwhile

```

Placeholder bits, denoted by x, are represented by -1 in the input vector or cell array of vectors. Repetition placeholder bits, y, are represented by -2. This function substitutes these placeholders as part of its scrambling operation. x and y also find in [3] section 5.5.5.6.

The scrambling sequence generator shall be initialized with  $c_{init}$  where

$$c_{init} = \eta_{RNTI} \cdot 2^{14} + \lfloor \frac{n_s}{2} \rfloor \cdot 2^9 + N_{ID}^{Cell} \quad (4.1)$$

at the start of each subframe where  $\eta_{RNTI}$  corresponds to the RNTI associated with the PUSCH transmission. Where the scrambling sequence  $c$  is generated by the following way described below

Pseudo-random sequences are defined by a length-31 Gold sequence. The output sequence  $c(n)$  of length  $M_{PN}$ , where  $n=0,1,\dots,M_{PN} - 1$  is defined by

$$c(n) = (x_1(n + N_c) + x_2(n + N_c)) \bmod 2 \quad (4.2)$$

$$x_1(n + 31) = (x_1(n + 3) + x(n)) \bmod 2 \quad (4.3)$$

$$x_2(n + 31) = (x_2(n + 3) + x_2(n + 2) + x_2(n + 1) + x_2(n)) \bmod 2 \quad (4.4)$$

where  $N_c = 1600$  and the first m-sequence shall be initialized with  $x_1(0) = 1, x_1(n) = 0, n = 1, 2, \dots, 30$ . The initialization of the second m-sequence is denoted by  $\sum_{i=0}^{30} x_2(i) \cdot 2^i$  with the value depending on the application of the sequence.

## 4.2 Modulation Mapper

The block of scrambled bits  $\tilde{b}(0), \tilde{b}(1), \dots, \tilde{b}(M_{bit} - 1)$  shall be modulated resulting in a block of complex-valued symbols  $d(0), \dots, d(M_{symp} - 1)$ . The given table specifies the modulation mappings applicable for the physical uplink shared channel.

Physical Channel	Modulation Schemes
PUSCH	QPSK and 16QAM

### 4.2.1 QPSK

In case of QPSK modulation, pairs of bits  $b(i)b(i + 1)$ , are mapped to complex-valued modulation symbols  $x = I + j * Q$ , where I and Q are in phase and Quadrature phase components according to given table

$b(i)b(i + 1)$	I	Q
00	$\frac{1}{\sqrt{2}}$	$\frac{1}{\sqrt{2}}$
01	$\frac{1}{\sqrt{2}}$	$-\frac{1}{\sqrt{2}}$
10	$-\frac{1}{\sqrt{2}}$	$\frac{1}{\sqrt{2}}$
11	$-\frac{1}{\sqrt{2}}$	$-\frac{1}{\sqrt{2}}$

The constellation diagram for QPSK shown in the following Figure 4.2a

### 4.2.2 16QAM

In case of 16-QAM, quadruplets of bits,  $b(i)b(i + 1)b(i + 2)b(i + 3)$ , are mapped to complex-valued modulation symbols  $x=I+j*Q$  according to table given below



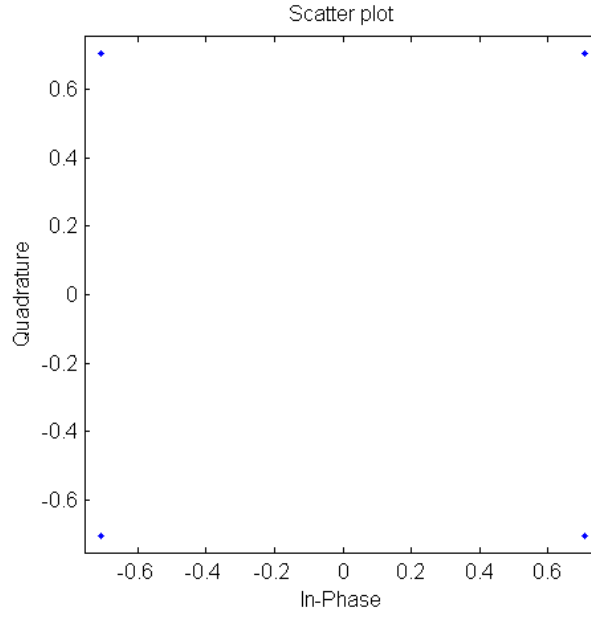


Figure 4.2a : QPSK Constellation.

$b(i)b(i+1)b(i+2)b(i+3)$	I	Q
0000	$\frac{1}{\sqrt{10}}$	$\frac{1}{\sqrt{10}}$
0001	$\frac{1}{\sqrt{10}}$	$\frac{3}{\sqrt{10}}$
0010	$\frac{3}{\sqrt{10}}$	$\frac{1}{\sqrt{10}}$
0011	$\frac{3}{\sqrt{10}}$	$\frac{3}{\sqrt{10}}$
0100	$\frac{1}{\sqrt{10}}$	$\frac{-1}{\sqrt{10}}$
0101	$\frac{1}{\sqrt{10}}$	$\frac{-3}{\sqrt{10}}$
0110	$\frac{3}{\sqrt{10}}$	$\frac{-1}{\sqrt{10}}$
0111	$\frac{3}{\sqrt{10}}$	$\frac{-3}{\sqrt{10}}$
1000	$\frac{-1}{\sqrt{10}}$	$\frac{1}{\sqrt{10}}$
1001	$\frac{-1}{\sqrt{10}}$	$\frac{3}{\sqrt{10}}$
1010	$\frac{-3}{\sqrt{10}}$	$\frac{1}{\sqrt{10}}$
1011	$\frac{-3}{\sqrt{10}}$	$\frac{3}{\sqrt{10}}$
1100	$\frac{-1}{\sqrt{10}}$	$\frac{-1}{\sqrt{10}}$
1101	$\frac{-1}{\sqrt{10}}$	$\frac{-3}{\sqrt{10}}$
1110	$\frac{-3}{\sqrt{10}}$	$\frac{-1}{\sqrt{10}}$
1111	$\frac{-3}{\sqrt{10}}$	$\frac{-3}{\sqrt{10}}$

The constellation diagram for 16 QAM shown in Figure 4.2b

### 4.3 Transform Precoder

Here the transform precoding nothing but DFT operation on modulation symbols. The block of complex-valued symbols  $d(0), \dots, d(M_{symp})$  is divided into  $\frac{M_{symp}}{M_{sc}^{FU\text{SCH}}}$  sets, each corresponding to one SC-FDMA

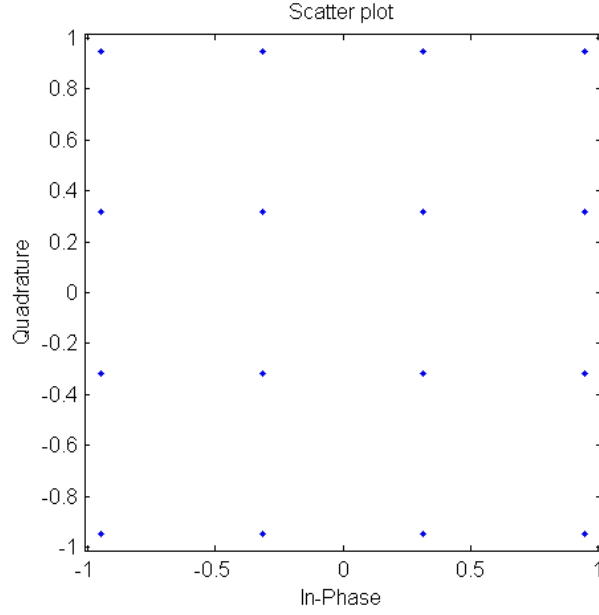


Figure 4.2b: 16 QAM Constellation

symbol. Transform precoding shall be applied according to

$$z(l.M_{sc}^{PUSCH} + k) = \frac{1}{\sqrt{M_{sc}^{PUSCH}}} \sum_{i=0}^{M_{sc}^{PUSCH}} d(l.M_{sc}^{PUSCH} + i).e^{-j\frac{2\pi ik}{M_{sc}^{PUSCH}}} \quad (4.5)$$

$$k = 0, \dots, M_{sc}^{PUSCH} - 1$$

$$l = 0, \dots, \frac{M_{symb}}{M_{sc}^{PUSCH}} - 1$$

resulting in a block of complex-valued symbols  $z(0), \dots, z(M_{symb} - 1)$ . The variable  $M_{sc}^{PUSCH} = M_{RB}^{PUSCH} \cdot N_{sc}^{RB}$ , where  $M_{RB}^{PUSCH}$  represents the bandwidth of the PUSCH in terms of resource blocks, and shall fulfill

$$M_{RB}^{PUSCH} = 2^{\alpha_2} \cdot 3^{\alpha_3} \cdot 5^{\alpha_5} \leq N_{UL}^{RB} \quad (4.6)$$

where  $\alpha_2, \alpha_3$  and  $\alpha_5$  are set of non negative integers.

#### 4.4 Uplink Reference Signals

The UL access is based on single-carrier FDMA and frequency-multiplexing reference signals with data transmissions would violate the single-carrier property resulting in increased Peak to Average Power Ratio(PAPR)/Cubic Metric(CM). Therefore, the uplink reference signals are strictly time-multiplexed to assure the single-carrier property of SC-FDMA and also uplink reference signals always UE specific signals.

Two types of uplink reference signals are supported:

- Demodulation reference signals (DMRS) used for channel estimation for PUSCH or PUCCH.
- Sounding reference signal (SRS) used to measure the uplink channel quality for channel sensitive scheduling.

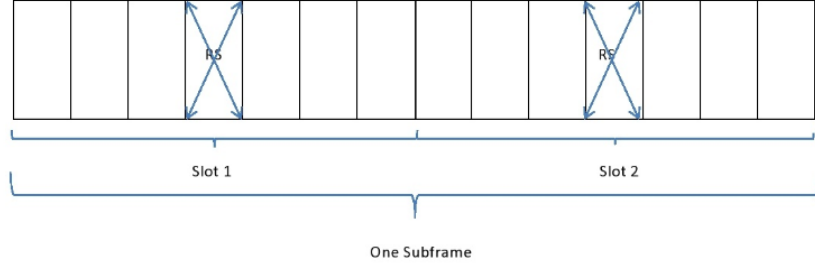


Figure 4.4a: Uplink DMRS for the normal cyclic prefix.

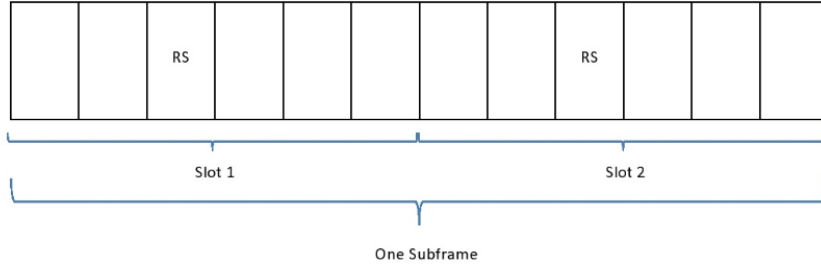


Figure 4.4b: Uplink DMRS for the Extended cyclic prefix

The uplink DMRS for normal cyclic prefix and extended cyclic prefix cases are shown in Figure 4.4a and 4.4b. DMRS for PUSCH are transmitted in the middle of the slot in symbol with  $l = 2, 3$  for the extended and normal cyclic prefix respectively. For PUCCH format 1, 1A and 1B, the demodulation reference signals are transmitted in three symbols ( $l = 2, 3, 4$ ) for the normal cyclic prefix and two symbols ( $l = 2, 3$ ) for the extended cyclic prefix. For PUCCH format 2, 2A and 2B, the demodulation reference signals are transmitted in two symbols ( $l = 1, 5$ ) for the normal cyclic prefix. For PUCCH format 2, the demodulation reference signal is transmitted in a single symbol ( $l = 3$ ) for the extended cyclic prefix case.

#### 4.4.1 Uplink Reference Signal Sequences

In order to enable low PAPR/CM, constant amplitude reference signal sequences are selected for the uplink. The same set of base sequences is used for demodulation and sounding reference signals. The reference signal sequence  $r_{u,v}^{(\alpha)}(n)$  is defined by a cyclic shift  $\alpha$  of a base sequence  $\bar{r}_{u,v}(n)$  according to:

$$r_{u,v}^{(\alpha)}(n) = e^{j\alpha n} \bar{r}_{u,v}(n), \quad 0 \leq n < M_{sc}^{RS} - 1 \quad (4.7)$$

Where

$$M_{sc}^{RS} = mN_{sc}^{RB}$$

where,  $M_{sc}^{RS}$  is the length of the reference signal sequence with  $1 \leq m \leq N_{RB}^{max,UL}$ . Multiple reference signal sequences are defined from a single base sequence by using different values of the cyclic shift  $\alpha$ .

The base sequences  $\bar{r}_{u,v}(n)$  are divided into 30 groups, where  $u \in \{0, 1, \dots, 29\}$  is the group number and  $v$  is the base sequence number within the group. For sequence lengths up to five resource blocks, that is  $M_{sc}^{RS} = mN_{sc}^{RB}$ ,  $1 \leq m \leq 5$  each sequence group contains a single base sequence ( $v = 0$ ). For sequence lengths greater than five resource blocks, that  $M_{sc}^{RS} = mN_{sc}^{RB}$ ,  $6 \leq m \leq N_{RB}^{max,UL}$ , each sequence group contains two base sequences ( $v = 0, 1$ ). The sequence group number  $u$  and the sequence number  $v$  within the group can be hopped in time to randomize the interference.

The definition of the base sequence  $\bar{r}_{u,v}(0), \dots, \bar{r}_{u,v}(M_{sc}^{RS} - 1)$  depends on the sequence length  $M_{sc}^{RS}$ . For sequence lengths of up to two resource blocks, computer-generated CAZAC sequences are used as reference signal sequences. For sequence lengths of more than two resource blocks, ZC sequences are used as the uplink reference signal sequences.

### Base sequences of length $3N_{sc}^{RB}$ or Larger

For  $M_{sc}^{RS} \geq 3N_{sc}^{RB}$ , the base sequence  $\bar{r}_{u,v}(0), \bar{r}_{u,v}(1), \dots, \bar{r}_{u,v}(M_{sc}^{RS} - 1)$  is given by

$$\bar{r}_{u,v}(n) = x_q(n \bmod N_{ZC}^{RS}), \quad 0 \leq n < M_{sc}^{RS} \quad (4.8)$$

where the  $q^{th}$  of Zadoff-Chu sequence is defined by

$$x_q(m) = e^{\frac{-j\pi \cdot q \cdot m(m+1)}{N_{ZC}^{RS}}}, \quad 0 \leq m \leq N_{ZC}^{RS} - 1 \quad (4.9)$$

with  $q$  is given by

$$q = \lfloor \bar{q} + 1/2 \rfloor + v \cdot (-1)^{\lfloor 2\bar{q} \rfloor} \quad (4.10)$$

$$\bar{q} = \frac{N_{ZC}^{RS}(u+1)}{31} \quad (4.11)$$

The length  $N_{ZC}^{RS}$  of the Zadoff-Chu sequence is given by the largest prime number such that  $N_{ZC}^{RS} < M_{sc}^{RS}$ . We note that for three resource blocks with  $M_{sc}^{RS} = 36$ , ZC sequence length is  $N_{ZC}^{RS} = 31$  as 31 is the largest prime number such that  $N_{ZC}^{RS} < M_{sc}^{RS}$ . We also know that with a ZC sequence length a prime number  $N_{ZC}^{RS}$  a total of  $(N_{ZC}^{RS} - 1)$  root sequences are available. With the smallest ZC sequence length of  $N_{ZC}^{RS} = 31$  for the three resource blocks, a total of 30 root sequences are available. It is for this reason that the number of sequence groups is limited to 30.

We know that that for sequence lengths up to five resource blocks, that is  $M_{sc}^{RS} = 60$ , each sequence group contains a single base sequence ( $v = 0$ ). However, when  $M_{sc}^{RS} = 72$ , the number of available ZC root sequences is 71, as 71 is the largest prime number such that  $N_{ZC}^{RS} < M_{sc}^{RS}$ . Given that we have 30 sequence groups, it now becomes possible to have more than one base sequence in a group. It should be noted that for  $M_{sc}^{RS} = 60$  and  $N_{ZC}^{RS} = 59$  and, therefore, two sequences cannot be provided within a group as this requires a total of at least 60 base or root sequences.

### Base sequences of length less than $3N_{sc}^{RB}$

For  $M_{sc}^{RS} = N_{sc}^{RB}$  and  $M_{sc}^{RS} = 2N_{sc}^{RB}$  the computer-generated CAZAC base sequence  $\bar{r}_{u,v}(n)$  is given by:

$$\bar{r}_{u,v}(n) = e^{\frac{j\pi\phi(n)}{4}}, \quad 0 \leq n \leq M_{sc}^{RS} - 1 \quad (4.12)$$

$u$	$\phi(0), \dots, \phi(11)$											
0	-1	1	3	-3	3	3	1	1	3	1	-3	3
1	1	1	3	3	3	-1	1	-3	-3	1	-3	3
2	1	1	-3	-3	-3	-1	-3	-3	1	-3	1	-1
3	-1	1	1	1	1	-1	-3	-3	1	-3	3	-1
4	-1	3	1	-1	1	-1	-3	-1	1	-1	1	3
5	1	-3	3	-1	-1	1	1	-1	-1	3	-3	1
6	-1	3	-3	-3	-3	3	1	-1	3	3	-3	1
7	-3	-1	-1	-1	1	-3	3	-1	1	-3	3	1
8	1	-3	3	1	-1	-1	-1	1	1	3	-1	1
9	1	-3	-1	3	3	-1	-3	1	1	1	1	1
10	-1	3	-1	1	1	-3	-3	-1	-3	-3	3	-1
11	3	1	-1	-1	3	3	-3	1	3	1	3	3
12	1	-3	1	1	-3	1	1	1	-3	-3	-3	1
13	3	3	-3	3	-3	1	1	3	-1	-3	3	3
14	-3	1	-1	-3	-1	3	1	3	3	3	-1	1
15	3	-1	1	-3	-1	-1	1	1	3	1	-1	-3
16	1	3	1	-1	1	3	3	3	-1	-1	3	-1
17	-3	1	1	3	-3	3	-3	-3	3	1	3	-1
18	-3	3	1	1	-3	1	-3	-3	-1	-1	1	-3
19	-1	3	1	3	1	-1	-1	3	-3	-1	-3	-1
20	-1	-3	1	1	1	1	3	1	-1	1	-3	-1
21	-1	3	-1	1	-3	-3	-3	-3	-3	1	-1	-3
22	1	1	-3	-3	-3	-3	-1	3	-3	1	-3	3
23	1	1	-1	-3	-1	-3	1	-1	1	3	-1	1
24	1	1	3	1	3	3	-1	1	-1	-3	-3	1
25	1	-3	3	3	1	3	3	1	-3	-1	-1	3
26	1	3	-3	-3	3	-3	1	-1	-1	3	-1	-3
27	-3	-1	-3	-1	-3	3	1	-1	1	3	-3	-3
28	-1	3	-3	3	-1	3	3	-3	3	3	-1	-1
29	3	-3	-3	-1	-1	-3	-1	3	-3	3	1	-1

Table 4.4: Definition of  $\phi(n)$  for  $M_{sc}^{RS} = N_{sc}^{RB}$

where the values of  $\phi(n)$  are given in Table 4.4 for  $M_{sc}^{RS} = N_{sc}^{RB}$ . The values  $\phi(0), \phi(1), \dots, \phi(23)$  for  $M_{sc}^{RS} = 2N_{sc}^{RB} = 24$  can be found in [2]. We note that the sequences are based on a constant amplitude QPSK alphabet with the following four alphabets:

$$\bar{r}_{u,v}(n) = e^{\frac{j\pi}{4}} = \frac{1}{\sqrt{2}} + \frac{j}{\sqrt{2}}, \phi(n) = 1 \quad (4.13)$$

$$\bar{r}_{u,v}(n) = e^{\frac{-j\pi}{4}} = \frac{1}{\sqrt{2}} - \frac{j}{\sqrt{2}}, \phi(n) = -1 \quad (4.14)$$

$$\bar{r}_{u,v}(n) = e^{\frac{3j\pi}{4}} = \frac{-1}{\sqrt{2}} + \frac{j}{\sqrt{2}}, \phi(n) = 3 \quad (4.15)$$

$$\bar{r}_{u,v}(n) = e^{\frac{-3j\pi}{4}} = \frac{-1}{\sqrt{2}} - \frac{j}{\sqrt{2}}, \phi(n) = -3 \quad (4.16)$$

## Group Hopping and Sequence Hopping

In order to randomize the inter-cell interference, sequence group hopping can be enabled by higher layers. In this case, the sequence-group number  $u$  in slot  $n_s$  is defined by a group-hopping pattern  $f_{gh}(n_s)$  and a sequence-shift pattern  $f_{ss}$  according to:

$$u = (f_{gh}(n_s) + f_{ss}) \bmod 30 \quad (4.17)$$

There are 17 different hopping patterns and 30 different sequence-shift patterns. Sequence-group hopping can be enabled or disabled by means of the parameter Group-hopping-enabled provided by higher layers. PUCCH and PUSCH have the same hopping pattern but may have different sequence-shift patterns.

The group-hopping pattern  $f_{gh}(n_s)$  is the same for PUSCH and PUCCH and given by

$$\begin{aligned} f_{gh}(n_s) &= 0 \quad \text{if Group Hopping Disabled} \\ &= \left( \sum_{i=0}^7 c(8n_s + i) \cdot 2^i \right) \bmod 30 \quad \text{if Group Hopping Enabled} \end{aligned}$$

where the pseudo-random sequence  $c(i)$  is defined in section 4.1 . The pseudo-random sequence generator shall be initialized with

$$c_{init} = \left\lfloor \frac{N_{ID}^{cell}}{30} \right\rfloor \quad (4.18)$$

at the beginning of each radio frame with cell specific value.

When the group hopping is not enabled  $f_{gh}(n_s)$  is set to zero. A total of 504 hopping patterns via 17 group-hopping patterns and 30 sequence shift patterns can be obtained. However , only a total of 504 hopping/shift patterns are used.

The group -hopping pattern  $f_{gh}(n_s)$  is the same for PUSCH and PUCCH. However,the sequence-shift pattern  $f_{ss}$  definition differs between PUCCH and PUSCH:

$$\begin{aligned} f_{ss}^{PUCCH} &= N_{ID}^{cell} \bmod 30 \\ f_{ss}^{PUSCH} &= \left( f_{ss}^{PUCCH} + \Delta_{ss} \right) \bmod 30 \end{aligned} \quad (4.19)$$

where,  $\Delta_{ss} \in \{0, 1, \dots, 29\}$  is configured by higher layers. Sequence hopping only applies for reference-signals of length  $M_{sc}^{RS} \geq 6N_{sc}^{RB}$ . For reference-signals of length  $M_{sc}^{RS} \leq 5N_{sc}^{RB}$ , the base sequence number  $v$  within the base sequence group is given by  $v = 0$ . When the sequence hopping enabled and group hopping is disabled the base sequence  $v$  with in the base sequence group in slot  $n_s$  is given by:

$$v = c(n_s), \quad (4.20)$$

where, the Pseudo random sequence  $c(i)$  is given in section 4.1 and takes values of either zero or one, which in turn determines the base sequence with  $v = 0$  or the base sequence with  $v = 1$ . The PN-sequence generator is initialized at the beginning of each radio frame with a cell-specific value as:

$$c_{init} = \left\lfloor \frac{N_{ID}^{cell}}{30} \right\rfloor \cdot 2^5 + f_{ss}^{PUSCH} \quad (4.21)$$

In other cases when sequence hopping is not enabled or group hopping is enabled, the base sequence number  $v$  within the base sequence group in slot  $n_s$  is always set to zero, that is  $v = 0$ .

#### 4.4.2 Demodulation Reference signals

The demodulation reference signals are specified for PUSCH and PUCCH. The demodulation reference signal sequence  $r^{PUSCH}()$  for rPSUCH is defined by:

$$r^{PUSCH}(m \cdot M_{sc}^{RS} + n) = r_{u,v}^{(\alpha)}(n), \quad m = 0, 1 \quad n = 0, \dots, (M_{sc}^{RS} - 1), \quad (4.22)$$

where  $r_{u,v}^{(\alpha)}(n)$  is the reference signal sequence given by Equation (4.7) and  $m=0,1$  represents the first and second slot with in a subframe. The length of the reference signal sequence is equal to the number of

Cyclic shift field	$n_{DMRS}^{(2)}$
000	0
001	2
010	3
011	4
100	6
101	8
110	9
111	10

Table 4.4(c): Mapping of cyclic shift field to  $n_{DMRS}^{(2)}$

resource elements or subcarriers used for PUSCH transmission, that is  $M_{sc}^{RS} = M_{sc}^{PUSCH}$ . The cyclic shift  $\alpha$  in a slot is given as:

$$\alpha = \frac{2\pi \left[ (n_{DMRS}^{(1)} + n_{DMRS}^{(2)} + n_{PRS}) \bmod 12 \right]}{12}, \quad (4.23)$$

where,  $n_{DMRS}^{(1)}$  is broadcast as part of the the system information . The value of  $n_{DMRS}^{(2)}$  are signaled in the UL scheduling assignment and are given in the Table 4.4(c). The  $n_{PRS}$  is given as:

$$n_{PRS} = \sum_{i=0}^7 c(i) * 2^i, \quad (4.24)$$

where the PN-sequence  $c(i)$  is given in section 4.1 , The PN-sequence generator is initialized at the beginning of each radio frame with a cell-specific value according to section 4.14. The demodulation reference signal sequence for PUSCH  $r^{PUSCH}()$  is multiplied with the amplitude scaling factor  $\beta_{PUSCH}$  and mapped in sequence starting with  $r^{PUSCH}(0)$  to the same set of physical resource blocks for the corresponding PUSCH transmission. The Constellation of DMRS is shown in the Figure 4.4(c).

## 4.5 Resource Element Mapping

The block of complex-valued symbols  $z(0), \dots, z(M_{symb} - 1)$  shall be multiplied with the amplitude scaling factor  $\beta_{PUSCH}$  in order to conform to the transmit power  $P_{PUSCH}$  specified in [2] and and mapped in sequence starting with  $z(0)$  to physical resource blocks assigned for transmission of PUSCH. The mapping to resource elements  $(k, l)$  corresponding to the physical resource blocks assigned for transmission and not used for transmission of reference signals and not reserved for possible SRS transmission shall be in increasing order of first the index  $k$ , then the index  $l$ , starting with the first slot in the subframe.

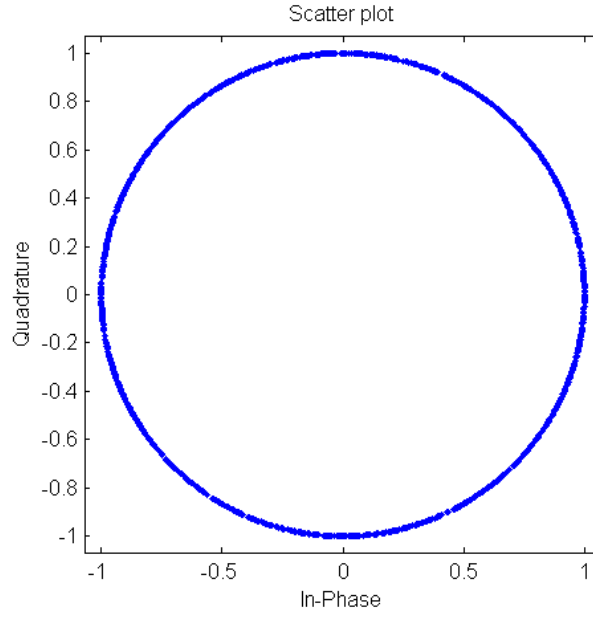


Figure 4.4(c) :Constellation of DMRS for  $M_{sc}^{RS}=100$  RB's

#### 4.6 SC-FDMA Signal Generation

The time-continuous signal  $s_l(t)$  in SC-FDMA symbol  $l$  in an UL slot is defined by

$$s_l(t) = \sum_{k=-\lfloor N_{RB}^{UL} N_{SC}^{RB} / 2 \rfloor}^{\lfloor N_{RB}^{UL} N_{SC}^{RB} / 2 \rfloor - 1} a_{k^{(-)},l} e^{j2\pi(k+1/2)\Delta f(t - N_{CP,l} T_s)}$$

for  $0 \leq t < (N_{cp,l} + N) * T_s$  where  $k^{(-)} = k + \lfloor N_{RB}^{UL} N_{SC}^{RB} / 2 \rfloor$ ,  $N = 2048$ ,  $\Delta f = 15KHz$  and  $a_{k,l}$  is the content of resource element

#### References

- [1] 3GPP TS 36.212: "Evolved Universal Terrestrial Radio Access (E-UTRA); Multiplexing and channel coding".
- [2] 3GPP TS 36.211: "Evolved Universal Terrestrial Radio Access (E-UTRA); Physical channels and modulation".
- [3] 3GPP TS 36.213: "Evolved Universal Terrestrial Radio Access (E-UTRA); Physical Layer Procedures".



## 5 | Transmitter Structure of PUCCH Formats 2,2a and 2b

The physical uplink channel supports multiple formats as shown in Table 5.1. The combination of uplink control information formats supported on PUCCH include hybrid-ARQ ACK/NACK using PUCCH format 1A or 1B, Channel Quality Indicator(CQI)/Precoding Matrix Indicator(PMI) using PUCCH format 2, CQI/PMI and hybrid ARQ ACK/NACK using PUCCH format 2A or 2B for the normal cyclic prefix or format 2 for extended cyclic prefix[2]. Formats 2A and 2B are supported for the normal cyclic prefix

PUCCH Format	Modulation Scheme	Number of bits per subframe $M_{bit}$
1	N/A	N/A
1A	BPSK	1
1B	QPSK	2
2	QPSK	20
2A	QPSK+BPSK	21
2B	QPSK+BPSK	22

Table 5.1: PUCCH Formats

only. The formats 1A and 1B are used for standalone transmission of single-bit and two-bits ACK/NACK respectively.

The format 2 is used when CQI/PMI is transmitted without ACK/NACK multiplexing using a (20,A) code or when CQI/PMI and ACK/NACK are jointly coded for the case of extended cyclic prefix[1]. We note that the number of channel bits in this case is 21 or 22 for single-bit and two-bits ACK/NACK feedback respectively. The modulation for single-bit ACK/NACK is BPSK while QPSK is used in all other cases. All PUCCH formats use a cyclic shift of a sequence in each symbol, where  $n_{cs}^{cell}(n_s, l)$  is used to derive the cyclic shift for different PUCCH formats.

$$n_{cs}^{cell}(n_s, l) = \sum_{i=0}^7 c(8N_{sym}^{UL} \cdot n_s + 8l + i)2^i, \quad (5.1)$$

where  $c(i)$  is the pseudo-random sequence [section 4.1]. The pseudo-random sequence generator is initialized with  $c_{init} = N_{ID}^{cell}$  at the beginning of each radio frame.

The physical resources used for PUCCH depend on two parameters,  $N_{RB}^{(2)}$  and  $N_{cs}^{(1)}$ , which are set by higher layers. The variable  $N_{RB}^{(2)} \geq 0$  denotes the bandwidth in terms of resource blocks that are reserved exclusively for PUCCH formats 2/2A/2B transmission in each slot. The variable  $N_{cs}^{(1)} \in \{0, 1, \dots, 8\}$  denotes the number of cyclic shift used for PUCCH formats 1/1A/1B in a resource block used for a mix of formats 1/1A/1B and 2/2A/2B. The resources used for transmission of PUCCH format 1/1A/1B and 2/2A/2B are

represented by the non-negative indices  $n_{pucch}^{(1)}$  and  $n_{pucch}^{(2)} < N_{RB}^2 N_{RB}^{sc} + \lceil \frac{N_{cs}^{(1)}}{8} \rceil \cdot (N_{sc}^{RB} - N_{cs}^{(1)} - 2)$ , respectively.

## 5.1 PUCCH Formats 2,2a and 2b

The block of bits  $b(0), \dots, b(M_{bit} - 1)$  is scrambled with a UE specific scrambling sequence, resulting in a block of scrambled bits  $\hat{b}(0), \dots, \hat{b}(M_{bit} - 1)$  according to

$$\hat{b}(i) = (b(i) + c(i)) \bmod 2, \quad (5.2)$$

where  $c(i)$  is the pseudo-random scrambling sequence  $c(i)$  equation 4.1. The scrambling sequence generator is initialized at the start of each subframe as:

$$c_{init} = (\lfloor \frac{n_s}{2} \rfloor + 1) \cdot (2 \cdot N_{ID}^{cell} + 1) \cdot 2^{16} + n_{RNTI} \quad (5.3)$$

The block of scrambled bits  $\hat{b}(0), \dots, \hat{b}(19)$  is modulated using QPSK modulation resulting in a block of complex valued modulation symbols  $d(0), \dots, d(9)$ . Each complex valued symbol  $d(0), \dots, d(9)$  is multiplied with a cyclically shifted length  $N_{seq}^{PUCCH} = 12$  sequence  $r_{u,v}^\alpha(n)$  according to:

$$z(N_{seq}^{PUCCH} \cdot n + i) = d(n) \cdot r_{u,v}^\alpha(i) \quad n = 0, 1, \dots, 9 \quad i = 0, 1, \dots, (N_{sc}^{RB} - 1), \quad (5.4)$$

where  $r_{u,v}^{(\alpha)}(i)$  is given by equation 4.7

The PUCCH format 2 mapping in a slot is shown in Figure 5.1 for the case of the normal cyclic prefix. In the case of the extended cyclic prefix, the second reference signal within the slot is dropped leaving five SC-FDMA symbols available for PUCCH. Therefore, the number of SC-FDMA symbols available for CQI/PMI transmission within a subframe is 10 for the case of both normal and extended cyclic prefixes. This allows carrying a total of 20 bits using QPSK modulation. For PUCCH formats 2A and 2B, the bits  $b(20), \dots, b(M_{bit} - 1)$  representing one or two bits ACK/NACK bits are modulated similarly to ACK/NACK in formats 1A and 1B as described in Table 5.2. This results in a single modulation symbol  $d(10)$ , which is used for the generation of the reference signal for PUCCH formats 2A and 2B. This modified reference signal carrying ACK/NACK is then mapped to the SC-FDMA symbol originally carrying the second reference signal within the slot as shown in Figure 5.1.

PUCCH Format	$b(20), \dots, b(M_{bit} - 1)$	$d(10)$
2A	0	1
	1	-1
2B	00	1
	01	-j
	10	j
	11	-1

Table 5.2: PUCCH Formats

## 5.2 PUCCH Mapping

The complex valued symbols  $z(i)$  is multiplied with amplitude scaling factor  $\beta_{PUCCH}$  according to power control algorithm and mapped to resource elements. PUCCH uses one resource block in each of

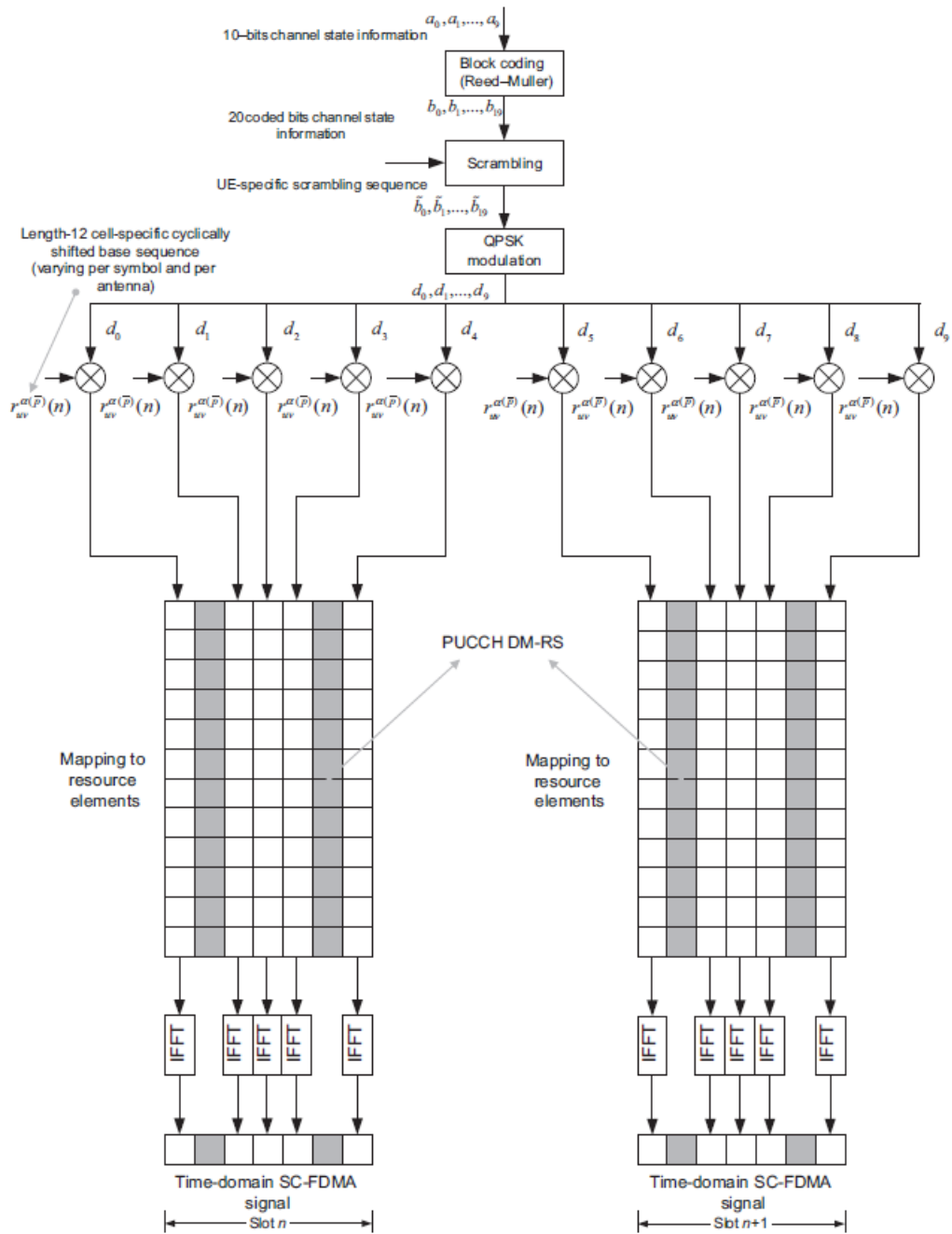


Figure 5.1: PUCCH Format Structure

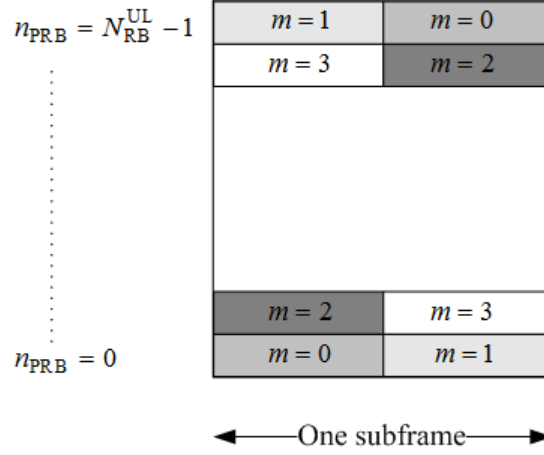


Figure 5.2:PUCCH Mapping to physical resource blocks

the two slots in a subframe. Within the physical resource block used for transmission, the mapping of  $z(i)$  to resource elements  $(k,l)$  not used for transmission of reference signals is in increasing order of first  $k$ , then  $l$  and finally the slot number, starting with the first slot in the subframe.

The resources used for the transmission of PUCCH formats 2/2A/2B are identified by a resource index  $n_{PUCCH}^{(2)}$  from which the cyclic shift  $\alpha$  is determined.

The physical resource block to be used for transmission of PUCCH in slot  $n_s$  is given by :

$$\begin{aligned} n_{PRB} &= \lfloor \frac{m}{2} \rfloor & \text{if } (m + n_s \bmod 2) = 0 \\ &= N_{RB}^{UL} - 1 - \lfloor \frac{m}{2} \rfloor & \text{if } (m + n_s \bmod 2) = 1 \end{aligned} \quad (5.5)$$

where the variable  $m$  depends on the PUCCH format. For formats 2,2A and 2B,  $m$  is given by

$$m = \lfloor \frac{n_{PUCCH}^{(2)}}{N_{sc}^{RB}} \rfloor \quad (5.6)$$

The mapping of PUCCH to physical resource blocks is illustrated in Figure 5.2

### 5.3 Demodulation Reference Signal

The demodulation reference signal sequence  $r^{PUCCH}(\cdot)$  for PUCCH is defined by

$$r^{PUCCH}(m' N_{RS}^{PUCCH} M_{sc}^{RS} + m M_{sc}^{RS} + n) = \bar{w}(m) z(m) r_{u,v}^{(\alpha)}(n) \quad (5.7)$$

Where

$$\begin{aligned} m &= 0, \dots, N_{RS}^{PUCCH} - 1 \\ n &= 0, \dots, M_{sc}^{RS} - 1 \\ m' &= 0, 1 \end{aligned}$$

For PUCCH formats 2a and 2b,  $z(m)$  equals  $d(10)$  for  $m=1$ , where  $d(10)$  is defined in Table 5.2. For all other cases,  $z(m) = 1$ .

The sequence  $r_{u,v}^{(\alpha)}(n)$  is given below with  $M_{sc}^{RS} = 12$  where the expression for the cyclic shift  $\alpha$  is

$u$	$\phi(0), \dots, \phi(11)$											
0	-1	1	3	-3	3	3	1	3	1	-3	3	3
1	1	1	3	3	3	-1	1	-3	-3	1	-3	3
2	1	1	-3	-3	-3	-1	-3	-3	1	-3	1	-1
3	-1	1	1	1	1	-1	-3	-3	1	-3	3	-1
4	-1	3	1	-1	1	-1	-3	-1	1	-1	1	3
5	1	-3	3	-1	-1	1	1	-1	-1	3	-3	1
6	-1	3	-3	-3	-3	3	1	-1	3	3	-3	1
7	-3	-1	-1	-1	1	-3	3	-1	1	-3	3	1
8	1	-3	3	1	-1	-1	-1	1	1	3	-1	1
9	1	-3	-1	3	3	-1	-3	1	1	1	1	1
10	-1	3	-1	1	1	-3	-3	-1	-3	-3	3	-1
11	3	1	-1	-1	3	3	-3	1	3	1	3	3
12	1	-3	1	1	-3	1	1	1	-3	-3	-3	1
13	3	3	-3	3	-3	1	1	3	-1	-3	3	3
14	-3	1	-1	-3	-1	3	1	3	3	3	-1	1
15	3	-1	1	-3	-1	-1	1	1	3	1	-1	-3
16	1	3	1	-1	1	3	3	3	-1	-1	3	-1
17	-3	1	1	3	-3	3	-3	-3	3	1	3	-1
18	-3	3	1	1	-3	1	-3	-3	-1	-1	1	-3
19	-1	3	1	3	1	-1	-1	3	-3	-1	-3	-1
20	-1	-3	1	1	1	1	3	1	-1	1	-3	-1
21	-1	3	-1	1	-3	-3	-3	-3	-3	1	-1	-3
22	1	1	-3	-3	-3	-3	-1	3	-3	1	-3	3
23	1	1	-1	-3	-1	-3	1	-1	1	3	-1	1
24	1	1	3	1	3	3	-1	1	-1	-3	-3	1
25	1	-3	3	3	1	3	3	1	-3	-1	-1	3
26	1	3	-3	-3	3	-3	1	-1	-1	3	-1	-3
27	-3	-1	-3	-1	-3	3	1	-1	1	3	-3	-3
28	-1	3	-3	3	-1	3	3	-3	3	3	-1	-1
29	3	-3	-3	-1	-1	-3	-1	3	-3	3	1	-1

Table 5.3: Definition of  $\phi(n)$  for  $M_{sc}^{RS} = N_{sc}^{RB}$

determined by the PUCCH format. For  $M_{sc}^{RS} = N_{sc}^{RB}$  and  $M_{sc}^{RS} = 2N_{sc}^{RB}$  the computer-generated CAZAC base sequence  $\bar{r}_{u,v}(n)$  is given by:

$$\bar{r}_{u,v}(n) = e^{\frac{j\pi\phi(n)}{4}}, \quad 0 \leq n \leq M_{sc}^{RS} - 1 \quad (5.8)$$

where the values of  $\phi(n)$  are given in Table 5.3 for  $M_{sc}^{RS} = N_{sc}^{RB}$ . The values  $\phi(0), \phi(1), \dots, \phi(23)$  for  $M_{sc}^{RS} = 2N_{sc}^{RB} = 24$  can be found in [2]. We note that the sequences are based on a constant amplitude QPSK alphabet with the following four alphabets:

$$\bar{r}_{u,v}(n) = e^{\frac{j\pi}{4}} = \frac{1}{\sqrt{2}} + \frac{j}{\sqrt{2}}, \phi(n) = 1 \quad (5.9)$$

$$\bar{r}_{u,v}(n) = e^{\frac{-j\pi}{4}} = \frac{1}{\sqrt{2}} - \frac{j}{\sqrt{2}}, \phi(n) = -1 \quad (5.10)$$

$$\bar{r}_{u,v}(n) = e^{\frac{3j\pi}{4}} = \frac{-1}{\sqrt{2}} + \frac{j}{\sqrt{2}}, \phi(n) = 3 \quad (5.11)$$

$$\bar{r}_{u,v}(n) = e^{\frac{-3j\pi}{4}} = \frac{-1}{\sqrt{2}} - \frac{j}{\sqrt{2}}, \phi(n) = -3 \quad (5.12)$$

The mapping of reference symbols in slot is shown in the Figure 5.3 for Normal cyclic prefix for PUCCH format 2,2A and 2B and Figure 5.4 for Extended cyclic prefix for PUCCH format 2.

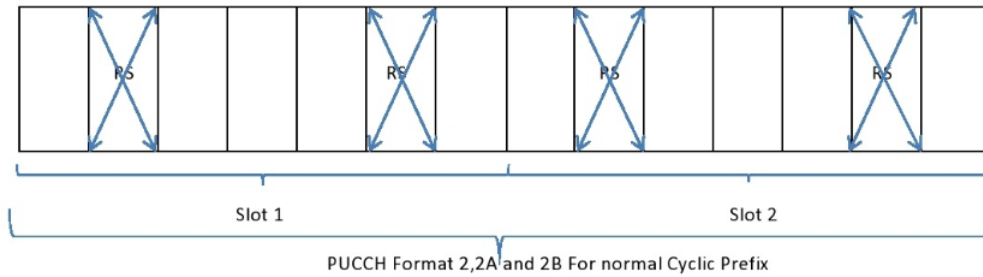


Figure 5.3: Demodulation reference signals for normal cyclic prefix

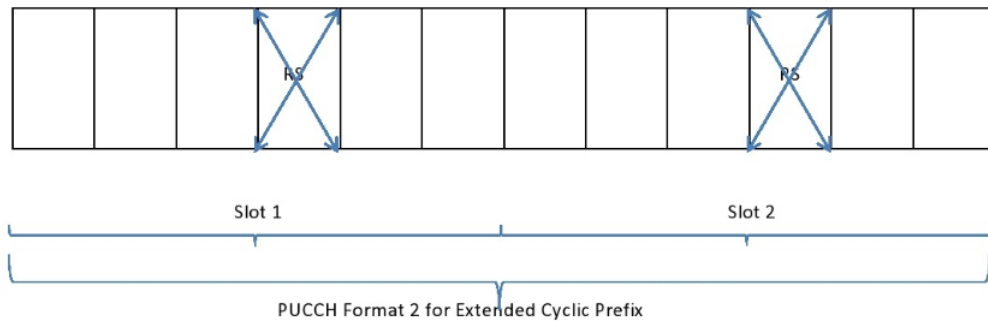


Figure 5.4: Demodulation reference signals for extended cyclic prefix

## References

- [1] 3GPP TS 36.212: "Evolved Universal Terrestrial Radio Access (E-UTRA); Multiplexing and channel coding".
- [2] 3GPP TS 36.211: "Evolved Universal Terrestrial Radio Access (E-UTRA); Physical channels and modulation".
- [3] 3GPP TS 36.213: "Evolved Universal Terrestrial Radio Access (E-UTRA); Physical Layer Procedures".

## 6 | Receiver Design for PUSCH

In the transmitter section, after the bit level scrambling process the modulation mapping converts message bit sequence into **PSK/QAM** symbols, performs **DFT** and **IFFT** on the symbols to convert them into time-domain signals, and sends them out through a (wireless) channel. Here one subframe is the TTI i.e. Transmission Time Interval which is  $1ms$  and it consists of 14 SCFDMA Symbols. The received signal is usually distorted by the channel characteristics. In order to recover the transmitted bits, the channel effect must be estimated and compensated in the receiver. The orthogonality allows each subcarrier component of the received signal to be expressed as the product of the transmitted signal and channel frequency response at the subcarrier. Thus, the transmitted signal can be recovered by estimating the channel response just at each subcarrier. In general, the channel can be estimated by using a preamble or pilot symbols known to both transmitter and receiver, which employ various interpolation techniques to estimate the channel response of the subcarriers between pilot tones.

Figure 6.1a illustrates PUSCH receiver operation from a multiple user access perspective in the uplink. Before performing the basic SC-FDMA demodulation process, the base station separates the users in the frequency domain during the subcarrier de-mapping process. Figure 6.1b shows the, two receiving antennas

### 6.1 Channel Estimation

Training symbols can be used for channel estimation, usually providing a good performance. The least squares (LS) channel estimator is widely used in practice due to its simplicity [1]. However, the frequency domain LS channel estimator results in approximately 3dB performance loss compared to the optimal linear minimum mean-square error (LMMSE) channel estimator [2]. Despite of the optimal channel estimation performance, the LMMSE channel estimator is not commonly used in practice due its very high complexity [1]. In the LTE uplink, a block of pilot symbols is transmitted periodically to estimate the channel. Figure 6.2 shows the slot structure adopted in the LTE uplink. Each slot consists of 7 transmission blocks, and the pilot block is placed in the middle of the slot [3]. In this chapter, a slow-variant channel is assumed (where the channel response is assumed to be the same during the slot period) and the channel estimate obtained in the pilot block is used to calculate the equalizer coefficients for the data blocks within the same slot.

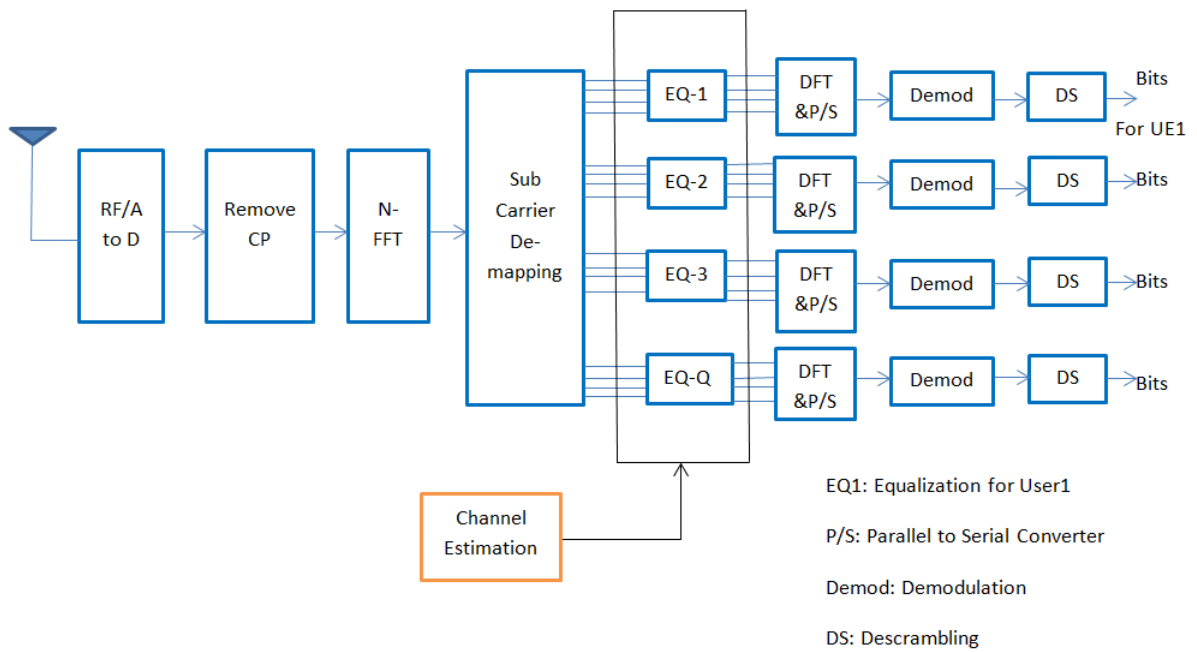


Figure 6.1a: PUSCH receiver structure from a multiple user access perspective with Q terminals in the uplink

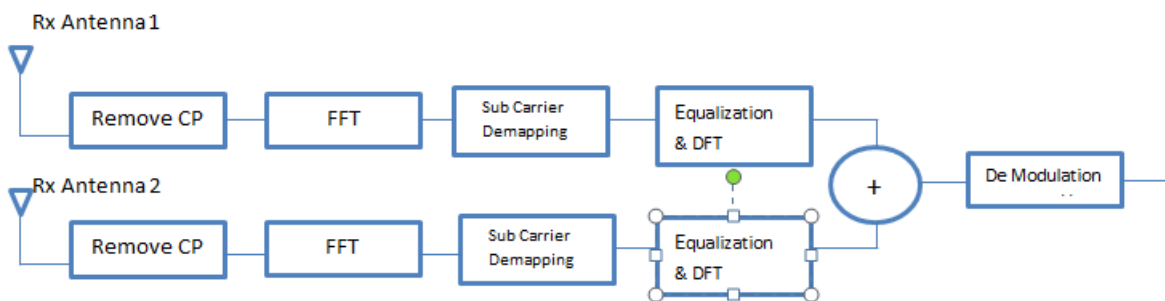


Figure 6.1b: PUSCH using 2 receiving antennas

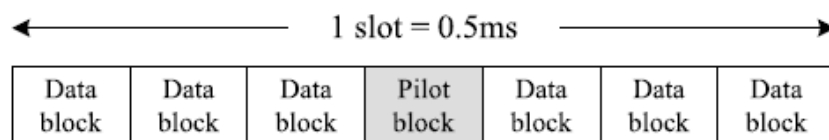


Figure 6.2: Slot Structure in LTE Uplink



### 6.1.1 Least Square Estimation

Let  $P_k$  denote the transmit pilot symbol on the  $k^{th}$  sub-carrier, where  $\sigma_p^2 = E[|P_k|^2]$  is the expected pilot symbol power. The received pilot symbol on the  $k^{th}$  sub-carrier is given by

$$Y_k = H_k P_k + N_k, \quad k = 0, \dots, K-1 \quad (6.1)$$

where  $K$  is the number of user sub-carriers,  $H_k$  is the  $k^{th}$  frequency channel response, and  $N_k$  is the  $k^{th}$  received noise with a variance of  $\sigma_n^2$ . Rewriting the 6.1 in the matrix form, the received pilot vector is denoted as  $\bar{\mathbf{Y}} = [Y_0, \dots, Y_{K-1}]^T$ , is given by

$$\bar{\mathbf{Y}} = \mathbf{P}\bar{\mathbf{H}} + \bar{\mathbf{N}} \quad (6.2)$$

where,  $\mathbf{P} = \text{diag}[P_0, \dots, P_{K-1}]$  is the frequency domain pilot matrix,  $\bar{\mathbf{H}} = [H_0, \dots, H_{K-1}]^T$  is the frequency domain channel vector and  $\bar{\mathbf{N}} = [N_0, \dots, N_{K-1}]^T$  is the received noise vector. In the LS estimation method, the aim is to minimize the squared difference between the observed signal and the desired signal [1]. Let  $\bar{\mathbf{H}}_{LS} = [H_{LS,0}, \dots, H_{LS,K-1}]^T$  denote the frequency domain least square frequency domain channel estimator vector, the cost function is

$$\begin{aligned} J_{LS} &= (\bar{\mathbf{Y}} - \mathbf{P}\bar{\mathbf{H}}_{LS})^H (\bar{\mathbf{Y}} - \mathbf{P}\bar{\mathbf{H}}_{LS}) \\ &= \bar{\mathbf{Y}}^H \bar{\mathbf{Y}} - \bar{\mathbf{Y}}^H \mathbf{P}\bar{\mathbf{H}}_{LS} - \bar{\mathbf{H}}_{LS}^H \mathbf{P}^H \bar{\mathbf{Y}} + \bar{\mathbf{H}}_{LS}^H \mathbf{P}^H \mathbf{P}\bar{\mathbf{H}}_{LS} \end{aligned} \quad (6.3)$$

Taking the derivation of  $J_{LS}$  with respect to  $\bar{\mathbf{H}}_{LS}^*$  and equating to zero,

$$\frac{\partial J_{LS}}{\partial \bar{\mathbf{H}}_{LS}^*} = \mathbf{P}^H \bar{\mathbf{Y}} - \mathbf{P}^H \mathbf{P}\bar{\mathbf{H}}_{LS} = \mathbf{O}_{K \times 1} \quad (6.4)$$

Solving the above equation for  $\bar{\mathbf{H}}_{LS}$  the LS frequency channel estimate is thus given by [1]

$$\bar{\mathbf{H}}_{LS} = (\mathbf{P}^H \mathbf{P})^{-1} \mathbf{P}^H \bar{\mathbf{Y}} \quad (6.5)$$

Since  $\mathbf{P}$  is a diagonal matrix, the LS channel estimate on the  $k^{th}$  subcarrier can be obtained as

$$\bar{H}_{LS,k} = \frac{P_k^*}{|P_k|^2} Y_k = \frac{Y_k}{P_k} \quad k = 0, 1 \dots K-1. \quad (6.6)$$

### Mean Square Error (MSE) of LS channel Estimator

Substituting (6.5) into (6.2), the LS channel estimate vector is given by

$$\bar{\mathbf{H}}_{LS} = \bar{\mathbf{H}} + \underbrace{(\mathbf{P}^H \mathbf{P})^{-1} \mathbf{P}^H \bar{\mathbf{N}}}_{\bar{\boldsymbol{\epsilon}}_{LS}} \quad (6.7)$$

where  $\bar{\boldsymbol{\epsilon}}_{LS} = [\epsilon_{LS,0}, \dots, \epsilon_{LS,K-1}]$  is the LS estimation noise vector. Hence the MSE of the LS channel estimate is given by

$$\begin{aligned} MSE &= \frac{1}{K} \text{tr} \left\{ E \left[ \bar{\boldsymbol{\epsilon}}_{LS} \bar{\boldsymbol{\epsilon}}_{LS}^H \right] \right\} \\ &= \frac{1}{K} \text{tr} \left\{ (\mathbf{P}^H \mathbf{P})^{-1} \mathbf{P}^H \underbrace{E[\mathbf{N}\bar{\mathbf{N}}^H]}_{\sigma_n^2 I_K} \mathbf{P} (\mathbf{P}^H \mathbf{P})^{-1} \right\} \\ &= \frac{\sigma_n^2}{K} \text{tr} (\mathbf{P}^H \mathbf{P})^{-1} \end{aligned} \quad (6.8)$$

It is shown in that the minimum MSE is attained if and only if  $(\mathbf{P}^H \mathbf{P})^{-1}$  is diagonal matrix and all the diagonal elements are equal (ie  $|p_k^2| = \sigma_p^2$ ). Hence, when the pilot symbols have a flat frequency spectrum, the minimum MSE of  $\frac{\sigma_n^2}{\sigma_p^2}$ .

### 6.1.2 LMMSE Channel Estimator

The LS channel estimator is widely used in practice due to its ease of implementation, amounting to the minimization of a least squares error criterion. By exploiting a prior knowledge of the channel statistics, the LMMSE estimator is optimal in the sense of minimizing the MSE of the channel estimate and hence provides the best channel estimation performance in terms of the lowest MSE.

The LS frequency channel estimate  $\bar{\mathbf{H}}_{\text{LS}}$  can be viewed as noisy observation of actual frequency of channel  $\bar{\mathbf{H}}$ . Let  $K \times K$  matrix  $\Theta$  denotes the LMMSE estimation matrix, the LMMSE channel estimate can be obtained by filtering  $\bar{\mathbf{H}}_{\text{LS}}$

$$\bar{\mathbf{H}}_{\text{LMMSE}} = \Theta \bar{\mathbf{H}}_{\text{LS}} \quad (6.9)$$

The cost function is defined as the MSE between  $\bar{\mathbf{H}}_{\text{LMMSE}}$  and  $\bar{\mathbf{H}}$  i.e.[1]

$$\begin{aligned} J_{\text{LMMSE}} &= \text{tr} \left\{ E \left[ (\bar{\mathbf{H}}_{\text{LMMSE}} - \bar{\mathbf{H}})(\bar{\mathbf{H}}_{\text{LMMSE}} - \bar{\mathbf{H}})^H \right] \right\} \\ &= \text{tr} \left\{ E \left[ (\Theta \bar{\mathbf{H}}_{\text{LS}} - \bar{\mathbf{H}})(\Theta \bar{\mathbf{H}}_{\text{LS}} - \bar{\mathbf{H}})^H \right] \right\} \\ &= \text{tr} \left\{ E \left[ (\Theta \bar{\mathbf{H}} + \Theta \bar{\epsilon}_{\text{LS}} - \bar{\mathbf{H}})(\Theta \bar{\mathbf{H}} + \Theta \bar{\epsilon}_{\text{LS}} - \bar{\mathbf{H}})^H \right] \right\} \\ &= \text{tr} \left\{ \Theta \mathbf{R}_{\bar{\mathbf{H}}\bar{\mathbf{H}}} \Theta^H - \Theta \mathbf{R}_{\bar{\mathbf{H}}\bar{\mathbf{H}}} + \Theta \left( \frac{\sigma_n^2}{\sigma_p^2} I_K \right) \Theta^H - \mathbf{R}_{\bar{\mathbf{H}}\bar{\mathbf{H}}} \Theta^H - \mathbf{R}_{\bar{\mathbf{H}}\bar{\mathbf{H}}} \right\} \end{aligned} \quad (6.10)$$

Where  $\mathbf{R}_{\bar{\mathbf{H}}\bar{\mathbf{H}}} = E[\bar{\mathbf{H}}\bar{\mathbf{H}}^H]$  is a  $K \times K$  channel correlation matrix and  $E[\bar{\epsilon}_{\text{LS}}\bar{\epsilon}_{\text{LS}}^H] = \frac{\sigma_n^2}{\sigma_p^2} I_K$ .

Taking the derivative of  $J_{\text{LMMSE}}$  with respect to  $\Theta^*$  and equating to zero we obtain

$$\frac{\partial J_{\text{LMMSE}}}{\partial \Theta^*} = \Theta \mathbf{R}_{\bar{\mathbf{H}}\bar{\mathbf{H}}} + \Theta \left( \frac{\sigma_n^2}{\sigma_p^2} I_K \right) - \mathbf{R}_{\bar{\mathbf{H}}\bar{\mathbf{H}}} = O_{K \times 1} \quad (6.11)$$

Solving the above equation for  $\Theta$ , The LMMSE estimation matrix is obtained as

$$\Theta = \mathbf{R}_{\bar{\mathbf{H}}\bar{\mathbf{H}}} \left( \mathbf{R}_{\bar{\mathbf{H}}\bar{\mathbf{H}}} + \frac{\sigma_n^2}{\sigma_p^2} I_K \right)^{-1} \quad (6.12)$$

By substituting the (6.12) into (6.9), the LMMSE channel estimation is given by [5]

$$\bar{\mathbf{H}}_{\text{LMMSE}} = \mathbf{R}_{\bar{\mathbf{H}}\bar{\mathbf{H}}} \left( \mathbf{R}_{\bar{\mathbf{H}}\bar{\mathbf{H}}} + \frac{\sigma_n^2}{\sigma_p^2} I_K \right)^{-1} \bar{\mathbf{H}}_{\text{LS}} \quad (6.13)$$

As shown in (6.13), a matrix multiplication is required to obtain the LMMSE channel estimate, and a matrix inversion is required for estimator coefficient calculation. Therefore, the LMMSE channel estimator requires a much higher complexity than the LS channel estimator.

### 6.1.3 DFT Based Channel Estimation with transform domain cutoff filter

As previously mentioned, the LS channel estimate can be viewed as the noisy observation of the actual channel response. By converting the frequency domain LS channel estimate to the time domain via the IDFT, the channel energy will be concentrated in a few time domain taps and the LS estimation noise will be distributed uniformly across all the taps. Finally, by converting the filtered time domain channel estimate back to the frequency domain via the DFT, a more accurate frequency domain channel estimate can be obtained for FDE coefficient calculation.

The conventional DFT-based channel estimation [6],[7] exploits the feature of OFDM systems having symbol length much larger than the length of channel impulse response(CIR).

The DFT-based channel estimation technique has been derived to improve the performance of LS channel estimation by eliminating the effect of noise outside the maximum channel delay. DFT Based Channel Estimation is based on the property that the energy of the channel is very concentrated in the time domain. The Figure 6.3 shows the DFT based channel estimator. Considered the channel estimation obtained from



Figure 6.3: DFT based Channel Estimator

the least squares ie  $\bar{H}_{LS}$  and apply the IDFT operation on the least square estimations. Then its gives the  $\bar{h}_{LS}$  which in the transform domain or time domain estimates

$$\bar{h}_{LS}(n) = \frac{1}{K} \sum_{k=0}^{K-1} \bar{H}_{LS}(k) e^{j\frac{2\pi nk}{K}} \quad 0 \leq n \leq K-1 \quad (6.14)$$

A de-noising filter is then applied in time domain to reduce noise. The transform domain cutoff filter  $w_{CF}(n)$  can be designed by simply keeping the transform domain samples at the "energy concentration" region as useful CIR samples and setting the samples at the "noise-only" region to be zeros[8],i.e.,

$$w_{CF}(n) = 1, \quad \text{if } 0 \leq n \leq f_c - 1, K - f_c \leq n \leq K - 1 \\ = 0, \quad \text{otherwise} \quad (6.15)$$

where  $f_c$  is the "cutoff" point of the transform domain filter.  $f_c$  is commonly chosen as channel length L or CP length  $N_{CP}$  if there is no knowledge about the channel length L [8]. Note that  $K-2 f_c$  samples have been removed by this hard cutoff filtering, which might also contain useful CIR information smearing into the "noise-only" region. The transform domain estimates after noise removing are then given by

$$\bar{h}_{nr}(n) = w_{CF}(n) \bar{h}_{LS}(n), \quad 0 \leq n \leq K-1 \quad (6.16)$$

Finally , the time domain filtered samples are transformed via a DFT block to get the final channel estimates back in frequency domain.

$$\bar{H}_{DFT}(k) = \sum_{n=0}^{K-1} \bar{h}_{nr}(n) e^{-j\frac{2\pi nk}{K}}, \quad 0 \leq k \leq K-1 \quad (6.17)$$

One additional improvement is to further suppress the noise effect in the transform domain by comparing time domain estimates powers with a threshold determined by the estimated noise power[7]. Thus the

noise removal filter further updated as (6.18).

$$\begin{aligned}
w_{CFNR} &= 1, & |\bar{h}_{LS}(n)|^2 &\geq \alpha \hat{\sigma}_n^2, & 0 \leq n \leq N_c - 1, K - N_c \leq n \leq K - 1 \\
&= 0, & |\bar{h}_{LS}(n)|^2 &< \alpha \hat{\sigma}_n^2, & 0 \leq n \leq N_c - 1, K - N_c \leq n \leq K - 1 \\
&= 0, & & & N_c \leq n < K - N_c
\end{aligned} \tag{6.18}$$

In (6.18),  $\hat{\sigma}_n^2$  denotes the estimated noise power and  $\alpha$  is a scaling factor that can be adjusted as a noise margin.

Assuming all the samples outside the energy concentration region contains noise only,[6] and [7] apply a noise power estimator by averaging the samples located in a "noise only" region, as is given by

$$\hat{\sigma}_n^2 = \frac{1}{K - 2N_c} \sum_{n=N_c}^{K-N_c-1} |\bar{h}_{LS}(n)|^2 \tag{6.19}$$

Thus the final channel estimates in the frequency domain with transform domain cutoff filter and in band noise removal can be obtained as

$$\bar{H}_{CFNR}(k) = \sum_{n=0}^{K-1} w_{CFNR}(n) \bar{h}_{LS}(n) e^{-\frac{j2\pi nk}{K}}, \quad 0 \leq k \leq K - 1 \tag{6.20}$$

Note that the above DFT based CE implementation method does not require any information about the channel and DFT/IDFT units are available blocks in the system. Thus it has very low implementation complexity.

#### 6.1.4 Linear Averaging Method

Any uplink UE will be allocated with only a part of available system bandwidth. In these scenarios conventional DFT method degrades significantly due to leakage of channel energy into adjacent taps, when partial frequency response is transformed to time domain. Multipath channel with an average delay spread of  $3\mu s$  will be in coherence across tones with in a Resource block [9]

$$\begin{aligned}
Y(k) &= H(k)X(k) + N(k) \\
\bar{H}_{LS}(k) &= \frac{Y(k)}{X(k)} \\
H_{avg}(k) &= \frac{1}{2\alpha - 1} \sum_{p=-\alpha}^{\alpha} \bar{H}_{LS}(k - p)
\end{aligned} \tag{6.21}$$

## 6.2 Equalization

An equalizer compensates for linear distortion introduced by the multipath propagation channel. For broadband channels, conventional time domain equalizers are impractical because of very long channel impulse response in the time domain. Frequency domain equalization (FDE) is more practical for such channels. Channel equalization is essentially an inverse filtering of the linear distortion introduced to the channel by the multipath propagation.

Using DFT, the frequency domain equalization can be easily implemented using modern digital signal

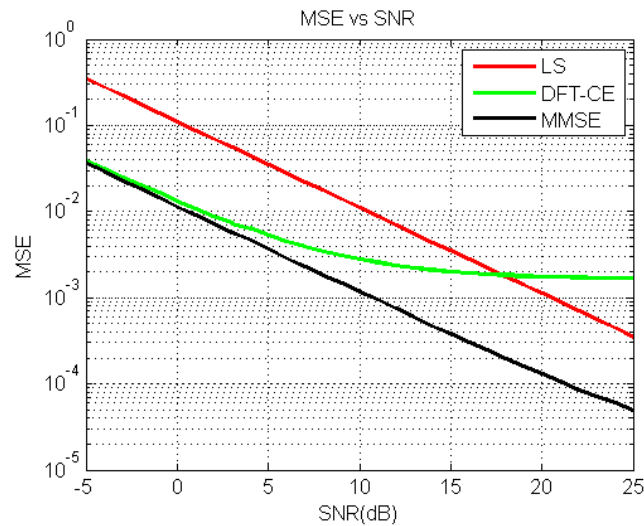


Figure 6.4: Different Channel Estimations with MSE vs SNR(dB)

processors (DSP). Because the DFT size does not grow linearly with the length of the channel response, the complexity of FDE is much lower than that of the equivalent time domain equalizer for broadband channels.

Single carrier modulation with frequency domain equalization (SC/FDE) is a practical technique for mitigating the effects of frequencyselective fading. It delivers performance similar to OFDM with essentially the same overall complexity, even for a long channel impulse response. The below figure shows the OFDMA and SCFDMA detection and equalization.

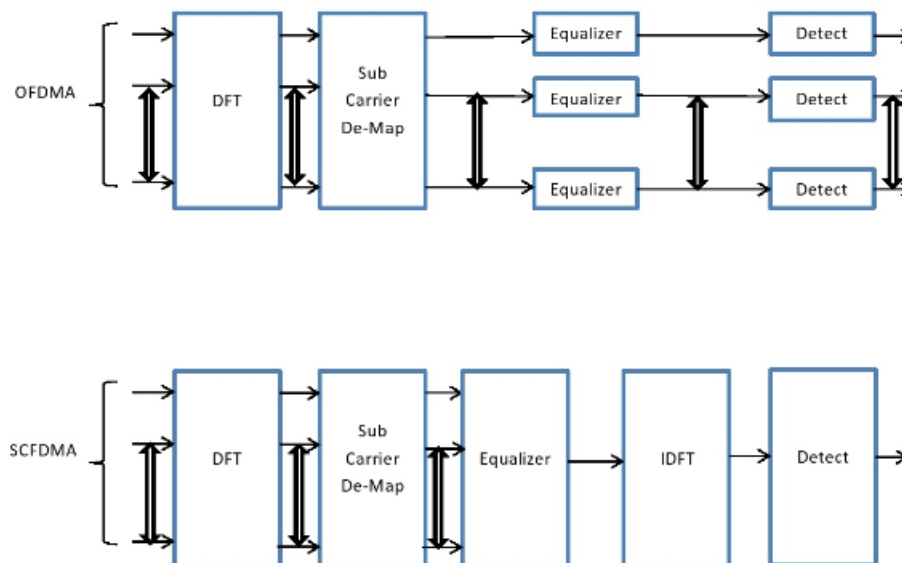


Figure 6.5: OFDMA and SCFDMA Detection and Equalization

### 6.2.1 ZF Equalization

The received SC FDMA symbol , after FFT and Sub Carrier Demapping is,

$$Y(k) = X(k)H(k) + N(k), \quad k = 0, 1, \dots, M_{sc}^{PUSCH} \quad (6.22)$$

where  $H(k)$  is estimated channel using pilot symbol and  $N(k)$  is Additive White Gaussian Noise Channel with complex normal distribution with mean zero and noise variance unity.

Now this received symbol is passed through the filter  $w(n)$  such that  $w(n) * h(n) = \delta(n)$ . In the Frequency domain  $W(k).H(k) = 1$ . So we can write  $W(k) = \frac{1}{H(k)}$ . The Zero forcing equalization is given by

$$\hat{X}(k) = \frac{Y(k)}{H(k)} \quad (6.23)$$

### 6.2.2 MMSE-LE Without Co-variance Estimation

A frequency domain vector valued MMSE filter is applied on received signal to minimize the effects of channel distortion.

$$\mathbf{Y}(k) = X(k)\mathbf{H}(k) + \mathbf{N}(k)$$

Receiver stacks up the frequency domain sample outputs from various antennas in vector format [10]

$$\begin{aligned} \mathbf{Y}(k) &= [Y_1(k) \dots Y_{N_r}(k)]^T \\ \mathbf{H}(k) &= [H_1(k) \dots H_{N_r}(k)]^T \\ \mathbf{N}(k) &= [N_1(k) \dots N_{N_r}(k)]^T \end{aligned}$$

Frequency domain filter 'W' will be operated on these stacked received output samples.

$$Z(k) = \mathbf{W}(k)\mathbf{Y}(k) = \sum_{l=1}^{N_r} W_l(k)Y_l(k) \quad (6.24)$$

We make use of orthogonality principle to derive equalizer coefficients

$$\mathbf{W}(k) = (R_{xx}^{-1}(k) + \mathbf{H}^\dagger(k)R_{nn}^{-1}(k)\mathbf{H}(k))^{-1}\mathbf{H}^\dagger(k)R_{nn}^{-1}(k) \quad (6.25)$$

### Theoretical Derivation

A frequency domain vector valued MMSE filter is applied on received signal to minimize the effect of channel distortion [10]

$$\begin{aligned} y(n) &= x(n) \odot h(n) + \underbrace{\sum_{t=1}^{T_r-1} x(n) \odot g_t(n)}_{\text{Co-channel Interference}} + \underbrace{\sum_{i=1}^{N_I} s(n)p_i(n)}_{\text{Adjacent-Channel Interference}} + \underbrace{n(n)}_{\text{AWNG}} \\ y_k &= h_{rx1}x_k + \sum_{m=1}^{t_r-1} g_m x_{m,k} + \sum_{i=0}^{n_I} l_i s_{i,k} + n_k \end{aligned} \quad (6.26)$$

Current setup is for  $2 \times 1$  MIMO system without adjacent channel interference

$$\begin{aligned}
y(k) &= x(k) \odot h(k) + n(k), \quad k = 0, 1, \dots, M_{sc}^{PUSCH} \\
\mathbf{y}(k) &= [y_1(k) \ y_2(k)]^T \\
\mathbf{h}(k) &= [h_1(k) \ h_2(k)]^T \\
\mathbf{n}(k) &= [n_1(k) \ n_2(k)]^T
\end{aligned} \tag{6.27}$$

Where  $n_1(k)$  and  $n_2(k)$  are iid complex Gaussian random variables with mean zero and variance  $\sigma^2$ . Applying M point FFT on  $\mathbf{y}(k)$

$$Y(k) = H(k)X(k) + N(k) \tag{6.28}$$

Applying Frequency domain vector valued MMSE Equalizer on  $Y(k)$

$$\hat{X}(k) = \sum_{l=1}^r W_l(k) Y_l(k) = \mathbf{W}(k) \mathbf{Y}(k) \tag{6.29}$$

$$\begin{aligned}
R_{yy}(k) &= E[\mathbf{Y}(k) \mathbf{Y}^\dagger(k)] \\
&= H(k) R_{xx}(k) H^\dagger(k) + R_{nn}(k) \\
R_{xy}(k) &= E[\mathbf{X}(k) \mathbf{Y}^\dagger(k)] \\
&= R_{xx}(k) H^\dagger(k) \\
R_{xx}(k) &= E[|X_k|^2] = m\sigma_x^2 \\
R_{nn}(k) &= E[\mathbf{N}(k) \mathbf{N}^\dagger(k)] = m\sigma_m^2 I
\end{aligned}$$

$$\begin{aligned}
W(k) &= R_{xx}(k) \mathbf{H}^\dagger(k) [\mathbf{H}(k) R_{xx}(k) \mathbf{H}^\dagger(k) + R_{nn}^{-1}]^{-1} \\
&= (R_{xx}^{-1}(k) + \mathbf{H}^{-1}(k) R_{nn}^{-1} \mathbf{H}(k))^{-1} \mathbf{H}^{-1}(k) R_{nn}^{-1}(k)
\end{aligned} \tag{6.30}$$

### 6.2.3 MMSE-LE With Co-variance Estimation

Frequency domain vector valued MMSE Filter where Interference plus Noise covariance is statistically estimated will be applied on received signal to minimize the effects of channel distortion and adjacent cell interference.

$$\mathbf{y}(k) = x(k) \mathbf{h}(k) + \underbrace{s(k) \mathbf{g}(k)}_{\text{Interference}} + \underbrace{n(k)}_{\text{Noise}} \tag{6.31}$$

we estimate Covariance of interference and noise across each Resource block as follows

$$\begin{aligned}
I_k^1 &= y_k^1 - h_k^1 x_k^P \\
I_k^2 &= y_k^2 - h_k^2 x_k^P \\
I &= [I_k^1 \quad I_k^2]^T
\end{aligned}$$

we assume channel to be at across sub-carriers per resource block

$$R_{i+n} = E[II^\dagger] = \frac{1}{12} \sum_{k=1}^{12} I_k I_k^\dagger$$

$$\text{diag}(R_{i+n}(k)) = [g_k^1 \quad g_k^2]^T \text{ in absence of noise}$$

$$R_{i+n}(k) = N_o N_r \text{ in absence of interference}$$

we invoke orthogonality principle to derive filter coefficients

$$w(k) = [R_{xx}^{-1} \mathbf{h}^\dagger R_{i+n}^{-1}(k) \mathbf{h}(k)]^{-1} \mathbf{h}^\dagger R_{i+n}^{-1}(k) \quad (6.32)$$

### 6.3 Inverse Precoding

As we know in the transmitter section, there is transform precoder (ie DFT) before inserting the data into the IFFT because to reduce the affect of PAPR. There is inverse process here ie IDFT before feeding the data into demodulation section.

$$\hat{d}(l.M_{sc}^{PUSCH} + k) = \frac{1}{\sqrt{M_{sc}^{PUSCH}}} \sum_{i=0}^{M_{sc}^{PUSCH}} \hat{z}(l.M_{sc}^{PUSCH} + i).e^{-j\frac{2\pi ik}{M_{sc}^{PUSCH}}}$$

$$k = 0, \dots, M_{sc}^{PUSCH} - 1$$

$$l = 0, \dots, \frac{M_{symb}}{M_{sc}^{PUSCH} - 1}$$

where  $\hat{z}$  is the received complex data after equalization and  $\hat{d}$  is the IDFT output.

### 6.4 Demodulation Section

Soft-demodulation, or more accurately soft-bit demodulation, is a demodulation process that estimates from the received demodulated symbols not only hard-bits (Boolean variable or binary digit: 0 or 1, or equivalently the polarity sign: positive or negative), but also their confidence levels. At the transmitter side, normally only hard-bits are involved, and they take the form of binary digits 0 or 1. However, at the receiver, particularly at the physical layer, these binary digits are more commonly represented as polarity signs, either negative or positive.

The soft bit is the LLR value i.e. The logarithmic ratio of probability of bit being 0 to the probability of the bit of being 1.

#### 6.4.1 Soft Demodulation of Binary Modulation in an AWGN Environment

The soft-demodulation process is normally straightforward in the case of binary modulation schemes, for instance BPSK. This characteristic is also valid in any 4-ary modulation scheme that is I-Q separable. hence can be regarded as dual-binary modulation schemes, for example Gray coded QPSK or Gray-coded 4-QAM schemes.

As we know the QPSK signal constellation is depicted in figure below having symbol energy  $E_{av} = 1$  and  $d$  in the figure equal to  $\frac{1}{\sqrt{2}}$  in an AWGN environment. Now suppose that a transmitter sends a modulated signal  $x$  through the AWGN channel  $n$  having zero mean and noise variance of  $\sigma^2$ . Denoting the received signal as  $r = r_I + r_Q = x + n$ , LLR of the received soft-bit from the real (or in-phase) component  $r_I$  [5]



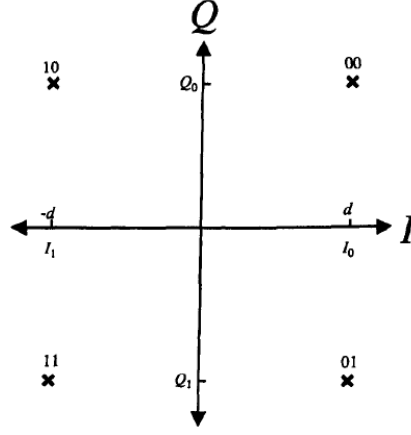


Figure 6.6: QPSK Constellation

$$LLR(b_I) = \log \left[ \frac{Pr(b_I = 0/r)}{Pr(b_I = 1/r)} \right] \quad (6.33)$$

According to Bayes Theorem,  $Pr\left(\frac{A}{B}\right) = \frac{Pr\left(\frac{B}{A}\right)Pr(A)}{Pr(B)}$

$$LLR(b_I) = \log \left[ \frac{\frac{Pr\left(\frac{r}{b_I=0}\right)Pr(b_I=0)}{Pr(r)}}{\frac{Pr\left(\frac{r}{b_I=1}\right)Pr(b_I=1)}{Pr(r)}} \right] \quad (6.34)$$

$$= \log \left[ \frac{Pr\left(\frac{r}{b_I=0}\right)}{Pr\left(\frac{r}{b_I=1}\right)} \right] + \log \left[ \frac{Pr(b_I = 0)}{Pr(b_I = 1)} \right] \quad (6.35)$$

Assuming the event of selecting bit  $b_I = 0, 1$  for transmission is equiprobable.

$$LLR(b_I) = \log \left[ \frac{\frac{1}{\sqrt{2\pi\sigma^2}} e^{-\frac{1}{2} \frac{(r_I-d)^2}{\sigma^2}}}{\frac{1}{\sqrt{2\pi\sigma^2}} e^{-\frac{1}{2} \frac{(r_I+d)^2}{\sigma^2}}} \right] \quad (6.36)$$

$$= \frac{2d}{\sigma^2} r_I \quad (6.37)$$

$$= \frac{2}{\sigma^2} \frac{r_I}{\sqrt{2}} \quad (6.38)$$

It follows that for imaginary (or quadrature) component case also, substitute the subscript Q for I. From this equation, it is evident that the LLR of a binary or dual-binary modulation scheme is just a simple function of the real or imaginary part of the received signal and its noise variance.

#### 6.4.2 Soft Demodulation in Rayleigh Fading Environment

Let Y denote either I or Q and  $\gamma$  denote the fading CSI that is represented by the estimated fading coefficient  $\hat{h}$ . The  $j^{th}$  bit LLR can be expressed as

$$LLR(b_Y^{(j)}) = \log \left[ \frac{Pr\left(\frac{b_Y^{(j)}=0}{z_Y}, \gamma\right)}{Pr\left(\frac{b_Y^{(j)}=1}{z_Y}, \gamma\right)} \right] \quad (6.39)$$

In this case

$$r = hx + n \quad (6.40)$$

and

$$\begin{aligned}
z &= z_I + jz_Q \\
&= \hat{h}^\dagger r \\
&= \hat{h}^\dagger (hx + n) \\
&= \hat{h}^\dagger hx + \hat{h}^\dagger n
\end{aligned}$$

Where  $\dagger$  represents the complex conjugation operation. Continuing the derivation, and assuming that the noise term  $\hat{h}^\dagger n$  is Gaussian distributed, it can be shown that

$$LLR(b_Y^{(j)}) = \log \left[ \frac{\sum_{y \in y_0^{(j)}} \frac{1}{\|\hat{h}\|^2 \sqrt{2\pi\sigma^2}} \exp\left(-\frac{1}{2\sigma^2 \|\hat{h}\|^2} (z_Y - \|\hat{h}\|^2 y)^2\right)}{\sum_{y \in y_1^{(j)}} \frac{1}{\|\hat{h}\|^2 \sqrt{2\pi\sigma^2}} \exp\left(-\frac{1}{2\sigma^2 \|\hat{h}\|^2} (z_Y - \|\hat{h}\|^2 y)^2\right)} \right] \quad (6.41)$$

$$= E_{y \in y_0^{(j)}} \frac{-1}{2\sigma^2 \|\hat{h}\|^2} \left( z_Y - \|\hat{h}\|^2 y \right)^2 - E_{y \in y_1^{(j)}} \frac{-1}{2\sigma^2 \|\hat{h}\|^2} \left( z_Y - \|\hat{h}\|^2 y \right)^2 \quad (6.42)$$

where E is operator is defined as

$$aEb = \log(\exp(a) + \exp(b)) \quad (6.43)$$

$$= \max(a, b) + \log(1 + \exp(-|a - b|)) \quad (6.44)$$

and  $y \in y_0^{(j)}$  denotes amplitude levels of modulation symbols constellation projected to Y axis corresponding to bit  $y^{(j)} = 0$ . Y represents I or Q axis, so  $z_y$  can mean either  $\text{Re}(Z)$  or  $\text{Im}(Z)$ . In QPSK case, there is only one member of y that satisfies  $y \in y_0^{(j)}$  that is  $y = +d$ .

So LLR reduces to

$$\begin{aligned}
LLR(b_y^{(j)}) &= \frac{-1}{2\pi \|\hat{h}\|^2} (z_y - \|\hat{h}\|^2 d)^2 + \frac{1}{2\pi \|\hat{h}\|^2} (z_y + \|\hat{h}\|^2 d)^2 \\
&= \frac{2Z_y}{\sigma^2} \\
&= \frac{\sqrt{2}z_y}{\sigma^2} \quad (6.45)
\end{aligned}$$

For the non binary operation is involved, operator E can be calculated recursively, for example

$$\begin{aligned}
\sum_{i=1}^3 a_i &= a_1 E a_2 E a_3 \\
&= a_1 E (a_2 E a_3) \quad (6.46)
\end{aligned}$$

In 16-QAM, however, there are two bits from each I and Q axis that make up a modulation symbol. The constellation representations of 16 QAM is Adopting  $\{i_l q_l i_0 q_0\}$  bit arrangement, where letter  $i$  signifies that the bits originate from I axis, this constellation point is made up of  $i_l = 0, i_0 = 1$  bits from I axis and  $q_l = 0, q_0 = 1$  bits from Q axis. For further convenience, the bit with subscript 1 will be referred to as MSB, whereas the other with subscript 0 will be called LSB.

It is apparent that for MSB

$$\begin{aligned}
y \in y_0^{(1)} &= \{d, 3d\} \\
y \in y_1^{(1)} &= \{-d, -3d\}
\end{aligned}$$

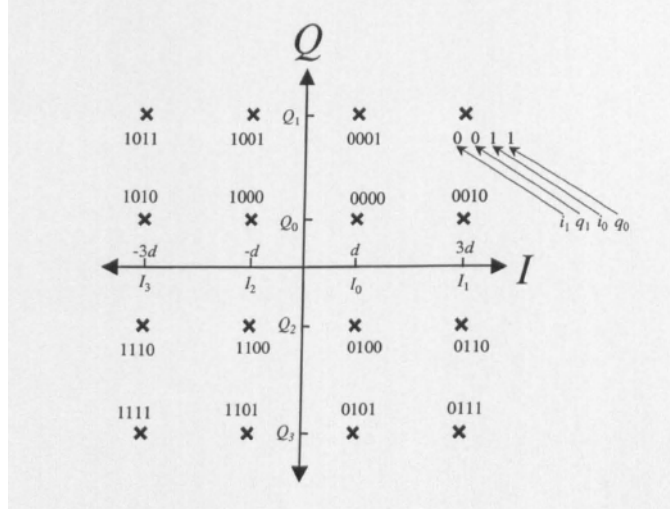


Figure 6.7: 16QAM Constellation

while for LSB

$$y \in y_0^{(0)} = \{-d, d\}$$

$$y \in y_1^{(0)} = \{-3d, 3d\}$$

Therefore for MSB

$$L_c(b_y^{(1)}) = E_{y=\{-d, -3d\}} \frac{-1}{2\sigma^2 \|\hat{\alpha}\|^2} (z_y - \|\hat{\alpha}\|^2 y)^2 - E_{y=\{d, 3d\}} \frac{-1}{2\sigma^2 \|\hat{\alpha}\|^2} (z_y - \|\hat{\alpha}\|^2 y)^2 \quad (6.47)$$

and for LSB

$$L_c(b_y^{(0)}) = E_{y=\{-d, d\}} \frac{-1}{2\sigma^2 \|\hat{\alpha}\|^2} (z_y - \|\hat{\alpha}\|^2 y)^2 - E_{y=\{-3d, 3d\}} \frac{-1}{2\sigma^2 \|\hat{\alpha}\|^2} (z_y - \|\hat{\alpha}\|^2 y)^2 \quad (6.48)$$

Due to simplicity of the exact soft-demodulation method for the QPSK case, there is no need of approximation. On the contrary, in the 16-QAM case, the calculation involves the computationally-intensive E operation. Therefore, in the following description and in the sections regarding the approximation methods, 16-QAM modulation is implied. The most obvious and straightforward approximation for this operation is, popularly applied in LogMAP decoding algorithm to produce its simpler version MaxLogMAP, the "taking the maximum" operation defined as follows

$$aMb \equiv \max(a, b) \quad (6.49)$$

Similar to the E operation, multiterm M operation can be performed recursively. Therefore, Therefore for MSB

$$L_c(b_y^{(1)}) = M_{y=\{-d, -3d\}} \frac{-1}{2\sigma^2 \|\hat{\alpha}\|^2} (z_y - \|\hat{\alpha}\|^2 y)^2 - M_{y=\{d, 3d\}} \frac{-1}{2\sigma^2 \|\hat{\alpha}\|^2} (z_y - \|\hat{\alpha}\|^2 y)^2 \quad (6.50)$$

and for LSB

$$L_c(b_y^{(0)}) = M_{y=\{-d, d\}} \frac{-1}{2\sigma^2 \|\hat{\alpha}\|^2} (z_y - \|\hat{\alpha}\|^2 y)^2 - M_{y=\{-3d, 3d\}} \frac{-1}{2\sigma^2 \|\hat{\alpha}\|^2} (z_y - \|\hat{\alpha}\|^2 y)^2 \quad (6.51)$$

### 6.4.3 BER vs SNR Plots for MMSE-LE with and without Co-variance Estimation

The BER vs SNRdB plots for MMSE LE with and without covariance estimation as shown below

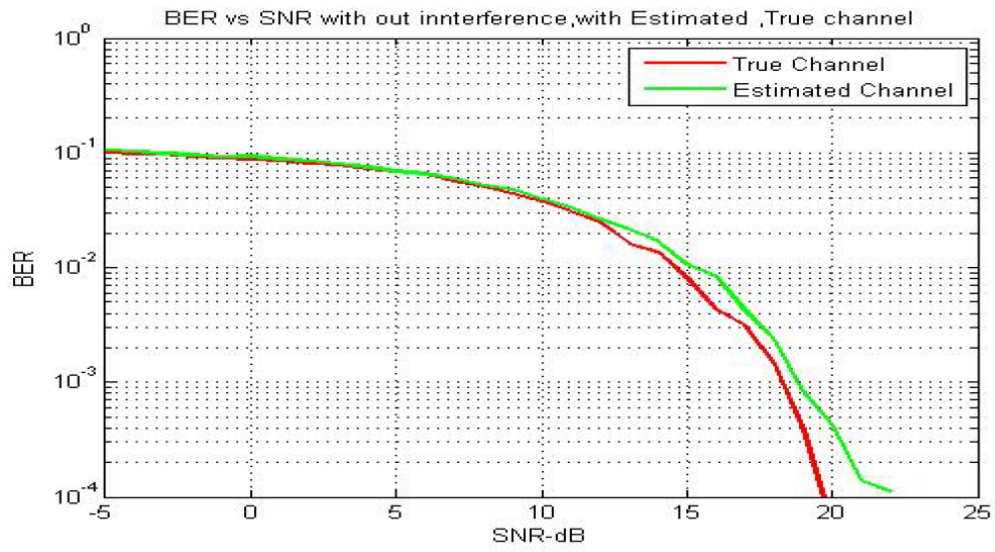


Figure 6.8(a): BER vs SNRdB for MMSE-LE without covariance estimation

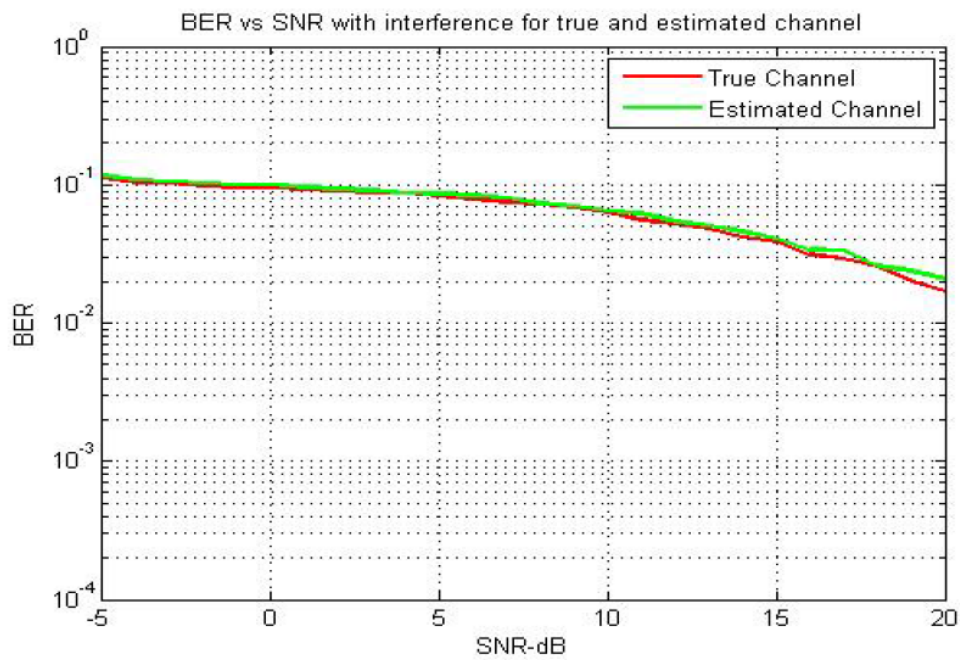


Figure 6.8(b): BER vs SNRdB for MMSE-LE with covariance estimation

## References

- [1]. S. Kay, *Fundamentals of Statistical Signal Processing, Volume I: Estimation Theory*, 1st ed. Upper Saddle River, New Jersey: Prentice Hall, 1993.
- [2] van de Beek, J.J., Edfors, O., Sandell, M. et al. (July 1995) On channel estimation in OFDM systems. *IEEE VTC'95*, vol. 2, pp. 815–819.
- [3] S. Sesia, I. Toufik, and M. Baker, *LTE - The UMTS Long Term Evolution: from Theory to Practice*. John Wiley and Son, 2009.
- [4] Coleri, S., Ergen, M., Puri, A., and Bahai, A. (2002) Channel estimation techniques based on pilot arrangement in OFDM systems. *IEEE Trans. on Broadcasting*, 48(3), 223–229.
- [5] “OFDM channel estimation by singular value decomposition,” *IEEE Trans. Commun.*, vol. 46, no. 7, pp. 931–939, Jul. 1998.
- [6] Y. Kang, K. Kim, and H. Park, “Efficient DFT-based channel estimation for OFDM systems on multipath channels,” *Communications, IET*, vol. 1, no. 2, pp. 197–202, Apr. 2007.
- [7] Y.-S. Lee, H.-C. Shin, and H.-N. Kim, “Channel estimation based on a time-domain threshold for OFDM systems,” *Broadcasting, IEEE Transactions on*, vol. 55, no. 3, pp. 656–662, Sep. 2009.
- [8] S. Wei and P. Zhiwen, “Iterative LS channel estimation for OFDM systems based on transform-domain processing,” in *Wireless Communications, Networking and Mobile Computing, 2007. WiCom 2007. International Conference on*, Sep. 2007, pp. 416–419.
- [9] Meilong Jiang, Guosen Yue, Narayan Prasad and Sampath Rangarajan, *Enhanced DFT-based Channel Estimation for LTE Uplink*, *IEEE VTC 2012-Spring* IEEE 978-1-4673-0990-5, 2012.
- [10] K. Kuchi, Limiting behavior of ZF/MMSE linear equalizers in wideband channels with frequency selective fading, *IEEE Commun. Lett.*, vol. 16, pp. 929-932, 2012



## 7 | Receiver design for PUCCH-Formats 2,2a and 2b

In LTE UL, PUCCH reports Scheduling Request(SR), DL Channel Quality Indicator (CQI) information, Precoding Matrix Indicator(PMI), Rank Indication(RI), and 1 or 2 Acknowledge/Non-Acknowledge (ACK/NACK) bits to eNodeB. PUCCH is divided into six transmission formats namely 1/1a/1b/2/2a/2b. These formats are defined by the type of transmitted information. The SR is transmitted via PUCCH, format 1. The SR requirement from UE is given only by power emissions in the control region in the resource grid. PUCCH format 1a/1b transmits a one or two-bit HARQ-ACK codeword which is modulated using the BPSK or QPSK modulation scheme. PUCCH format 2 carries CQI/PMI and RI information. The format 2 codeword has a length from 5 to 13 bits. It uses the QPSK modulation scheme. In the case of format 2a/2b codeword, one or two bit HARQ-ACK information is only added to format 2. In the case of format 2a, a one bit HARQ-ACK codeword is modulated using BPSK and in the case of format 2b, a two bit HARQ-ACK codeword is modulated using QPSK [1,2].

Demodulation Reference Signals(DMRS) are time multiplexed with the data symbols on PUCCH and occupy the same bandwidth as its PUCCH data transmission for a given UE [2]. These Reference Signals (RSs) are primarily used for channel estimation. However, one of the RSs for PUCCH formats 2a/2b is based on transmitted ACK/NACK in UE, and then the receivers at eNodeB have no complete priori-knowledge about RSs and can not utilize them to do channel estimation.

The overall PUCCH signal processing chain is depicted in Figures (7.1) and (7.2). These signal processing chains became the base for the developed link level PUCCH model.

Format 2, CQI/PMI and RI, is channel coded using the (20,A) Reed-Muller code, where 'A' is the length of input codeword in bits [1]. When channel coding is performed, the output sequence of 20 bits in length is multiplexed with the one or two-bit HARQ-ACK codeword and scrambled using a cell-specific pseudo-random sequence  $c(n)$ . The scrambled data are modulated using QPSK and BPSK modulation.

Next, the modulated and spread signal is led to the resource mapping block and IFFT is performed. After the addition of a cyclic prefix (CP), the signal in the time domain enters the transmission channel. PUCCH resources are always doubled (additional frequency diversity) and placed on the edge of time- frequency resource grid.

The received signal after FFT/DFT operation is given by

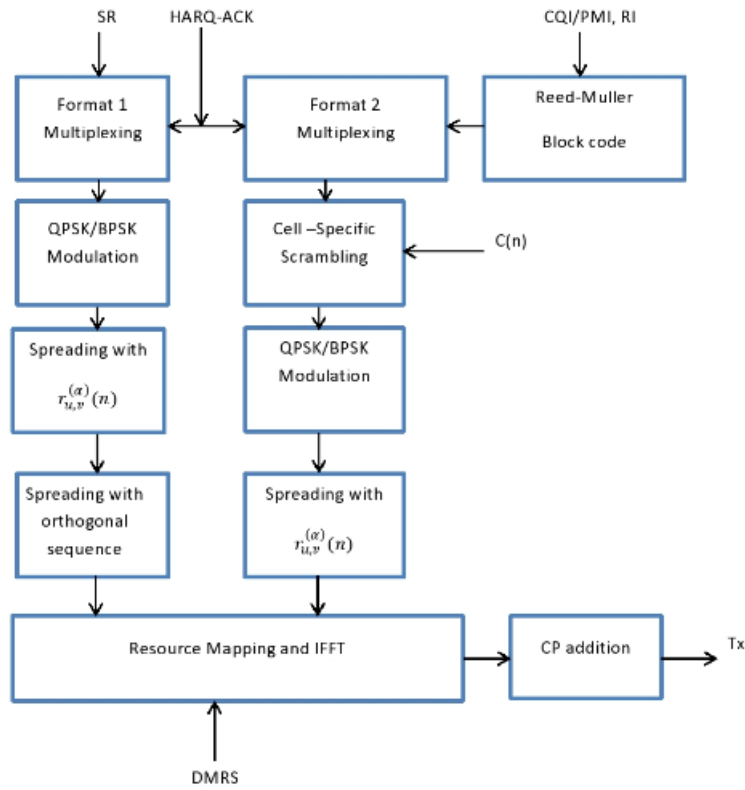


Figure 7.1: PUCCH Signal Processing in Transmitter

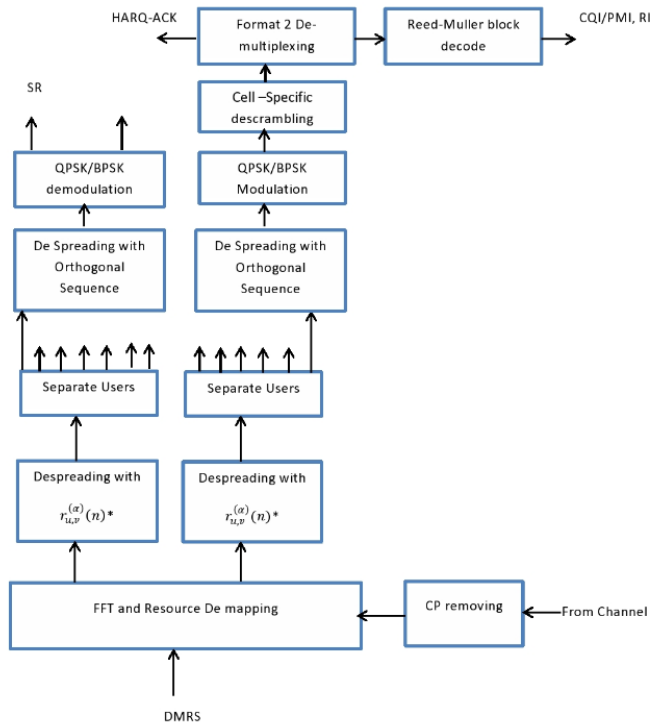


Figure 7.2: PUCCH Signal Processing in Receiver



$$\mathbf{Y} = \mathbf{H}\mathbf{X} + \mathbf{N} \quad (7.1)$$

$$\mathbf{Y} = [Y_1, \dots, Y_r]^T$$

$$\mathbf{X} = [X_1, \dots, X_t]^T$$

$$\mathbf{H} = \begin{bmatrix} H_{11} & H_{12} & \dots & H_{1t} \\ H_{21} & H_{22} & \dots & H_{2t} \\ \vdots & \vdots & \dots & \vdots \\ H_{r1} & H_{r2} & \dots & H_{rt} \end{bmatrix}$$

$$\mathbf{N} = [N_1, \dots, N_r]^T$$

$\mathbf{N}$  is the Additive White Gaussian Noise Channel (AWGN) of size  $r \times 1$ . Where  $r$  is the number of receiving antennas and  $t$  is the number of transmitting antennas.

## 7.1 Channel Estimation

The channel Estimation can be based on

- Least Square Estimation (LS)
- Linear MMSE Estimation (LMMSE)
- DFT Based Channel Estimation (DFT-CE)
- 2D-Minimum Mean Square Estimation (2D-MMSE)

### 7.1.1 LS Estimation

As discussed in section (6.1.1), the LS frequency channel estimates is given by [3]

$$\bar{H}_{LS,k} = \frac{Y_k}{P_k}, \quad k = 0, 1, \dots, M_{sc}^{PUCCH} \quad (7.2)$$

Where  $Y_k$  is Recieved symbol on  $k$ th subcarrier,  $P_k$  is Pilot symbol on  $k$ th subcarrier and  $M_{sc}^{PUCCH}$  is number of subcarriers allocated to PUCCH.

Without using any knowledge of the statistics of the channels, the LS estimators are calculated with very low complexity, but they suffer from a high Mean Square Error (MSE).

The (MSE) of LS estimate is given by the Equation (6.8).

In case of PUCCH format 2a/2b only one Reference Symbol(RS) is available since the second RS is modulated by ACK/NACK so that the performance of channel estimation which is based on only one RS is poor. The following procedure give the a coherent demodulation algorithm for estimated second symbol in a slot for format 2a/2b [4] assuming that channel characteristics are with in the coherence time in a slot.

#### Parameter Description:

Symbols  $\mathbf{R}_1$  and  $\mathbf{R}_5$  are represents the Reference Symbol 1 and Reference Symbol 5 in receiver and symbol  $\mathbf{r}_1$  and  $\mathbf{r}_5$  are represent Reference Symbol 1 and Reference Symbol 5 in transmitter . Data symbol of CQI is represent by symbol  $\mathbf{Y}$ , and  $\mathbf{H}$  is impulse response of resources grid.

#### Algorithm Flow:

The algorithm is suitable for PUCCH format 2a/2b and can be summarized as follows and flow chart for

the algorithm shown in Figure (7.3)

STEP 1: Extract the RSs  $\mathbf{R}_1$  and  $\mathbf{R}_5$  from the resource grid in the receiver.

STEP 2: Channel Estimates can be obtained from the first RS since it known to both transmitter and receiver.

$$H_1(k) = \frac{R_1(k)}{r_1(k)}, \quad k = 0, 1 \dots M_{sc}^{PUCCH}$$

STEP 3: The second RS  $\mathbf{R}_5$  is generated by RS  $\mathbf{r}_5$  which is modulated by information of ACK and impulse response  $\mathbf{H}_5$ . Where  $\mathbf{r} = [\alpha_1, \dots, \alpha_N]$  where  $N = 12$  and  $\alpha_i$  is is subcarrier which is include complex symbol, and then coherent with RS  $\mathbf{r}$  which is not include the ACK information, where

$$S_r = \sum_{i=1}^N \frac{R_{5,i} \cdot r_i^*}{R_{1,i}}$$

STEP 4:  $S_r$  will be dispose with special QPSK demodulation by PUCCH, specific reference Table 5.2, and original ACK bit is obtained. RS  $\mathbf{r}_5$  can be generated by original ACK bit.

STEP 5: The second Impulse response  $\mathbf{H}_5$  is obtained by channel estimation with RS  $\mathbf{R}_5$  and RS  $\mathbf{r}_5$  which regenerate in local, where  $H_{5,k} = \frac{R_{5,k}}{r_{5,k}}$ .

STEP 6: All Impulse response  $H(k, l)$  in resources grid is obtained by linear interpolation with two Impulse response  $H_1$  and  $H_5$  of reference signal, and then extract symbol Y which include CQI information from resources grid and signal detection.

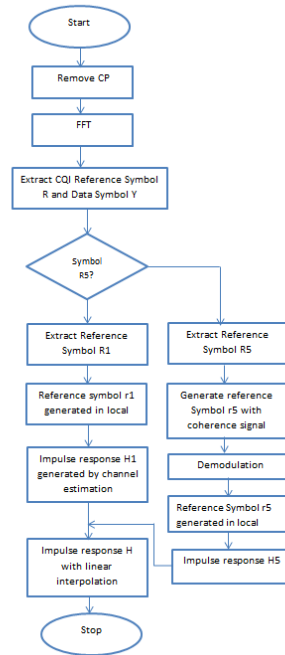


Figure 7.3: Algorithm Flow of PUCCH Channel Estimation (Formats 2a/2b)

### 7.1.2 LMMSE Estimation

Consider the LS solution given in the Equation (7.2), can be written in the vector form

$$\bar{\mathbf{H}}_{LS} = \mathbf{X}_D^{-1} \mathbf{Y} \triangleq \tilde{\mathbf{H}} \quad (7.3)$$

Where  $\mathbf{X}_D$  is the diagonal matrix of pilot symbols. Using the weight matrix  $\mathbf{W}$ , define  $\hat{\mathbf{H}} = \mathbf{W}\tilde{\mathbf{H}}$  which corresponds to MMSE estimate.

MSE of the channel estimates is given as

$$J(\tilde{\mathbf{H}}) = E\{\|\mathbf{e}\|^2\} = E\{\|\mathbf{H} - \tilde{\mathbf{H}}\|^2\} \quad (7.4)$$

Then, the MMSE channel estimation method finds a better estimate in terms of  $\mathbf{W}$  in such a way that the MSE in Equation (7.4) is minimized. The orthogonality principle states that the estimation error vector  $\mathbf{e} = \mathbf{H} - \hat{\mathbf{H}}$  is orthogonal to  $\tilde{\mathbf{H}}$ , such that

$$\begin{aligned} \mathbf{E}[\mathbf{e}\tilde{\mathbf{H}}^\dagger] &= \mathbf{E}[(\mathbf{H} - \hat{\mathbf{H}})\tilde{\mathbf{H}}^\dagger] \\ &= \mathbf{E}[(\mathbf{H} - \mathbf{W}\tilde{\mathbf{H}})\tilde{\mathbf{H}}^\dagger] \\ &= \mathbf{E}\{\mathbf{H}\tilde{\mathbf{H}}^\dagger\} - \mathbf{W}\mathbf{E}\{\tilde{\mathbf{H}}\tilde{\mathbf{H}}^\dagger\} \\ &= \mathbf{R}_{\mathbf{H}\tilde{\mathbf{H}}} - \mathbf{W}\mathbf{R}_{\tilde{\mathbf{H}}\tilde{\mathbf{H}}} = 0 \end{aligned} \quad (7.5)$$

Where  $\mathbf{R}$  is the cross correlation matrix, and  $\tilde{\mathbf{H}}$  is the LS channel estimate given as,

$$\tilde{\mathbf{H}} = \mathbf{X}_D^{-1}\mathbf{Y} = \mathbf{H} + \mathbf{X}_D^{-1}\mathbf{N} \quad (7.6)$$

Solving Equation (7.5) for  $\mathbf{W}$  yields

$$\mathbf{W} = \mathbf{R}_{\mathbf{H}\tilde{\mathbf{H}}}\mathbf{R}_{\tilde{\mathbf{H}}\tilde{\mathbf{H}}}^{-1} \quad (7.7)$$

Where  $\mathbf{R}_{\tilde{\mathbf{H}}\tilde{\mathbf{H}}}$  is the auto correlation matrix of  $\tilde{\mathbf{H}}$  given as

$$\begin{aligned} \mathbf{R}_{\tilde{\mathbf{H}}\tilde{\mathbf{H}}} &= \mathbf{E}\{\tilde{\mathbf{H}}\tilde{\mathbf{H}}^\dagger\} \\ &= \mathbf{E}\{(\mathbf{X}_D^{-1}\mathbf{Y})(\mathbf{X}_D^{-1}\mathbf{Y})^\dagger\} \\ &= \mathbf{E}\{(\mathbf{H} + \mathbf{X}_D^{-1}\mathbf{N})(\mathbf{H} + \mathbf{X}_D^{-1}\mathbf{N})^\dagger\} \\ &= \mathbf{E}\{\mathbf{H}\mathbf{H}^\dagger + \mathbf{X}_D^{-1}\mathbf{N}\mathbf{H}^\dagger + \mathbf{H}\mathbf{N}^\dagger(\mathbf{X}_D^{-1})^\dagger + \mathbf{X}_D^{-1}\mathbf{N}\mathbf{N}^\dagger(\mathbf{X}_D^{-1})^\dagger\} \\ &= \mathbf{E}\{\mathbf{H}\mathbf{H}^\dagger\} + \mathbf{E}\{\mathbf{X}_D^{-1}\mathbf{N}\mathbf{N}^\dagger(\mathbf{X}_D^{-1})^\dagger\} \\ &= \mathbf{E}\{\mathbf{H}\mathbf{H}^\dagger\} + \frac{\sigma_n^2}{\sigma_x^2}\mathbf{I} \end{aligned} \quad (7.8)$$

and  $\mathbf{R}_{\mathbf{H}\tilde{\mathbf{H}}}$  is the cross-correlation matrix between the true channel vector and temporary channel estimate vector in the frequency domain. Using Equation (7.7), the MMSE channel estimate follows as

$$\begin{aligned} \hat{\mathbf{H}} &= \mathbf{W}\tilde{\mathbf{H}} \\ &= \mathbf{R}_{\mathbf{H}\tilde{\mathbf{H}}}\mathbf{R}_{\tilde{\mathbf{H}}\tilde{\mathbf{H}}}^{-1}\tilde{\mathbf{H}} \\ &= \mathbf{R}_{\mathbf{H}\tilde{\mathbf{H}}}\left(\mathbf{R}_{\mathbf{H}\mathbf{H}} + \frac{\sigma_n^2}{\sigma_x^2}\mathbf{I}\right)^{-1}\tilde{\mathbf{H}} \end{aligned} \quad (7.9)$$

Where  $\dagger$  is the complex conjugation.

### 7.1.3 DFT Based Channel Estimation

DFT Based Channel Estimation is based on the property that the energy of the channel is very concentrated in the time domain.

Thus the final channel estimates in the frequency domain with transform domain cutoff filter and in band noise removal can be obtained as, section (6.1.3)

$$\hat{H}_{CFNR}(k) = \sum_{n=0}^{K-1} w_{CFNR}(n) \hat{h}_{LS}(n) e^{-\frac{j2\pi nk}{K}}, \quad 0 \leq k \leq K - 1 \quad (7.10)$$

Where  $K = M_{sc}^{PUCCH}$ , number of subcarriers allocated to PUCCH.

Note that the above DFT based CE implementation method does not require any information about the channel and DFT/IDFT units are available blocks in the system. The Figures 7.4, 7.5 and 7.6 shows the Mean Square Error (MSE) performance of different channel estimates for PUCCH format 2 and format 2a.

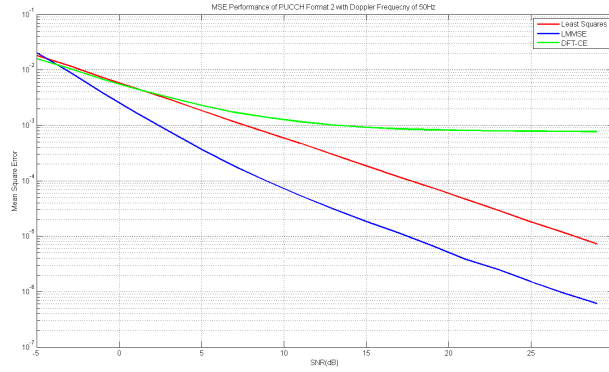


Figure 7.4: MSE Performance of PUCCH Format 2, with  $F_d=100$  Hz

#### 7.1.4 2D-MMSE

2D-MMSE is very well suited for estimating the channel over frequency tones. As we know in PUCCH format 2 there are 2 reference symbols in a slot. In 2D-MMSE statistics of channel are exploited to derive the estimates over the complete 12x7 resource grid from the received pilot symbols or reference symbols. Let  $x_p(m, n)$  are the two pilot sequences in a slot where  $m=2,6$  and  $n=1,2,..12$ . The received signal is

$$y_p(m, n) = x_p(m, n) * h_p(m, n) + n(m, n) \quad (7.11)$$

In the frequency domain

$$\mathbf{Y}_p = \mathbf{X}_p \mathbf{H}_p + \mathbf{N}_p \quad (7.12)$$

Where  $\mathbf{Y}_p = [Y_p(2, 1) \ Y_p(2, 2) \ \dots \ Y_p(2, 12) \ Y_p(6, 1) \ Y_p(6, 2) \ \dots \ Y_p(6, 12)]^T$  of size 24x1 and  $X_p$  is the diagonal matrix of size 24x24.

$$X_p = \begin{bmatrix} X_p(2, 1) & 0 & \dots & 0 & 0 & 0 & \dots & 0 \\ 0 & X_p(2, 2) & \dots & 0 & 0 & 0 & \dots & 0 \\ \vdots & \vdots & \ddots & 0 & 0 & 0 & \dots & 0 \\ 0 & 0 & 0 & X_p(2, 12) & 0 & 0 & \dots & 0 \\ 0 & 0 & 0 & 0 & X_p(6, 1) & 0 & \dots & 0 \\ 0 & 0 & 0 & 0 & 0 & X_p(6, 2) & \dots & 0 \\ \vdots & \vdots & \vdots & \vdots & \vdots & \vdots & \ddots & 0 \\ 0 & 0 & 0 & 0 & 0 & 0 & 0 & X_p(6, 24) \end{bmatrix}$$

and  $\mathbf{H}_p = [H_p(2, 1) \ H_p(2, 2) \ \dots \ H_p(2, 12) \ H_p(6, 1) \ H_p(6, 2) \ \dots \ H_p(6, 12)]^T$  of size 24x1.

Channel estimates of over all resource elements  $H(m_i, n_k)$   $i=1, \dots, 7$  and  $k=1, \dots, 12$  are found using channel statistics  $Y_p, X_p$

$$H = W.Y_p \quad (7.13)$$

$$W = R_{HY_p} R_{Y_p Y_p}^{-1} \quad (7.14)$$

$$R_{Y_p Y_p} = E[(X_p H_p + N_p + X_{ip} G_{ip})(X_p H_p + N_p + X_{ip} G_{ip})^H] \quad (7.15)$$

Assume received signal of intended user is uncorrelated with interfere user and AWGN, then

$$R_{Y_p Y_p} = E[X_p H_p H_p^H X_p^H] + \sum_i P_i I + N_o I \quad (7.16)$$

$$= X_p E[H_p H_p^H] X_p^H + R_{nn} \quad (7.17)$$

$$\text{Where } R_{nn} = N_o I + \sum_i P_i \quad (7.18)$$

$P_i$  is the interference power of  $i^{th}$  user and  $R_{HY_p}$  is given by

$$R_{HY_p} = R_{HH_p} X_p^H \quad (7.19)$$

To get the cross correlation and auto correlation coefficients between pilot locations and non pilot locations we assume a constant PDP and constant doppler spectrum of channel.

$$R_\tau(\Delta t) = \text{sinc}(2f_d \Delta t) \quad (7.20)$$

$$R_f(\Delta f) = e^{-j\pi f} \text{sinc}(\tau \Delta f) \quad (7.21)$$

$$R_x(k, l) = (R_f(m_p - m) \Delta f)(R_\tau(k_p - k) \Delta t) \quad (7.22)$$

## 7.2 Interpolation

This interpolation technique is applicable for the channel estimates of LS and LMMSE. Let  $H(k, l)$  is the unknown impulse response of the slot where  $k$  is  $0, 1, \dots, M_{sc}^{PUCCH}$  and  $l$  is  $0, 1, \dots, 6$ . Here linear interpolation is adopted which is defined as follows:

$$H(k, l) = \frac{l_2 - l}{l_2 - l_1} * H(k, l_1) + \frac{l - l_1}{l_2 - l_1} * H(k, l_2) \quad (7.23)$$

Where  $l_1$  and  $l_2$  represents the position of RS,  $H(k, l_1)$  and  $H(k, l_2)$  impulse response of two reference symbols.

### 7.3 Equalization

#### 7.3.1 ZF Equalization

The received OFDMA symbol , after FFT/DFT and Sub Carrier Demapping is,

$$Y_r(k, l) = X(k, l)H_r(k, l) + N_r(k, l), \quad (7.24)$$

where 'r' indicates the number of receiving antennas here in this case 2 receiving antennas,  $k = 0, 1, \dots, M_{PUCCH}^{sc} - 1$ ,  $l = 0, 1 \dots 6$  and  $H(k, l)$  are subcarrier index and symbol number in a slot and  $N(k, l)$  is AWGN Channel with complex normal distribution with mean zero and noise variance unity. The ZF weighting matrix (filter) that decomposes the received signal into its component streams is given by the following equation [6]:

$$\mathbf{G}_{GF} = \sqrt{\frac{N_{Tx}}{E_s}} (\mathbf{H}^H \mathbf{H})^{-1} \mathbf{H}^H \quad (7.25)$$

#### 7.3.2 MMSE Equalization

A frequency domain vector valued MMSE filter is applied on received signal to minimize the effects of channel distortion[6]. The MMSE weighting matrix (filter) is given by the following expression [6]:

$$\mathbf{G}_{MMSE} = \sqrt{\frac{N_{Tx}}{E_s}} (\mathbf{H}^H \mathbf{H} + \frac{N_{Tx} N_o}{E_s} \mathbf{I})^{-1} \mathbf{H}^H \quad (7.26)$$

where I is an  $N_{Rx} \times N_{Rx}$  identity matrix

### 7.4 Demodulation

Soft-demodulation, or more accurately soft-bit demodulation, is a demodulation process that estimates from the received demodulated symbols not only hard-bits (Boolean variable or binary digit: 0 or 1, or equivalently the polarity sign: positive or negative), but also their confidence levels. At the transmitter side, normally only hard-bits are involved, and they take the form of binary digits 0 or 1. However, at the receiver, particularly at the physical layer, these binary digits are more commonly represented as polarity signs, either negative or positive.

The soft bit is the LLR value i.e. The logarithmic ratio of probability of bit being 0 to the probability of the bit of being 1.

#### 7.4.1 Soft Demodulation of Binary Modulation in an AWGN Environment

The soft-demodulation process is normally straightforward in the case of binary modulation schemes, for instance BPSK. This characteristic is also valid in any 4-ary modulation scheme that is I-Q separable. hence can be regarded as dual-binary modulation schemes, for example Gray coded QPSK or Gray-coded 4-QAM schemes.

As we know the QPSK signal constellation is depicted in figure below having symbol energy  $E_{av} = 1$  and

d in the figure equal to  $\frac{1}{\sqrt{2}}$  in an AWGN environment. Now suppose that a transmitter sends a modulated signal  $x$  through the AWGN channel  $n$  having zero mean and noise variance of  $\sigma^2$ . Denoting the received signal as  $r = r_I + r_Q = x + n$ , LLR of the received soft-bit from the real (or in-phase) component  $r_I$  [5]

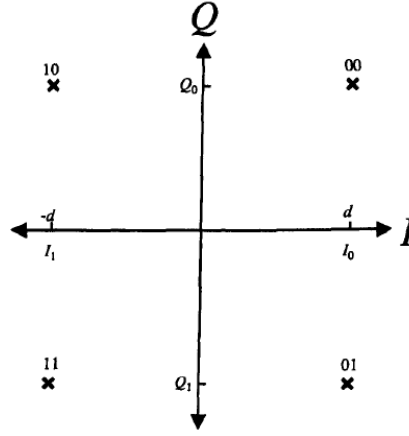


Figure 7.7: QPSK Constellation

$$LLR(b_I) = \log \left[ \frac{Pr(b_I = 0/r)}{Pr(b_I = 1/r)} \right] \quad (7.27)$$

According to Bayes Theorem,  $Pr\left(\frac{A}{B}\right) = \frac{Pr\left(\frac{B}{A}\right)Pr(A)}{Pr(B)}$

$$LLR(b_I) = \log \left[ \frac{\frac{Pr\left(\frac{r}{b_I=0}\right)Pr(b_I=0)}{Pr(r)}}{\frac{Pr\left(\frac{r}{b_I=1}\right)Pr(b_I=1)}{Pr(r)}} \right] \quad (7.28)$$

$$= \log \left[ \frac{Pr\left(\frac{r}{b_I=0}\right)}{Pr\left(\frac{r}{b_I=1}\right)} \right] + \log \left[ \frac{Pr(b_I = 0)}{Pr(b_I = 1)} \right] \quad (7.29)$$

Assuming the event of selecting bit  $b_I = 0, 1$  for transmission is equiprobable.

$$LLR(b_I) = \log \left[ \frac{\frac{1}{\sqrt{2\pi\sigma^2}} e^{-\frac{1}{2} \frac{(r_I-d)^2}{\sigma^2}}}{\frac{1}{\sqrt{2\pi\sigma^2}} e^{-\frac{1}{2} \frac{(r_I+d)^2}{\sigma^2}}} \right] \quad (7.30)$$

$$= \frac{2d}{\sigma^2} r_I \quad (7.31)$$

$$= \frac{2}{\sigma^2} \frac{r_I}{\sqrt{2}} \quad (7.32)$$

It follows that for imaginary (or quadrature) component case also, substitute the subscript Q for I. From this equation, it is evident that the LLR of a binary or dual-binary modulation scheme is just a simple function of the real or imaginary part of the received signal and its noise variance.

#### 7.4.2 Soft Demodulation in Rayleigh Fading Environment

Let Y denote either I or Q and  $\gamma$  denote the fading CSI that is represented by the estimated fading coefficient  $\hat{h}$ . The  $j^{th}$  bit LLR can be expressed as

$$LLR(b_Y^{(j)}) = \log \left[ \frac{Pr\left(\frac{b_Y^{(j)}=0}{z_Y}, \gamma\right)}{Pr\left(\frac{b_Y^{(j)}=1}{z_Y}, \gamma\right)} \right] \quad (7.33)$$

In this case

$$r = hx + n \quad (7.34)$$

and

$$\begin{aligned} z &= z_I + jz_Q \\ &= \hat{h}^\dagger r \\ &= \hat{h}^\dagger (hx + n) \\ &= \hat{h}^\dagger hx + \hat{h}^\dagger n \end{aligned}$$

Where  $\dagger$  represents the complex conjugation operation. Continuing the derivation, and assuming that the noise term  $\hat{h}^\dagger n$  is Gaussian distributed, it can be shown that

$$LLR(b_Y^{(j)}) = \log \left[ \frac{\sum_{y \in y_0^{(j)}} \frac{1}{\|\hat{h}\|^2 \sqrt{2\pi\sigma^2}} \exp\left(-\frac{1}{2\sigma^2 \|\hat{h}\|^2} (z_Y - \|\hat{h}\|^2 y)^2\right)}{\sum_{y \in y_1^{(j)}} \frac{1}{\|\hat{h}\|^2 \sqrt{2\pi\sigma^2}} \exp\left(-\frac{1}{2\sigma^2 \|\hat{h}\|^2} (z_Y - \|\hat{h}\|^2 y)^2\right)} \right] \quad (7.35)$$

$$= E_{y \in y_0^{(j)}} \frac{-1}{2\sigma^2 \|\hat{h}\|^2} \left( z_Y - \|\hat{h}\|^2 y \right)^2 - E_{y \in y_1^{(j)}} \frac{-1}{2\sigma^2 \|\hat{h}\|^2} \left( z_Y - \|\hat{h}\|^2 y \right)^2 \quad (7.36)$$

where E is operator is defined as

$$aEb = \log(\exp(a) + \exp(b)) \quad (7.37)$$

$$= \max(a, b) + \log(1 + \exp(-|a - b|)) \quad (7.38)$$

and  $y \in y_0^{(j)}$  denotes amplitude levels of modulation symbols constellation projected to Y axis corresponding to bit  $y^{(j)} = 0$ . Y represents I or Q axis, so  $z_y$  can mean either Re(Z) or Im(Z). In QPSK case, there is only one member of y that satisfies  $y \in y_0^{(j)}$  that is  $y = +d$ .

So LLR reduces to

$$\begin{aligned} LLR(b_y^{(j)}) &= \frac{-1}{2\pi \|\hat{h}\|^2} (z_y - \|\hat{h}\|^2 d)^2 + \frac{1}{2\pi \|\hat{h}\|^2} (z_y + \|\hat{h}\|^2 d)^2 \\ &= \frac{2Z_y}{\sigma^2} \\ &= \frac{\sqrt{2}z_y}{\sigma^2} \end{aligned} \quad (7.39)$$

For the non binary operation is involved, operator E can be calculated recursively, for example

$$\begin{aligned} \sum_{i=1}^3 a_i &= a_1 E a_2 E a_3 \\ &= a_1 E (a_2 E a_3) \end{aligned} \quad (7.40)$$

In 16-QAM, however, there are two bits from each I and Q axis that make up a modulation symbol. The constellation representations of 16 QAM is Adopting  $\{i_l q_l i_0 q_0\}$  bit arrangement, where letter  $i$  signifies that the bits originate from I axis, this constellation point is made up of  $i_l = 0, i_0 = 1$  bits from I axis and  $q_l = 0, q_0 = 1$  bits from Q axis. For further convenience, the bit with subscript 1 will be referred to as



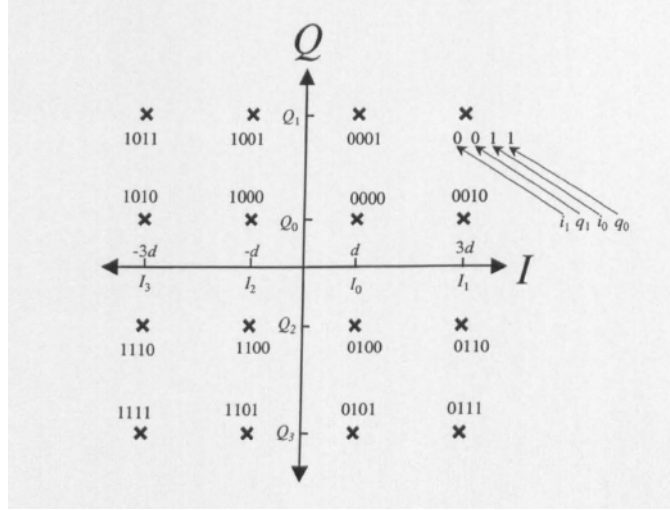


Figure 7.8: 16QAM Constellation

MSB, whereas the other with subscript 0 will be called LSB.

It is apparent that for MSB

$$y \in y_0^{(1)} = \{d, 3d\}$$

$$y \in y_1^{(1)} = \{-d, -3d\}$$

while for LSB

$$y \in y_0^{(0)} = \{-d, d\}$$

$$y \in y_1^{(0)} = \{-3d, 3d\}$$

Therefore for MSB

$$L_c(b_y^{(1)}) = E_{y=\{-d,-3d\}} \frac{-1}{2\sigma^2 \|\hat{\alpha}\|^2} (z_y - \|\hat{\alpha}\|^2 y)^2 - E_{y=\{d,3d\}} \frac{-1}{2\sigma^2 \|\hat{\alpha}\|^2} (z_y - \|\hat{\alpha}\|^2 y)^2 \quad (7.41)$$

and for LSB

$$L_c(b_y^{(0)}) = E_{y=\{-d,d\}} \frac{-1}{2\sigma^2 \|\hat{\alpha}\|^2} (z_y - \|\hat{\alpha}\|^2 y)^2 - E_{y=\{-3d,3d\}} \frac{-1}{2\sigma^2 \|\hat{\alpha}\|^2} (z_y - \|\hat{\alpha}\|^2 y)^2 \quad (7.42)$$

Due to simplicity of the exact soft-demodulation method for the QPSK case, there is no need of approximation. On the contrary, in the 16-QAM case, the calculation involves the computationally-intensive E operation. Therefore, in the following description and in the sections regarding the approximation methods, 16-QAM modulation is implied. The most obvious and straightforward approximation for this operation is, popularly applied in LogMAP decoding algorithm to produce its simpler version MaxLogMAP, the "taking the maximum" operation defined as follows

$$aMb \equiv \max(a, b) \quad (7.43)$$

Similar to the E operation, multiterm M operation can be performed recursively. Therefore, Therefore for MSB

$$L_c(b_y^{(1)}) = M_{y=\{-d,-3d\}} \frac{-1}{2\sigma^2 \|\hat{\alpha}\|^2} (z_y - \|\hat{\alpha}\|^2 y)^2 - M_{y=\{d,3d\}} \frac{-1}{2\sigma^2 \|\hat{\alpha}\|^2} (z_y - \|\hat{\alpha}\|^2 y)^2 \quad (7.44)$$

and for LSB

$$L_c(b_y^{(0)}) = M_{y=\{-d,d\}} \frac{-1}{2\sigma^2 \|\hat{\alpha}\|^2} (z_y - \|\hat{\alpha}\|^2 y)^2 - M_{y=\{-3d,3d\}} \frac{-1}{2\sigma^2 \|\hat{\alpha}\|^2} (z_y - \|\hat{\alpha}\|^2 y)^2 \quad (7.45)$$

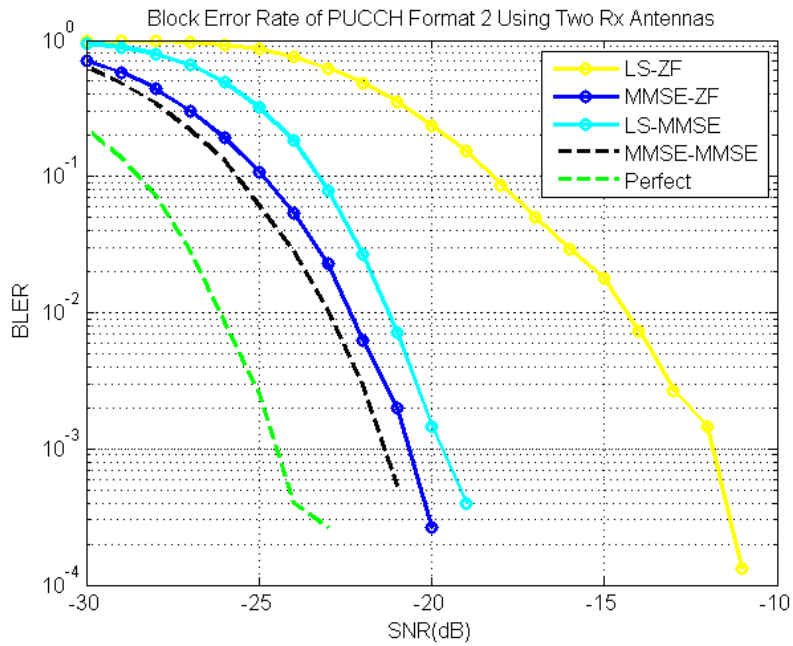


Figure 7.9(a): BLER vs SNRdB for PUCCH Format2

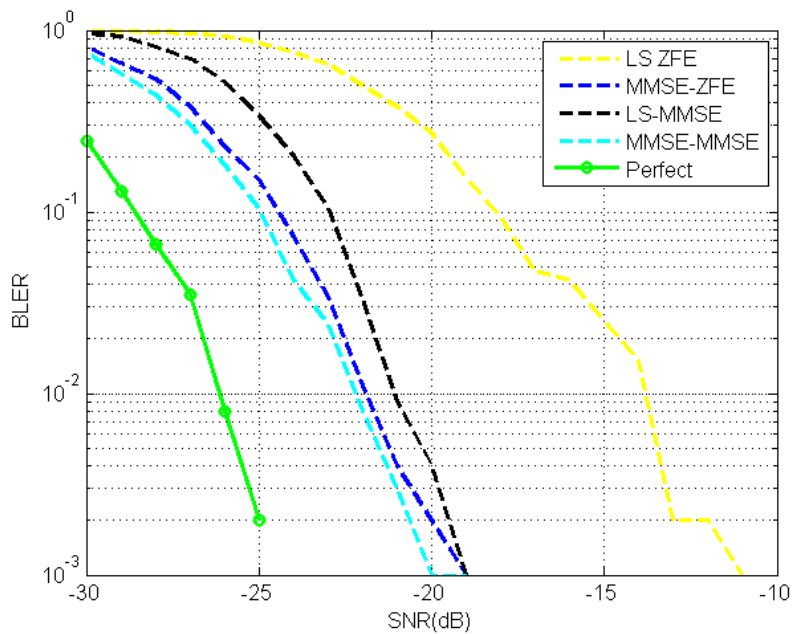


Figure 7.9(b): BLER vs SNRdB for PUCCH Format2a

### 7.4.3 Block Error Plots for PUCCH

The block error rate plots for PUCCH Format 2 and 2a are given below figures 7.9(a) and 7.9(b)

### References

- [1] 3GPP TS 36.212: "Evolved Universal Terrestrial Radio Access (E-UTRA); Multiplexing and channel coding".

[2] 3GPP TS 36.211: "Evolved Universal Terrestrial Radio Access (E-UTRA); Physical channels and modulation".

[3] Sinem Coleri, Mustafa Ergen, Anuj Puri, "Channel Estimation Techniques Based on Pilot Arrangement in OFDM Systems", IEEE Transactions on Broadcasting, VOL.48,N0.3,Sept2002:223-229.

[4] Fatang Chen, "Research On Method of PUCCH Channel Estimation Based on UCI Separate Coding", IPCSIT vol.43 2012 .

[5] B Sklar "Digital Communications Fundamentals and Applications".

[6] K. Kuchi, Limiting behavior of ZF/MMSE linear equalizers in wideband channels with frequency selective fading, IEEE Commun. Lett., vol. 16, pp. 929-932, 2012



# 8 | CQI Decoding algorithm for PUSCH and PUCCH

For uplink control information, both aperiodic and periodic reporting are supported. The periodic reporting of Channel Quality Indicator(CQI), Precoding Matrix Indicator(PMI), and Rank Indicator(RI) is carried out using PUCCH while aperiodic is done on the PUSCH data channel is shown in the Figure 8.1. The reporting types supported on PUCCH include wideband CQI and UE selected subband CQI. With

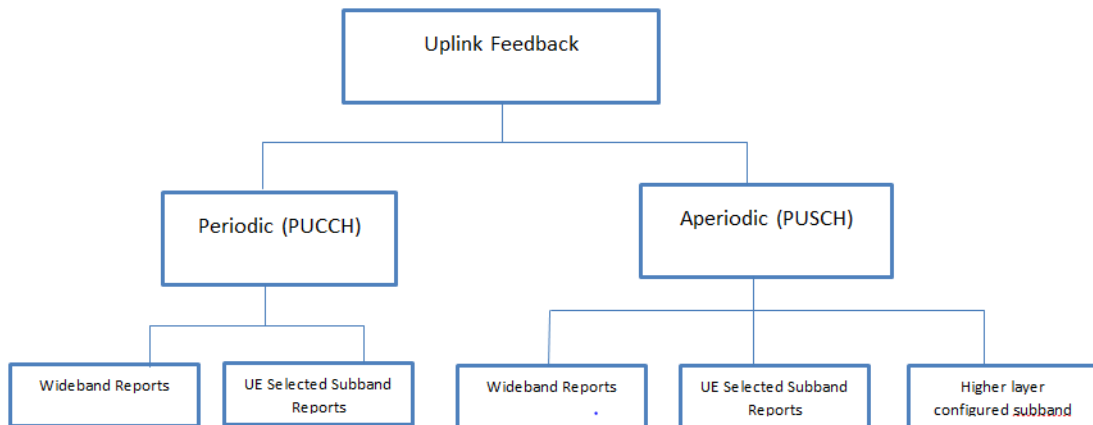


Figure 8.1: Uplink Reporting Schemes

aperiodic reporting on PUSCH, in addition to wideband CQI and UE selected subband CQI, higher layer configured subband CQI reporting is also supported [1].

## 8.1 Channel Coding for Periodic Reporting

Three forms of channel coding are used for periodic reporting on PUCCH, one for CQI/PMI, another for hybrid ARQ ACK/NACK and scheduling request and finally one for a combination of CQI/PMI and hybrid ARQ ACK/NACK[2]. The CQI/PMI bits input to the channel coding block are denoted by  $a_1, a_1, \dots, a_A$ , where A is the number of bits and depend on the transmission format. These bits are coded using a variable Reed-Muller(RM) (20,A)[1,3] code whose codewords are linear combinations of the 13 basis sequences denoted  $M_{i,n}$  as given in Table 8.1. The 13 basis sequences allow to code a maximum of 13 PUCCH payload bits, which is the case when two bits of ACK/NACK are jointly coded with a maximum

i	$M_{i,0}$	$M_{i,1}$	$M_{i,2}$	$M_{i,3}$	$M_{i,4}$	$M_{i,5}$	$M_{i,6}$	$M_{i,7}$	$M_{i,8}$	$M_{i,9}$	$M_{i,10}$	$M_{i,11}$	$M_{i,12}$
0	1	1	0	0	0	0	0	0	0	0	1	1	0
1	1	1	1	0	0	0	0	0	0	1	1	1	0
2	1	0	0	1	0	0	1	0	1	1	1	1	1
3	1	0	1	1	0	0	0	0	1	0	1	1	1
4	1	1	1	1	0	0	0	1	0	0	1	1	1
5	1	1	0	0	1	0	1	1	1	0	1	1	1
6	1	0	1	0	1	0	1	0	1	1	1	1	1
7	1	0	0	1	1	0	0	1	1	0	1	1	1
8	1	1	0	1	1	0	0	1	0	1	1	1	1
9	1	0	1	1	1	0	1	0	0	1	1	1	1
10	1	0	1	0	0	1	1	1	0	1	1	1	1
11	1	1	1	0	0	1	1	0	1	0	1	1	1
12	1	0	0	1	0	1	0	1	1	1	1	1	1
13	1	1	0	1	0	1	0	1	0	1	1	1	1
14	1	0	0	0	1	1	0	1	0	0	1	0	1
15	1	1	0	0	1	1	1	1	0	1	1	0	1
16	1	1	1	0	1	1	1	0	0	1	0	1	1
17	1	0	0	1	1	1	0	0	1	0	0	1	1
18	1	1	0	1	1	1	1	1	0	0	0	0	0
19	1	0	0	0	0	1	1	0	0	0	0	0	0

Table 8.1: Basis sequence for(20,A)

of 11 bits of CQI/PMI. The bit sequence after encoding denoted by  $b_0, b_1, \dots, b_{B-1}$  is given as:

$$b_i = \sum_{n=0}^{A-1} (a_n \cdot M_{i,n}) \text{mod } 2 \quad i = 0, 1, 2, \dots, (B-1) = 19 \quad (8.1)$$

## 8.2 Channel Coding for Aperiodic Reporting

The aperiodic reporting is performed by transmission of control information on PUSCH. The channel coding for hybrid ARQ ACK/NACK, rank indication (RI) and CQI/PMI is done independently. The channel coding schemes used for aperiodic reporting are summarized in given table.

Channel Coding Scheme	Control Information
Simplex(3,2)code	Two-bits ACK/NACK
	Two-bits rank information
Variable RM(32,o) block code	CQI/PMI payload $\leq 11$ bits
Tail-biting convolutional code	CQI/PMI payload $> 11$ bits

The CQI/PMI bits input to the channel coding block are denoted by  $o_0, o_1, o_2, o_3, \dots, o_{O-1}$ , where  $O$  is the number of bits. For CQI/PMI payload sizes greater than 11 bits, the information is coded using a tail-biting convolutional code. For payload sizes of 11 bits or less, the CQI/PMI is coded using a variable Reed–Muller (RM)(32,o) block code [1,3]. The codewords of the (32,o) block code are a linear combination of 11 basis sequences denoted  $M_{i,n}$  and given in Table 8.2. The 11 basis sequences allow one to encode a maximum of 11 bits of CQI/PMI. The encoded CQI/PMI block is denoted  $b_0, b_1, b_2, b_3, \dots, b_{B-1}$  and

i	$M_{i,0}$	$M_{i,1}$	$M_{i,2}$	$M_{i,3}$	$M_{i,4}$	$M_{i,5}$	$M_{i,6}$	$M_{i,7}$	$M_{i,8}$	$M_{i,9}$	$M_{i,10}$
0	1	1	0	0	0	0	0	0	0	0	1
1	1	1	1	0	0	0	0	0	0	1	1
2	1	0	0	1	0	0	1	0	1	1	1
3	1	0	1	1	0	0	0	0	1	0	1
4	1	1	1	1	0	0	0	1	0	0	1
5	1	1	0	0	1	0	1	1	1	0	1
6	1	0	1	0	1	0	1	0	1	1	1
7	1	0	0	1	1	0	0	1	1	0	1
8	1	1	0	1	1	0	0	1	0	1	1
9	1	0	1	1	1	0	1	0	0	1	1
10	1	0	1	0	0	1	1	1	0	1	1
11	1	1	1	0	0	1	1	0	1	0	1
12	1	0	0	1	0	1	0	1	1	1	1
13	1	1	0	1	0	1	0	1	0	1	1
14	1	0	0	0	1	1	0	1	0	0	1
15	1	1	0	0	1	1	1	1	0	1	1
16	1	1	1	0	1	1	1	0	0	1	0
17	1	0	0	1	1	1	0	0	1	0	0
18	1	1	0	1	1	1	1	1	0	0	0
19	1	0	0	0	0	1	1	0	0	0	0
20	1	0	1	0	0	0	1	0	0	0	1
21	1	1	0	1	0	0	0	0	0	1	1
22	1	0	0	0	1	0	0	1	1	0	1
23	1	1	1	0	1	0	0	0	1	1	1
24	1	1	1	1	1	0	1	1	1	1	0
25	1	1	0	0	0	1	1	1	0	0	1
26	1	0	1	1	0	1	0	0	1	1	0
27	1	1	1	1	0	1	0	1	1	1	0
28	1	0	1	0	1	1	1	0	1	0	0
29	1	0	1	1	1	1	1	1	1	0	0
30	1	1	1	1	1	1	1	1	1	1	1
31	1	0	0	0	0	0	0	0	0	0	0

Table 8.2: Basis sequence for(32,o)

given as:

$$b_i = \sum_{n=0}^{O-1} (o_n \cdot M_{i,n}) \text{ mod } 2 \quad i = 0, 1, 2, \dots, (B-1) = 31 \quad (8.2)$$

The output bit sequence  $q_0, q_1, \dots, q_{Q-1}$  is obtained by circular repetition of the encoded CQI/PMI block as follows:

$$q_i = b_{(i \text{ mod } B)}, \quad i = 0, 1, 2, \dots, (Q-1) \quad (8.3)$$

### 8.3 Decoding algorithm for APeriodic report-Long CQI

The number of CQI bits may vary between 5 and 11 depending on whether wideband or narrowband CQI reports are transmitted. If the number of CQI bits is less than seven, then the encoding matrix (32 x 6) is a standard RM (1, 5) code which is processed with interleaver. In the standard, they are the vectors from  $M_0$  to  $M_5$ . Otherwise, the encoding matrix (32 x 11) consists of above RM vectors and five masks. The masks are listed as follows:

$M_6$  : 00100110011100011011100011001110

$M_7$  : 00001101101011110010001011010110  
 $M_8$  : 00110111000110000100001110111110  
 $M_9$  : 01100010111011011000010110110010  
 $M_{10}$  : 11111111111111110000111101000010

Because the encoder of CQI is based on RM code, many decoding algorithms for RM codes have been researched in [4], [5], and [6]. These algorithms include hard-decision decoding and soft-decision decoding. As for decoding for CQI, the bipolarity change for codeword, interleaving and eliminating infection of the masks should be considered before decoding codeword with Fast Hadamard Transform(FHT). As for decoding for CQI, the bipolarity change for codeword, interleaving and eliminating infection of the masks should be considered before decoding codeword with FHT. The interleaving of codeword is shown in the Figure 8.2 When the number of bit in each encoding block is larger than six, the length

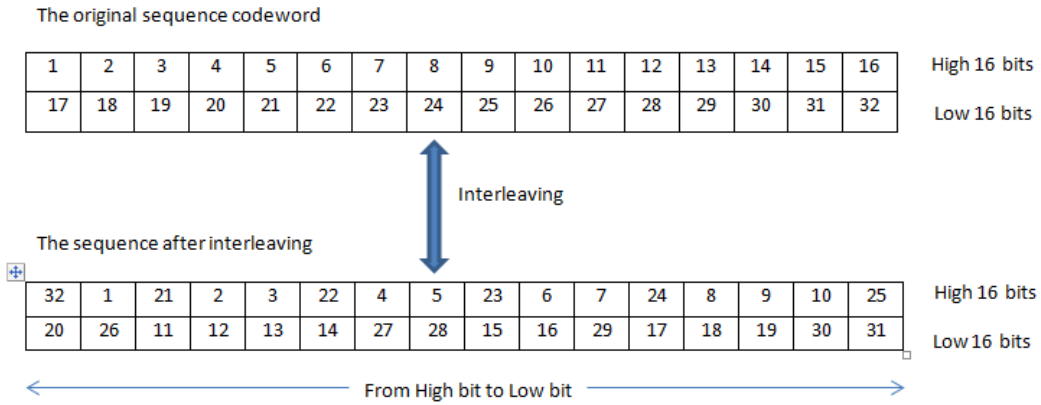


Figure 8.2: The order of interleaving for Codeword

of codeword through CQI encoder is 32 bits. On the receiver, infection caused by mask sequences  $M_7, M_8, M_9, M_{10}, M_{11}$  in encoding should be eliminated first [7]. There are 32 kinds of linear combination for these five mask sequences in the encoder matrix, and every linear combination can be obtained through the following steps:

Let the value of  $i$  be an integer from 0 to 31.

**STEP 1:**  $a_0, a_1, a_2, a_3, a_4$  are the five bits of binary number of  $i$ . i.e.  $a_k = F(i)$  where  $k=0,1,2,3,4$

The function  $F(i)$  transforms  $i$  from decimal to binary. The linear combination is

$$\mathbf{v}_n = a_{i,0} \cdot M_7 + a_{i,1} \cdot M_8 + a_{i,2} \cdot M_9 + a_{i,3} \cdot M_{10} + a_{i,4} \cdot M_{11}$$

where  $n=1,2,\dots,32$  and  $i=0,1,\dots,31$ .

Then, the mask matrix, denoted by  $M_D$ , that consist of vectors which are transformed with mode 2 operation and bipolar transformation for above 32 linear combinations. So,  $M_D = [\mathbf{v}_1 \mathbf{v}_2 \dots \mathbf{v}_{32}]^T$  and each row in  $M_D$  is  $\mathbf{v}_n, n=1,2,\dots,32$ . When the value of  $i$  is 31,  $a_{i,0}, a_{i,1}, a_{i,2}, a_{i,3}, a_{i,4}$ , are all '1'. In this case, the linear combinations of five mask sequences forms  $\mathbf{v}_{32}$ . Received word that processed by interleaving (Figure.8.2. shows the order of interleaving for codeword) and bipolar changing multiply with  $\mathbf{v}_{32}$  can eliminate the infection of mask sequences.

Assuming that the received word is  $\mathbf{c} = (c_1, c_2, \dots, c_{32})$ , then whole decoding process is given as follows:

**STEP 2:** Bipolar transformation for the decision block:



$$\tilde{\mathbf{c}} = 1 - 2 * c_i, \quad \text{where } i = 0, 1, \dots, 31 \quad (8.4)$$

$$(8.5)$$

**STEP 3:** According to Figure 8.2 for interleaving.

**STEP 4:** Construct the mask matrix  $M_D$  based on the mask sequence in the CQI encoder. Where  $M_D = [v_1, v_2, \dots, v_{32}]^T$  and  $\mathbf{v}_n = a_{i,0} \cdot M_7 + a_{i,1} \cdot M_8 + a_{i,2} \cdot M_9 + a_{i,3} \cdot M_{10} + a_{i,4} \cdot M_{11}$ .

**STEP 5:** Bipolar transformation for each element  $M_D$ . Then changes the row order according to Figure 8.2 and the result is the decoding matrix  $\bar{M}_D$

**STEP 6:** Multiply every bit of  $\tilde{\mathbf{c}}$  with corresponding bit of each row in  $\bar{M}_D$ . Each row is a vector 1x32.

**STEP 7:** Making FHT for each vector in (5), Then the results can make up a matrix 32x32, which is denoted by  $D_{32 \times 32}$ .

**STEP 8:** Finding out the element, denoted as K, whose magnitude is the largest in  $D_{32 \times 32}$ . Then decodes the word according to the number of row and column corresponds with K.

**STEP 9:** Transforming the row and column index of K to five binary bits separately. These bits are then decoded to  $o_7, o_8, o_9, o_{10}, o_{11}$  and  $o_2, o_3, o_4, o_5, o_6$  respectively. Then obtaining  $o_1$  according to the sign of K, thus, if K is positive number,  $o_1$  is '0' and  $o_1$  is '1' otherwise.

### 8.3.1 Decoding algorithm for Aperiodic report -Short CQI

When the number of bit in every encoding block is less than seven, there is no mask sequences inflection for the codeword. So the procedure of decoding for received word is simplified compared to above situation.

Interleaving and bipolar transformation process is only needed for the received word while not for the mask matrix. Find the element in the word with largest magnitude after FHT and then decode them on the basis of the column number and the sign of it.

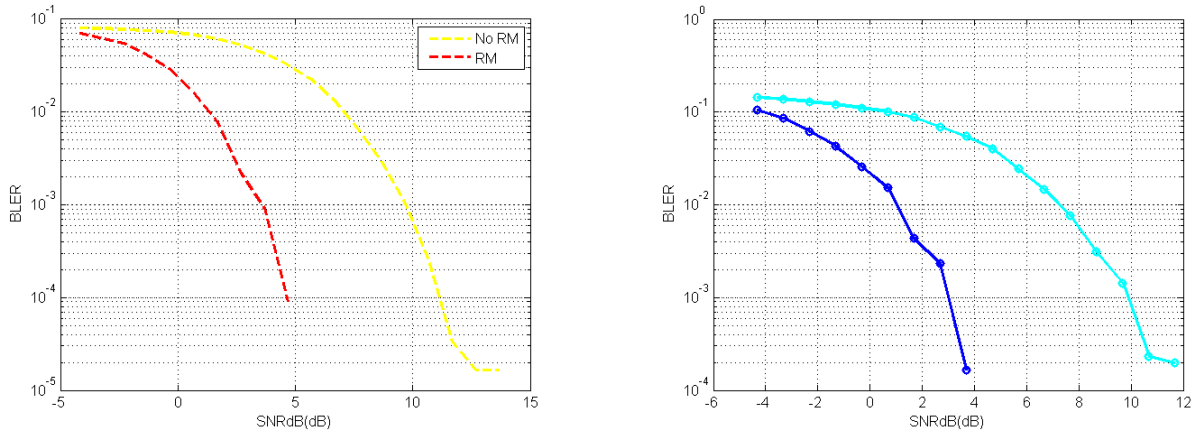


Figure 8.3: Simulation of Long and Short CQI

### 8.4 Decoding algorithm for Periodic report-CQI

The decoding algorithm for CQI information in PUCCH is similar to PUSCH only difference in construction of mask matrix  $M_D$ . Here there totally 7 mask sequence from these mask sequence it can form the

mask matrix of size 128x32. Perform the FHT on the received word with each row and find out the index which gives maximum magnitude . Transform the row and column index of that magnitude value into binary bits  $o_7, o_8, o_9, o_{10}, o_{11}, o_{13}, o_{13}$  and  $o_2, o_3, o_4, o_5, o_6$  respectively. Then obtaining  $o_1$  according to the sign of magnitude, thus, if magnitude is positive number,  $o_1$  is '0' and  $o_1$  is '1' otherwise.

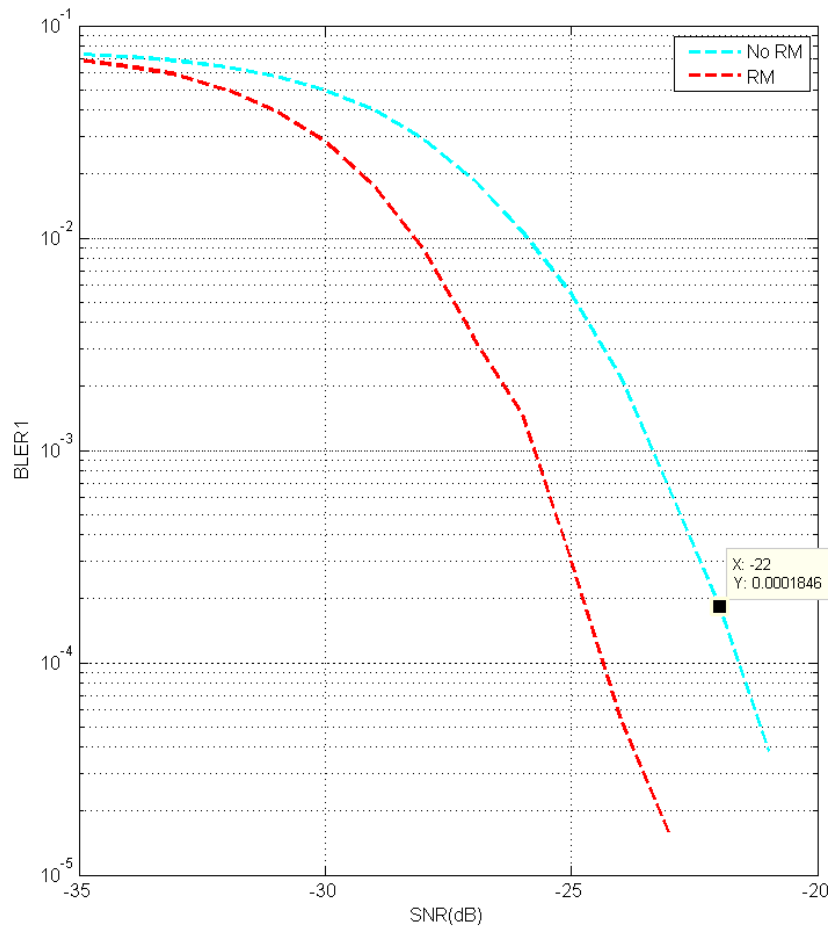


Figure 8.4: Simulation of CQI decoding algorithm in PUCCH

## References

- [1] 3GPP TS 36.212: "Evolved Universal Terrestrial Radio Access (E-UTRA); Multiplexing and channel coding".
- [2] 3GPP TS 36.211: "Evolved Universal Terrestrial Radio Access (E-UTRA); Physical channels and modulation".
- [3] " Reed Muller Error Correcting Codes ", Ben cooke.
- [4] David Chase, "A Class of Algorithms for Decoding Block Codes With Channel Measurement Information", IEEE TRANSACTIONS ON INFORMATION THEORY, VOL, IT-8, NO.1, JANUARY 1972

[5] Kenneth G. Paterson, Alan E. Jones, "Efficient Decoding Algorithm for Generalized Reed-Muller Codes", IEEE TRANSACTION ON COMMUNICATIONS, VOL48,NO.8,AUGUST 2000

[6] Ilya Dumer, Kirill Shabunov, "Soft-Decision of Reed-Muller Codes Recursive Lists",IEEE TRANSACTIONS ON INFORMATION THEORY, VOL.52,N0.3,MARCH 2006

[7] " Decoding Algorithm with FHT for CQI in 3GPP-LTE ", Minling Li and Dahai Han . 2010 International Conference on Computer Application and System Modeling.



# 9 | Miscellaneous-Concepts

## 9.1 Orthogonal Frequency Division Multiplexing (OFDM)

The basic principle of OFDM is to divide the available spectrum into narrowband parallel channels referred to as subcarriers and transmit information on these parallel channels at a reduced signaling rate. The goal is to let each channel experience almost flat-fading simplifying the channel equalization process. The name OFDM comes from the fact that the frequency responses of the subchannels are overlapping and orthogonal. The subchannel frequency  $f_k = k * \Delta f$ , where  $\Delta f$  is the subcarrier spacing. Each subcarrier is modulated by a data symbol and an OFDM symbol is formed by simply adding the modulated subcarrier signals.

The baseband signal with in OFDM symbol can be written as:

$$S(t) = \sum_{k=0}^{N-1} X(k) * e^{j2\pi k \Delta f t}, \quad (9.1)$$

where N represents the number of subcarriers,  $X(k)$  complex modulation symbol transmitted on the  $k$ th subcarrier  $e^{j2\pi k \Delta f t}$  and  $\Delta f$  subcarrier spacing.

The orthogonality of OFDM subcarriers can be lost when the signal passes through a time-dispersive radio channel due to inter-OFDM symbol interference. However, a cyclic extension of the OFDM signal can be performed [1] to avoid this interference. In cyclic prefix extension, the last part of the OFDM signal is added as cyclic prefix (CP) in the beginning of the OFDM signal which is illustrated in figure

The cyclic prefix length is generally chosen to accommodate the maximum delay spread of the wireless channel. The addition of the cyclic prefix makes the transmitted OFDM signal periodic and helps in avoiding inter-OFDM symbol and inter-subcarrier interference.

The OFDM transmitter and receiver model is given in and .At the receiver, the estimate of the complex modulation symbol  $X(m)$  is obtained by multiplying the received signal with  $e^{-j2\pi m \Delta f t}$  and integrating over an OFDM symbol duration as below:

$$\begin{aligned} \hat{X}(m) &= \frac{1}{T_s} \int_0^{T_s} [z(t) + s(t)] * e^{-j2\pi m \Delta f t} dt \\ &= \frac{1}{T_s} \int_0^{T_s} z(t) * e^{-j2\pi m \Delta f t} dt + \frac{1}{T_s} \int_0^{T_s} s(t) * e^{-j2\pi m \Delta f t} dt, \end{aligned} \quad (9.2)$$

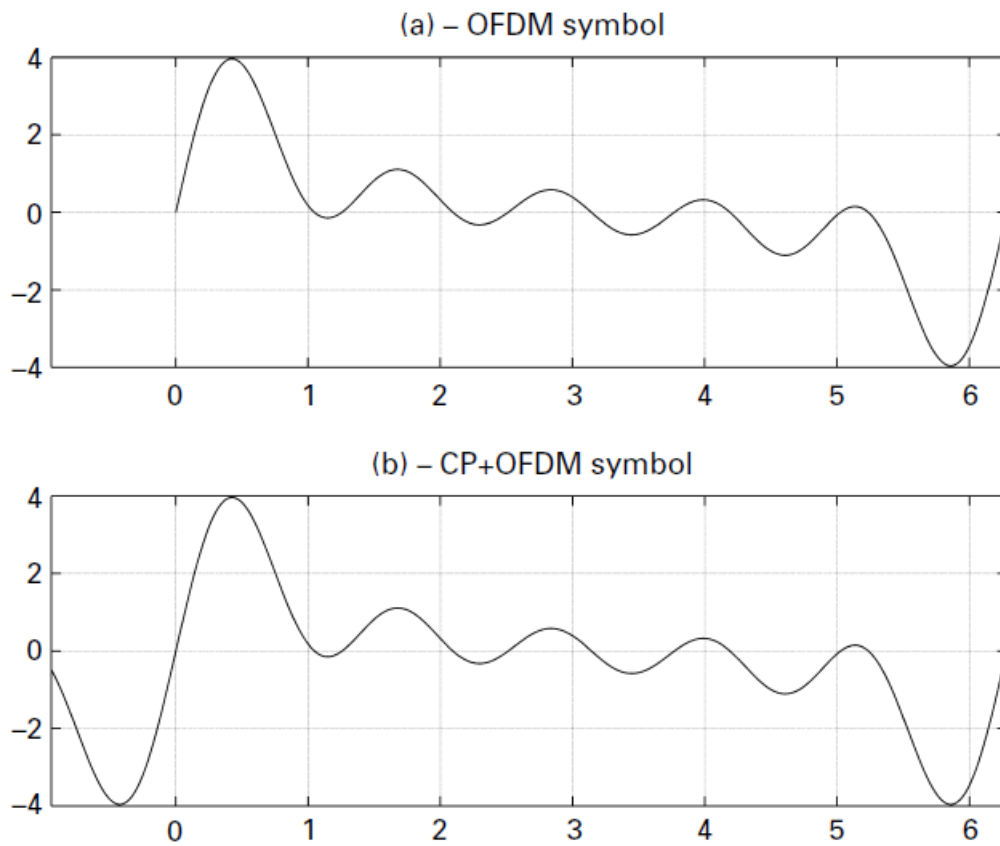


Figure 9.1: An illustration of cyclic prefix extension of OFDM symbol.

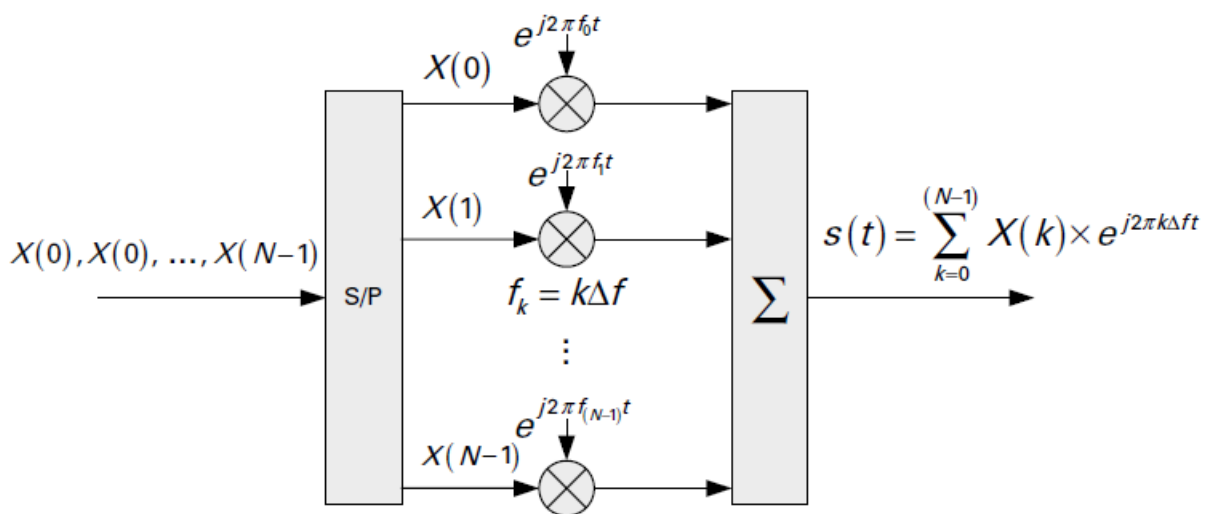


Figure 9.2: OFDM continuous-time transmitter model using banks of subcarrier oscillators.

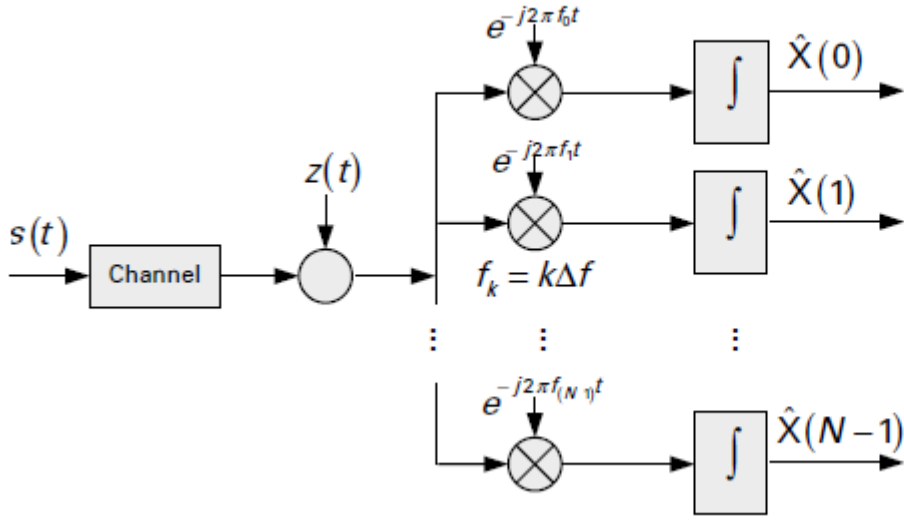


Figure 9.3: OFDM continuous-time receiver model using banks of subcarrier oscillators.

We assume perfect time and frequency synchronization and ignore the effect of wireless channel. Under these assumptions, the only source of signal degradation is AWGN component  $z(t)$ . By letting

$$\hat{z} = \frac{1}{T_s} \int_0^{T_s} z(t) * e^{-j2\pi k \Delta f t} dt, \quad (9.3)$$

we can written as (5.2)

$$\begin{aligned} \hat{X}(m) &= \frac{1}{T_s} \sum_{k=0}^{N-1} X(k) \int_0^{T_s} e^{j2\pi k \Delta f t} e^{-j2\pi m \Delta f t} dt + \hat{z} \\ &= \frac{1}{T_s} \sum_{k=0}^{N-1} X(k) \int_0^{T_s} e^{j2\pi (k-m) \Delta f t} dt + \hat{z} \\ &= X(m) + \hat{z}, \end{aligned} \quad (9.4)$$

We note that under the assumptions of perfect time and frequency synchronization and also that the wireless channel does not cause any time or frequency dispersion, the transmitted data message is perfectly recovered with the only source of degradation being the noise. This is guaranteed by the mutual orthogonality of OFDM subcarriers over the OFDM symbol duration  $T_s$  as below:

$$\begin{aligned} \frac{1}{T_s} \int_0^{T_s} e^{j2\pi (k-m) \Delta f t} dt &= 1 & k = m \\ &= 0 & k \neq m \end{aligned} \quad (9.5)$$

We can represent the OFDM baseband transmit signal in the following form:

$$s(t) = \sum_{k=0}^{N-1} \sum_{n=-\infty}^{\infty} X_n(k) e^{j2\pi k \Delta f t} \text{rect}(t - nT_s), \quad (9.6)$$

where  $n$  is the OFDM symbol number and the rectangular filter is defined as:

$$\begin{aligned} \text{rect} &= \frac{1}{\sqrt{T_s}} & 0 \leq t \leq T_o \\ &= 0 & \text{elsewhere} \end{aligned} \quad (9.7)$$

Until now we discussed OFDM transmitter and receiver implementation using banks of subcarrier oscillators. A more efficient processing for OFDM using discrete Fourier transform (DFT) and hence eliminating the need for banks of subcarrier oscillators was presented by Weinstein and Ebert [2].

By assuming  $N$  times sampling of the OFDM symbol at time instants of  $t = \frac{m}{N}T_s$ , we can rewrite (5.1) as below:

## References

- [1] Peled, A. and Ruiz, A., "Frequency domain data transmission using reduced computational complexity algorithms," IEEE International Conference on Acoustics, Speech, and Signal Processing ICASSP '80, vol. 5, pp. 964–967, Apr. 1980.
- [2] Weinstein, S. B. and Ebert, P. M., "Data transmission by frequency-division multiplexing using the discrete Fourier transform," IEEE Transactions on communications, vol. COM-19, no. 5, pp. 628–634, Oct. 1971.
- [3] "Research On Method Of PUCCH Channel Estimation Based On UCI Separate Coding" (ICETC2012) IPCSIT vol.43 (2012) © (2012) IACSIT Press, Singapore